AFFDL-TR-73-56

EFFECTS OF STRUCTURAL HEATING ON THE SONIC FATIGUE OF AEROSPACE VEHICLE STRUCTURES

M. J. JACOBSON
F. E. FINWALL
NORTHROP CORPORATION
HAWTHORNE, CALIFORNIA

JANUARY 1974

TECHNICAL REPORT AFFDL-TR-73-56

AIR FORCE FLIGHT DYNAMICS LABORATORY
AIR FORCE SYSTEMS COMMAND
WRIGHT-PATTERSON AIR FORCE BASE, OHIO 45433

NOTICE

When Government drawings, specifications, or other data are used for any purpose other than in connection with a definitely related Government procurement operation, the United States Government thereby incurs no responsibility nor any obligation whatsoever; and the fact that the Government may have formulated, furnished, or in any way supplied the said drawings, specifications, or other data, is not to be regarded by implication or otherwise as in any manner licensing the holder or any other persons or corporation, or conveying any rights or permission to manufacture, use or sell any patented invention that may in any way be related thereto.

Copies of this report should not be returned unless return is required by security considerations, contractual obligations, or notice on a specific document.

AIR FORCE/55780/4 February 1974 — 150

EFFECTS OF STRUCTURAL HEATING ON THE SONIC FATIGUE OF AEROSPACE VEHICLE STRUCTURES

M. J. JACOBSON
P. E. FINWALL
NORTHROP CORPORATION

FOREWORD

The research work reported herein was conducted by the Northrop Corporation, Aircraft Division, Hawthorne, California, for the Aero-Acoustics Branch, Vehicle Dynamics Division, Air Force Flight Dynamics Laboratory, Wright-Patterson Air Force Base, Ohio, under Contract F33615-72-C-1198. This research is part of a continuing effort to establish tolerance levels and design criteria for acoustic fatigue prevention under the exploratory development program of the Air Force Systems Command. The effort was conducted under Project 4437.

Mr. O. F. Maurer was the Project Engineer. This study was performed during the period March 1972 to March 1973.

The manuscript was released by the authors in March 1973 for publication, and was assigned the Northrop number NOR 73 - 45.

The work was performed at Northrop with Dr. M. J. Jacobson serving as the Principal Investigator under the technical guidance of Dr. C. Hwang - both in the Structures Research and Technology Department - and under the supervision of Mr. C. Rosenkranz, Manager of the Structures Research and Technology Department, wherein the analysis and design were conducted. Major tasks were carried out under the direction of Mr. P. E. Finwall, who directed the test program, and Mr. J. G. Buttrey, who directed the fabrication program. Dr. W. S. Pi of Northrop provided valuable advice in developing an analytic criterion for the onset of oil canning.

This technical report has been reviewed and is approved.

WALTER J. MYKYTOW
Ass't. for Research & Technology
Vehicle Dynamics Division

ABSTRACT

The results of an analytic and experimental investigation to identify and determine the influence of effects of structural heating on the dynamic response characteristics of randomly excited aerospace structures and on the combined environment-acoustic fatigue properties of structural components are presented. Thermal and thermal-acoustic tests were conducted on 2024-T81 aluminum alloy, Ti-6Al-4V titanium alloy and Rene' 41 nickel-base alloy panel specimens. Effects of the temperature increase and sound pressure on the stress response and oil canning of the panels were observed. A semi-empirical criterion for predicting oil canning of panels in thermal-acoustic environments was developed. Shaker tests were conducted on 2024-T81 aluminum alloy specimens to determine the effect of the different sequences and combinations of heating and shaker excitation on the fatigue life of the specimens when oil canning is a factor. Elevated temperature fatigue tests under steady-state random (shaker) excitation were also conducted with Ti-6Al-4V titanium alloy and Rene' 41 nickel-base alloy specimens.

CONTENTS

CONTENTS (CONTINUED)

ILLUSTRATIONS

ILLUSTRATIONS (CONTINUED)

TABLES

TABLES (CONTINUED)

SYMBOLS AND NORMAL UNITS

SYMBOLS		UNITS
A_o	Amplitude of thermal buckle	inch
A, B, C	Nondimensional constants (in Appendix A)	
D	Bending rigidity	lb. in.
E	Young's modulus	psi
K	Generalized stiffness	lb/in^3
F	Temperature	degrees Fahrenheit
M	Generalized mass	lb sec^2/in^3
S	Spectral density of pressure	psi^2/Hz
S_i	Nondimensional stress (with i an integer)	
SPL	Sound pressure level	db re 20 N/m^2
t	Temperature	degrees Farenheit
a	Length	inch
b	Width	inch
ϵ	Strain	inch/inch
f	Frequency	Hz
h	Thickness	inch
σ	Stress	psi
w	Deflection	inch
w	Rms deflection	inch-rms
Γ	Nondimensional participation factor	
α	Coefficient of thermal expansion	inch/inch/F
γ	Weight density	lb/in^3
ζ	Nondimensional viscous damping factor	
ν	Poisson's ratio	
ρ	Mass density	lb sec^2/in^4
cr	Critical (when used as a subscript)	

I. INTRODUCTION

There has been a definite need for analysis and design methods for structures in thermal-acoustic environments, since there are many instances of simultaneous applications of noise and heat to portions of present and projected high performance aircraft, including V/STOL aircraft. The noise sources include the engine air intake duct turbulence, jet engine exhaust, and high-speed flight during which the aircraft skin is acted on by boundary layer noise and high temperatures induced by aerodynamic heating.

The program reported herein was conducted to determine the influence of the major effects of structural heating on the dynamic response characteristics of randomly excited aerospace structures and on the acoustic fatigue properties of structural components in the combined environment. As a part of the investigation, analytical studies and experiments were conducted to establish qualitative and quantitative information on the combined environment effects due to different combinations of acoustic and thermal loading and their relative importance in the combined environment-acoustic fatigue problem. A description of the analytical, design, and test methods that were used, as well as the results and conclusions that were drawn from the analytical and experimental investigation, are incorporated into this report.

A major goal of the program was the achievement of a better understanding of acoustic fatigue in thermal environments. This is of significance, since there have been only a few reported investigations during the last several years (e.g., References 1, 2, and 3) that supply data on structures in combined acoustic-thermal environments. The aforementioned investigations were limited in scope and did not result in design charts for general usage comparable to those of References 4 and 5 for room temperature and intense noise environments. In fact, the few reported investigations were (intentionally) not formulated to produce a thorough study into the nature and influence of thermal effects on dynamic stress response and fatigue in acoustic environments.

The program was organized in the following manner. A preliminary investigation was conducted to obtain information to serve as a guide for the finalization of the program. In the preliminary investigation, a study was made to determine the various aircraft structural heating conditions and to identify thermal effects as they influence fatigue life in the combined thermal and acoustic environment. Structures were considered which are heated up to 1200F and are exposed simultaneously and/or intermittently to a high intensity acoustic environment. Also in the preliminary investigation, a review of the materials for elevated temperature applications was conducted, and the final selection of materials for use in the experimental program was made. During the review of the materials, a literature search was performed to obtain basic material properties such as mechanical and thermal properties.

Following the preliminary investigation, a combined analytical and experimental investigation was conducted to determine the thermal effects

on dynamic stress response and fatigue. Items such as the spatial distribution of temperature, thermal buckling, oil canning, thermal load cycling, and acoustic load cycling were considered.

The objective of the test program was to obtain data to support and check the analysis. The thermal-acoustic test program was conducted to obtain experimental data on oil canning and the dynamic strain response in thermal-acoustic environments. The thermal-shaker test program was conducted to determine the effects of different sequences and simultaneous applications of the thermal and acoustic loads on oil canning and fatigue failures.

The overall test program included the fabrication and test of ten panel specimens in a combined acoustic-thermal environment, of thirty beam-type specimens for tests in a combined vibratory-thermal environment, and of nineteen coupons for static tests at ambient and elevated temperature to qualify the test materials (and, as a by-product, generate materials data). Materials used in the experimental program were the 2024-T81 aluminum alloy, the Ti-6Al-4V titanium alloy, and the Rene' 41 nickel-base alloy.

A method for predicting oil canning of originally flat panels in thermal-acoustic environments was developed and evaluated against test data that were obtained in the experimental program. The experimental strain data were also evaluated as a function of sound pressure level, temperature, and other pertinent parameters.

An overview of structural heating conditions and their effect on structures in thermal-acoustic environments is in Section II. The investigation of thermal effects on the dynamic stress response of acoustically loaded panels and the newly developed criterion for predicting oil canning of multi-bay metallic panels are reported in Section III. The investigation of thermal effects on fatigue is reported in Section IV. The conclusions from the entire program are in Section V.

The criteria for the selection of materials for the test program, the method of manufacturing the specimens, and the results of the material qualification tests are in Appendix A. Many details of the thermal-acoustic test program are in Appendix B and of the thermal-shaker test program are in Appendix C.

II. GENERAL CONSIDERATIONS

II.1 BACKGROUND

Aircraft structural components such as engine air intake ducting and rear fuselage and empennage structures which are located in the vicinity of the jet engine exhaust have experienced combined heating and random dynamic excitation which result from the acoustic or pseudoacoustic noise emitted by the jet efflux. In addition, in the VTOL and V/STOL operational modes of projected advanced aircraft, combined thermal and acoustic environments can be expected in areas of the wing and/or fuselage structure – the locations and magnitudes being highly dependent upon vehicle/engine configurations. The combined thermal-acoustic environment can also occur in different operational modes of reentry vehicles such as the space shuttle.

In examining the test data, it is apparent that the effects of the combined environment on panel life may be more severe than a linear superposition of the effects of the separate environments. In the lower ranges of structural heating, a high intensity acoustic environment is the predominant factor in contributing to structural damage and fatigue. At higher temperatures, the contributions of the thermal effects may prevail and, when enhanced by an acoustic load, may cause early structural failure.

A completely rigorous analytical method of obtaining the combined effects of the thermal and acoustic loading is unavailable. Therefore, present practices of design for structural components to withstand the combined thermal-acoustic loading rely heavily on component testing in a simulated environment. From such tests (which are more in the nature of qualification tests), quantitative data on the contribution of the various thermal effects to the damage are generally not available.

A particular goal of this program was to obtain a better quantitative measure of the effects in the combined environments. There are various reasons, some of which are described below, why the thermal effects in a combined environment are often more severe than the thermal effects in separate environments. The various reasons include:

- Thermal tensile stresses (usually near a boundary) in the skin due to its non-uniform temperature, heat sinks at the boundaries, etc., act in combination with vibratory stresses caused by acoustic excitation. These combined stresses can lead to early fatigue failures.

- Thermal compressive stresses in the panel interior reduce the panel flexural stiffness which permits an increase in the panel deflection and stresses caused by acoustic excitation and can lead to an early fatigue failure even in the absence of thermal buckling and/or dynamic buckling. The same factors mentioned above that cause tensile stresses at a panel (or bay) boundary will cause compressive stresses in the panel (or bay) interior.

- The reduction in Young's modulus and material strength at elevated temperature reduces the panel stiffness and strength and can lead to an early acoustic failure for the reasons just mentioned above.

- large stress reversals that occur during the oil canning of thermally buckled panels in sufficiently high intensity acoustic environments can lead to early fatigue failures.

II.2 STRUCTURAL HEATING CONDITIONS

Thermal and acoustic environments that are applicable to existing and expected operating conditions of aerospace vehicles (e.g., advanced high-speed jet aircraft, V/STOL aircraft, and the space shuttle system) were examined. From this investigation, the combined and separate thermal and dynamic environments were finalized for investigation during the remainder of the program.

In general, the thermal conditions can be adequately defined for aerospace structural systems given the vehicle type and operating regime. The particular structural heating conditions that may exist on flight vehicle structures are highly dependent on such factors as the detailed structural arrangement, the type of vehicle, its mission profile, and the means of propulsion. Representative environmental temperatures and sound pressure levels that were considered are in Table I. The reviewed data in Table I did not include quantitative information on structurally non-uniform temperature distributions in the combined environments. Because of three-dimensional temperature gradients that occur when heat is applied to typical aircraft structural configurations, such as skin supported by heavy frames, a spatially non-uniform temperature in the structure is to be expected, especially prior to the time when steady-state temperatures are reached.

In the thermal-acoustic test program, steady-state temperature conditions existed in the test conditions. In the shaker test program, some tests were conducted under steady-state temperature conditions and other tests were conducted under uniform heating conditions that produced temperature increases up to approximately 300F per minute in the shaker test specimens.

Thermal and thermal-acoustic service environments may be characterized by either rapid temperature variations, slow cyclic temperature variations, or steady-state temperature conditions. The qualitative effect of these different thermal environments on stresses and fatigue life are reviewed below.

II.2.(a) Rapid Temperature Variations

In the absence of an acoustic environment, the stress-time relation of a thin beam, thin plate, or thin panel depends on whether there is rapid heating and/or cooling during the temperature cycle. When there is extremely rapid heating (or cooling), vibratory thermal stresses (References 6 through 8) may develop with an amplitude of the same order of magnitude as the steady state stress, corresponding to the stabilized temperature. Furthermore, if in an acoustic environment there is rapid heating (or cooling) in raising (or lowering) the panel temperature from one temperature to another temperature and permitting the panel temperature to stabilize at the second level for some extended time period before

TABLE I. COMBINED ENVIRONMENT TEMPERATURE-ACOUSTIC DATA

AIRCRAFT	ENVIRONMENTAL TEMPERATURE (F)	SPL (db)	CAUSE	TEMPERATURE-TIME RELATION
Fighter	500–600	150–158	Aerodynamic heating of aircraft structure	Constant temperature in cruise condition at constant altitude
Fighter	Up to 1200F in aircraft using "uncooled" engines (1)	Up to 165	Jet exhaust in the vicinity of aircraft structure	The temperature may remain constant for long periods of time during flight
V/STOL Fighter	200–300	About 158	Jet exhaust that is reflected from ground during take-off	These temperatures and SPLs are not sustained after take-off
Space Shuttle	350	162	Boundary layer turbulence	These temperatures and SPLs occur during the transonic phase of the ascent

(1) By "cooled" engines are meant bypass engines that feature a self-cooled afterburner design. "Uncooled" engines do not have that design feature.

returning to the initial temperature and subsequently repeating the temperature cycle, then the effect of the stresses from the combined thermal and acoustic loading may produce a structural fatigue life different than the fatigue life that would have resulted from the acoustic environment alone or the thermal environment alone.

II.2. (b) Temperature Cycling with Large Periods

If the temperature cycling of structures is not rapid, then the vibratory thermal stresses become negligible. In the case of slow heating and cooling of thin beams in the absence of an acoustic environment, it is unlikely that sufficiently high thermal stresses can be generated to produce a fatigue failure unless there are considerable bending deflections because of buckling. In the case of thin plates that are slowly heated and cooled in the absence of an acoustic environment, sufficiently high stresses (especially at the corners of the plate (e.g., see Reference 9) may be generated through the plate thickness to produce a fatigue failure because of the cyclic thermal stresses. In the case of thin plates that are slowly heated and cooled in the presence of an acoustic environment, the fluctuating stresses from the acoustic loading are higher at the center of the ends of the plate than at the corners of the plates. In such a combined thermal-acoustic environment, the fluctuating stresses from the acoustic loading may combine with the cyclic stresses from the slow temperature cycling to produce a fatigue life different than the fatigue life that would have resulted from the acoustic loading alone or the slow temperature cycling alone.

II.2(c) Steady-State Temperatures

There may be situations when an elevated temperature is reached and maintained for long periods of time when acoustic excitation exists. At the steady-state elevated temperature, the fatigue life of a panel in an acoustic environment is influenced by temperature in several ways -- for example, (1) by oil canning, if it occurs, (2) by stress changes as a result of temperature-dependent material properties and (3) by an average in-plane thermal stress that is induced throughout the structure due to boundary constraints.

II.3 THERMAL-ACOUSTIC EFFECTS

Heating of structural components produces a variety of thermal effects on the material, the acoustic response, and the acoustic fatigue life. The principal thermal-acoustic effects are reviewed below.

II.3.(a) Changes in Dynamic Properties

By dynamic properties are meant those material properties of the structural components that affect the structural dynamic response characteristics. For this program, the structural dynamic response characteristics were defined as natural frequencies and associated modal shapes, deflection and strain response to acoustic excitation, and dynamic buckling. The dynamic material properties are the material modulus of elasticity, internal damping, and thermal coefficient of expansion; and a discussion of these parameters as they relate to this program follows.

Heating changes the material modulus of elasticity which can be characterized quantitatively by Young's modulus and the shear modulus of many metallic materials. (For analytic purposes, most metals are considered isotropic.) For many materials, modulus of elasticity as a function of temperature is in the literature (e.g., MIL-HDBK-5). A change in the elasticity will produce a change in the dynamic response characteristics of the structural components since all the dynamic response characteristics are a function of Young's modulus which is temperature dependent.

Heating can also change the structural damping. If the heating changes the internal damping of the metals, then the heating is altering a dynamic property of the material. Investigations of internal damping as a function of temperature and response frequency have been reported (e.g., References 10, 11 and 12). In practical service applications, material choices are made so that significant metallurgical changes will not occur in the operating environment. Therefore, the effect of heating on the internal damping of aircraft panels in service was not considered to be significant in this program.

The damping of structural components is also influenced by the damping at the boundary which can be a function of temperature of the component and the boundary member(s). In practice, it is difficult to measure separately the damping at the boundary and the internal damping, and no attempt was made to measure that difference in this program. The changes in overall damping are manifested by changes in the deflection and stress response under random acoustic excitation. When the structural response is predominantly unimodal, the random deflection and stress responses are inversely proportional to the square root of the viscous damping factor, a relationship which is exact for the response of one degree of freedom spring-dashpot-mass system, which is often used to simulate the small deflection response of panels subjected to random broadband, acoustic excitation.

Another material property that can be affected by temperature and thus influence the dynamic response is the thermal coefficient of expansion. The thermal coefficient of expansion in combination with the boundary conditions and temperature distribution determines the thermal stresses which may play a significant role in the dynamic response; however, the thermal coefficient of expansion is not particularly sensitive to temperature changes - particularly for the practical useful operational temperature ranges for many structural materials.

II.3(b) Modifications in Dynamic Characteristics

The heat distribution over an aerospace structure and the associated temperature gradients can significantly modify the dynamic characteristics of structural components. Heating generates compressive thermal stresses in (1) a region(s) of a structural panel with a significantly non-uniform inplane temperature build-up due to heat sinks on its boundaries or due to non-uniform heating and (2) an entire panel with essentially uniform temperature but with boundaries that prevent thermal expansion. When sufficiently large, these compressive thermal stresses can produce thermal bending and buckling in the absence of an acoustic environment. Furthermore, when large inplane compressive stresses exist which are not large enough to produce thermal buckling, these

compressive thermal stresses can significantly reduce the component apparent stiffness. This reduction may be characterized by (1) a significant reduction in the fundamental frequency of a panel or otherwise give rise to a nonlinear behavior, depending on the thermal distribution and dynamic mode shape, and (2) an increase in the maximum out-of-plane deflection and the maximum panel bending stress when an acoustic pressure loading acts normal to the surface of a panel.

When the power spectral density of the excitation does not contain uniform spatial and/or frequency content, then a change in the natural frequency(ies) and modal shape(s) of the responding mode(s) may result in a significant modification of the dynamic response characteristics.

A temperature gradient through the thickness of a stiffened or unstiffened panel can produce a curvature which stiffens the panel, increases its fundamental frequency, and tends to reduce the stress response to acoustic excitation and therefore tends to increase the acoustic fatigue life. However, an increase in curvature because of heating may also lead to oil canning (see the next subsection) which tends to increase stresses and reduce the acoustic fatigue life.

As was stated in the previous subsection, heating affects the dynamic properties of the materials which, in turn, influence the dynamic response. It was noted in Reference 1 that the effect of the thermal stresses on panel stiffness was much more important than the effect of heating on Young's modulus (i.e., the panel elasticity) in producing an early acoustic fatigue failure in the thermal environment. For service applications, the effects of the generated thermal stresses may always be more important on the acoustic fatigue life than the effects of the changes in Young's modulus (just as was the case in Reference 1) because the change in Young's modulus from ambient temperature to the planned operating temperatures is usually not considered drastic for the useful operational temperature range of materials.

II.3.(c) Dynamic Buckling or Oil Canning

A temperature gradient through the thickness of a stiffened or unstiffened panel can produce bending of the panel into a curved shape. For normal heating rates of aircraft panels with thin skins it is unlikely that a significant temperature variation exists through the thickness of a thin, unstiffened panel or through the thickness of the portion of the thin skin of stiffened panels that is not in contact with or close to the stiffeners. Data in the test program verify this.

Thermal buckling of initially flat panels is also manifested by curvature. A curved panel is susceptible to dynamic buckling or oil canning which, for this program, is defined as the phenomenon when a curved panel has at least two equilibrium positions and under acoustic pressure loading intermittently snaps back and forth between them, as well as vibrates continuously about one or the other of them. Random acoustic excitation with oil canning produces higher rms stresses than random acoustic excitation without oil canning. The higher rms stresses and the large stress reversals as the panels snap through the flat position in moving towards one curved equilibrium position from the other promote earlier fatigue failures.

In Reference 13, the oil canning of an initially curved bay of a cross-stiffened graphite-epoxy test panel when the overall sound pressure level reached 148 db is reported. The initial curvature itself was a result of thermal stresses that were developed from the cool down (during the manufacture of the panel) to room temperature from the 250F temperature at which the stiffeners were bonded to skin. There was a significant increase in measured rms strain response when the oil canning occurred.

II.3.(d) Strength Degradation

Fatigue strength parameters for most metallic structural materials are affected in a manner similar to static strength parameters in a thermal environment. That is, their effective temperature ranges and rate of strength deterioration at higher temperatures are much the same (Reference 14). In addition, the fatigue limit tends to decrease with increasing temperatures (Reference 15).

On the positive side, most materials tend to be less notch sensitive at high temperatures (where notch sensitivity is measured by the strength reduction factor, K_f). One exception is austenitic steel, which has shown greater notch sensitivity up to 1100F to 1200F. Also, the effect of surface treatment is less important at high temperatures.

The candidate materials that were considered for use in the test program were aluminum alloys, titanium alloys, ferritic stainless steels, austenitic stainless steels, and nickel-base alloys. For the conventional aircraft structural alloys of the five aforementioned materials, the fatigue strength at any life decreases as the temperature and time of exposure increases above certain limits. The magnitude of decrease is related to a number of factors, including the material type and the structural configuration. The nickel-base alloys are used in environments with the highest elevated temperatures, the stainless steels at somewhat lesser elevated temperatures, followed by the titanium alloys at somewhat lower maximum elevated temperatures, and the aluminum alloys at the lowest elevated temperatures.

The structural configuration affects the uniformity of the temperature variation in a structural system and the subsequent dimensional changes during thermal cycling. These effects depend on the type of structural arrangements and are additive to any working stress existing in a particular member. Such induced stresses may ultimately determine the type of material used.

II.3.(e) Thermal Fatigue

When all local areas of a structural component are free to expand and the structural component is subjected to heating, a completely unconstrained thermal expansion process occurs. Restraint of this expansion (for example, because of immovable boundary conditions or because of heat sinks in zones near the boundary that result in a temperature gradient along the structural component) introduces thermal stresses into the component. The thermal stress depends on the temperature as well as the distribution of the material area and the material thermal properties. Repetitive application of thermal stresses can produce a thermal fatigue which is a structural fatigue condition that is similar to low cycle, high stress fatigue induced by mechanical loading. Recent thermal fatigue studies include work by Spera (Reference 16).

Panels with low bending rigidities undergo sufficiently large out-of-plane displacements to result in only elastic strains in many situations. However, if the thermal stress is sufficiently high, a plastic strain will result for ductile materials. Subsequent temperature cycles will result in a hysteresis loop with no further plastic flow. The amount of strain hardening or softening present will determine the ultimate position of this loop. Studies have indicated that in comparing high temperature, mechanical fatigue tests with thermal fatigue at equal values of cyclic plastic strain, the thermally cycled specimens have the lowest life (References 17 and 18). The net effect may be a modified S-N curve in the low cycle range.

The high cycle acoustic fatigue is often characterized by a zero average stress and by the rms stress and time to failure for different spectral contents that can be classified as either narrow-band or broad-band. The low cycle thermal fatigue is characterized by a relatively high average stress. The prediction of fatigue life of structural components in such combined thermal-acoustic environments depends on the method of combining the effects of low cycle fatigue and high cycle fatigue. Methods such as modified Goodman diagrams for constant life situations have been used widely when discrete frequency, constant amplitude stresses are superimposed on an average stress. There are no modified Goodman diagrams in general use in the case of random response to mechanical excitation that may be superimposed on a slowly-varying thermal stress.

II.3.(f) Other Effects

Other effects, such as creep, were not considered in this program.

III. THERMAL EFFECTS ON THE DYNAMIC STRESS RESPONSE

III.1 OVERVIEW

An interrelated analytical and experimental program was formulated and conducted to determine the principal thermal effects on the dynamic stress response. The results were evaluated, and procedures for the testing, analysis, and design of acoustic fatigue resistant structures were developed and are reported herein.

III.2 SUMMARY OF TEST PROGRAM

Ten test specimens (Table II and III) were fabricated and subjected to thermal and thermal-acoustic tests.

In Table II, the first two characters in the alphanumeric designation of a test specimen refers to the test condition. The third alphanumeric character is the specimen number for that test condition. For example, specimen A-3-2 is the second test specimen for test condition A-3.

TABLE II. THERMAL-ACOUSTIC TEST SPECIMENS AND TEST CONDITIONS

Test Specimen Designation	Test Condition	Material	Configuration	Photograph
A-1-1	A-1	2024-T81	Unstiffened beam	Figure 6
A-1-2	A-1	2024-T81	Unstiffened beam	-
A-2-1	A-2	2024-T81	Unstiffened plate	-
A-2-2	A-2	2024-T81	Unstiffened plate	Figure B-1
A-3-1	A-3	2024-T81	3-Bay Panel	-
A-3-2	A-3	2024-T81	3-Bay Panel	Figure B-2
A-4-1	A-4	Ti-6Al-4V	3-Bay Panel	Figure B-3
A-4-2	A-4	Ti-6Al-4V	3 Bay Panel	-
A-5-1	A-5	René 41	3-Bay Panel	Figures B-4
A-5-2	A-5	René 41	3-Bay Panel	and B-5

TABLE III. DESCRIPTION OF THERMAL-ACOUSTIC TEST SPECIMENS

Quantity	Material	Configuration (1)	Overall Specimen Dimensions (inch)	Unsupported Specimen Dimensions (inch)
2	2024-T81	Unstiffened Beam	10.0 x 1.0	8.4 x 1.0
2	2024-T81	Unstiffened Plate	18.0 x 10.0	16.4 x 8.4
2	2024-T81	3-Bay Panel	18.0 x 18.0	16.4 x 16.4
2	Ti-6Al-4V	3-Bay Panel	18.0 x 18.0	16.4 x 16.4
2	René 41	3-Bay Panel	18.0 x 18.0	16.4 x 16.4

(1) The thickness of all skins and stiffener details was 0.040 inch.

The two unstiffened 2024-T81 aluminum alloy beams were fabricated and tested to determine the thermal effects with a one-dimensional varying temperature distribution; the two unstiffened 2024-T81 aluminum alloy plates were fabricated and tested to determine the thermal effects with a two-dimensional varying temperature distribution; and the three-bay panels were fabricated and tested to determine the thermal effects with a three-dimensional varying temperature distribution. Because of two unsupported free edges of the unstiffened beams, in combination with their relatively thin skin and heat sinks at the clamped boundaries, a one-dimensional varying temperature distribution was expected for these specimens; because of the relatively thin skins and the heat sinks at the clamped boundaries of the unstiffened plates, a two-dimensional varying temperature distribution was expected for these specimens; and because of the stiffeners and the heat sinks at the clamped boundaries of the stiffened panels, a three-dimensional varying temperature was expected for these specimens. (The expected temperature distributions were essentially obtained in all of the tests.)

Experimental strain data, damping data, temperatures, and natural frequencies were sought during the tests of the acoustic panels for use in assessing the thermal effects on stress response. The data were carefully examined to determine the existence of thermal buckling and/or dynamic buckling and their onset if possible (dynamic buckling was not expected in the absence of thermal buckling).

III.3 DESCRIPTION OF THERMAL-ACOUSTIC TEST SPECIMENS

There were two specimens for each combination of material and configuration so that two identical specimens could be tested at each condition. A manufacturing drawing of the three-bay panels is in Figure 1. Rivet selections are in Table IV. The bay dimensions were considered typical for various applications and the repetition of some of the dimensions was to permit the need of only one test fixture.

The test section of the three-bay panels was considered to consist of the central bay, the stiffeners, and the adjacent parts of the other bays. The central bay was designed with nominal dimensions of 16.0 x 8.0 inches (i.e., with an aspect ratio of 2, which is typical of many applications). This type of three-bay panel was used before (Reference 19) in ambient temperature-acoustic tests of stiffened panels (Figure 2) with 7075-T6 skins and riveted stiffeners. With the panels of Figure 2, acoustic fatigue failures occurred in the skin along the line of rivets midway between the clamped edges at 3 hours (for one panel) and 5-1/2 hours (for another panel) of broad band acoustic excitation at 160 db overall sound pressure level.

The knowledge that the configuration of Figure 2 led to fatigue lives of over one hour at 160 db SPL was a factor in selecting the design of Figure 1 for this program. An objective of this thermal-acoustic test program was to obtain strain response data before a fatigue failure occurred during tests of short duration up to 160 db. The objective was successfully achieved since no acoustic fatigue failures occurred during the test program.

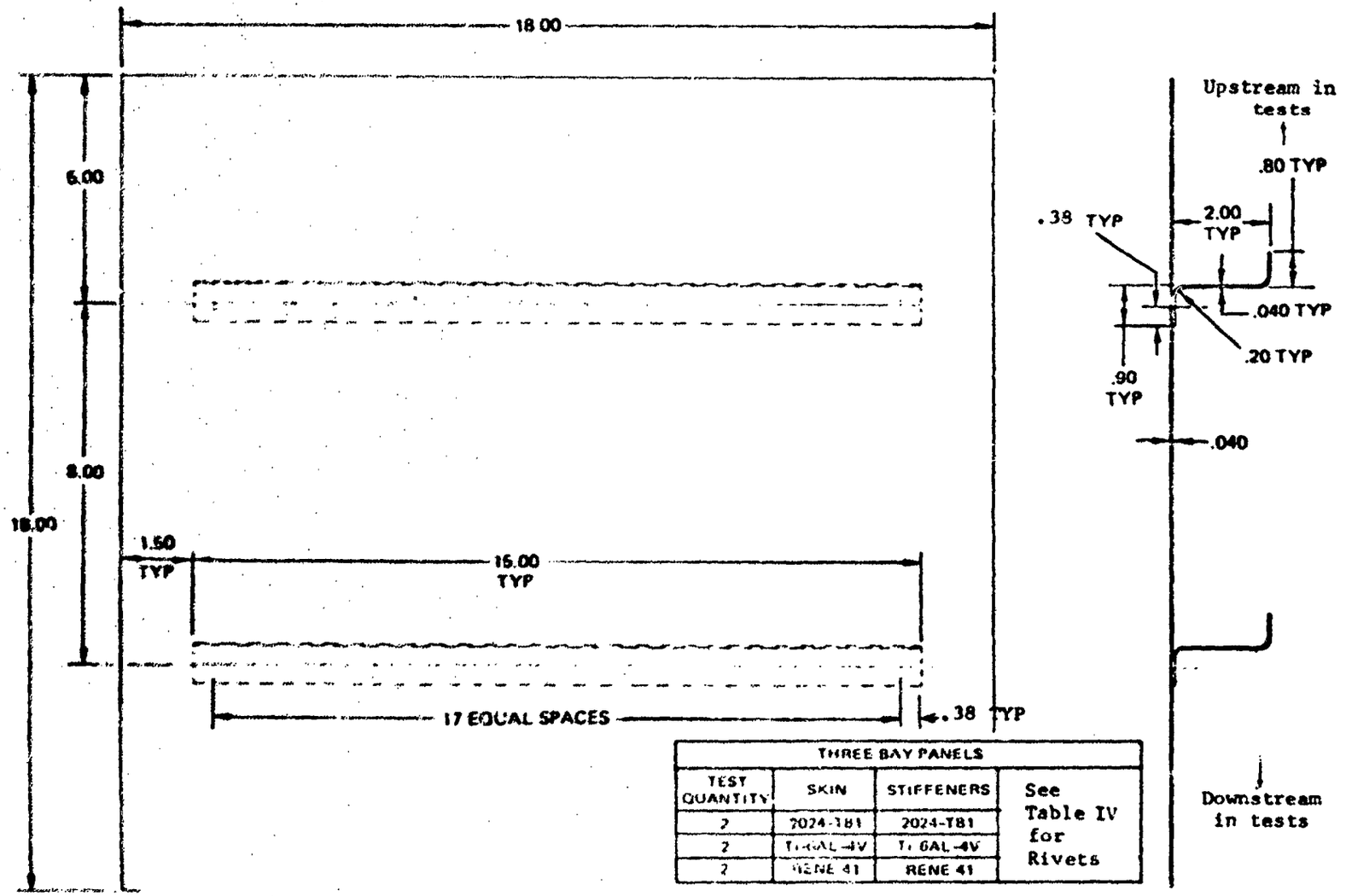

THREE BAY PANELS			
TEST QUANTITY	SKIN	STIFFENERS	See Table IV for Rivets
2	7024-T81	2024-T81	
2	Ti-6AL-4V	Ti-6AL-4V	
2	RENE 41	RENE 41	

FIGURE 1. THREE BAY THERMAL-ACOUSTIC TEST PANELS

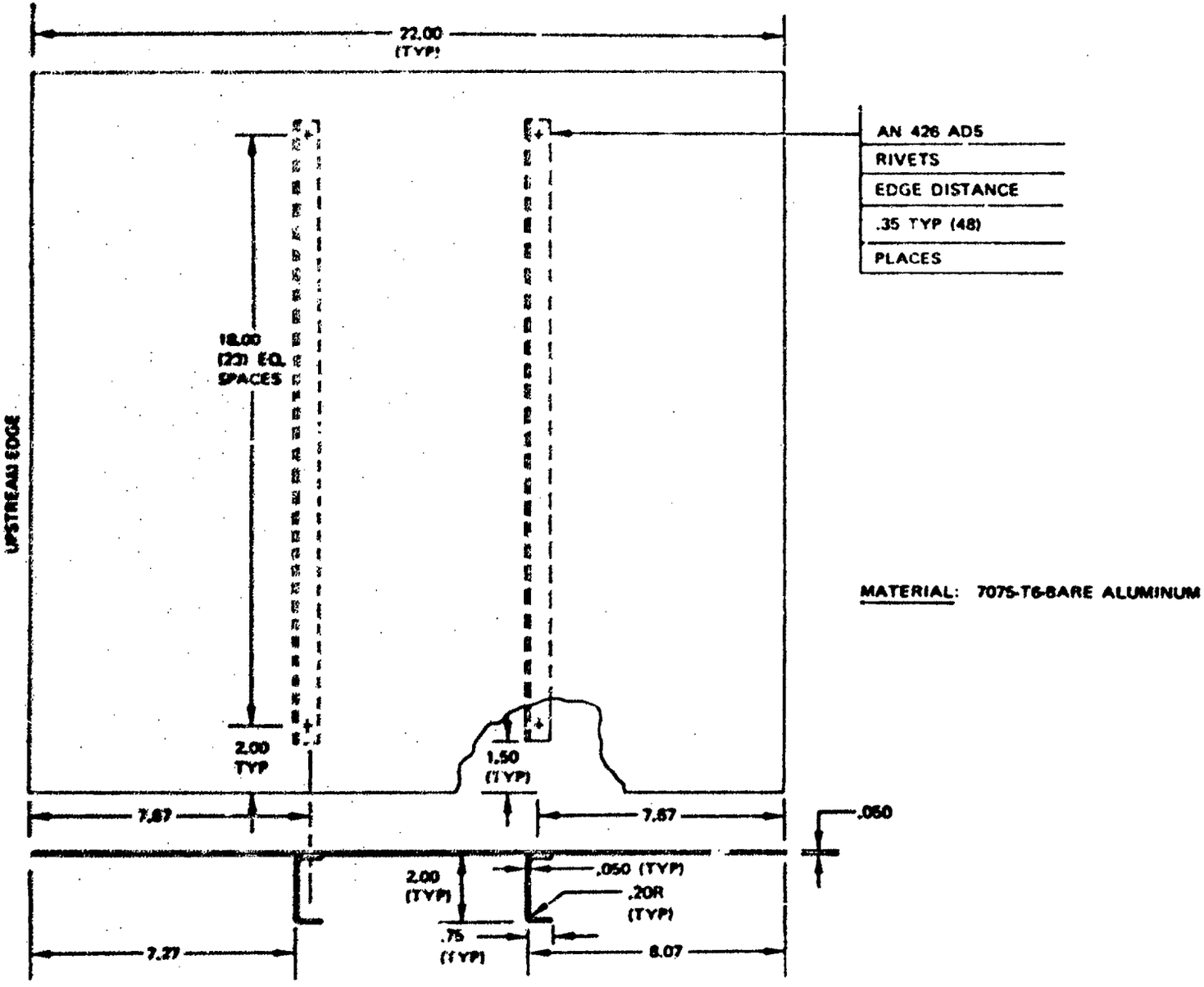

FIGURE 2 - ACOUSTIC TEST PANELS FROM A PREVIOUS PROGRAM

TABLE IV. RIVET SELECTION

Specimen Description	Skin Thickness (inch)	Stiffener Thickness (inch)	Rivets
3-Bay 2024-T81 acoustic panels	.040	.040	MS20470-AD5 (protruding head)
2024-T81 shaker specimens	.063	.063	MS20426-AD5 (countersunk)
3-Bay Ti-6Al-4V acoustic panels	.040	.040	CSE 903B-5 (protruding head)
Ti-6Al-4V shaker specimens	.063	.063	CSR 902B-5 (countersunk)
3-Bay Rene' 41 acoustic panels and shaker specimens	.040	.040	NAS1198-5 (protruding head)

Six of the ten acoustic-thermal test specimens were three-bay panels and only the three-bay panels included all the test materials. This reflected the belief that results from three-bay panels tests will more closely simulate the test results of cross-stiffened panels that are often used in practice. Only 2024-T81 aluminum alloy specimens were used in the unstiffened beam and plate tests since their test results relative to the three-bay 2024-T81 aluminum alloy panel test results were expected to indicate the effect of one-dimensional and two-dimensional varying temperatures for all three test materials.

III.4 GENERAL TEST PROCEDURE

The test procedures and instrumentation were designed to produce the end product, i.e., test data, in an efficient, repeatable, and reliable manner. The test data that were sought for the beam, plate and three-bay panel thermal-acoustic tests are outlined below:

- Frequency response - natural frequencies
- Mode damping
- Strain levels as a function of acoustic level and temperature distribution
- Temperature distribution
- Acoustic spectrum levels and overall levels

The following discussion outlines the test procedure that was the basis for the tests of the ten thermal-acoustic specimens.

The test specimens were instrumented with a set of high temperature strain gages and thermocouples. Then each test specimen was installed in its fixture, which provided the required boundary conditions. The specimens were then tested at the ambient temperature to determine resonance frequencies, mode shapes and modal damping characteristics. Low level discrete frequency loudspeaker excitation was used for this determination.

Next the test specimen was mounted in the progressive wave acoustic test chamber opposite the radiant heating module. The initial thermal tests were at ambient sound pressure level. The thermal-acoustic tests were then conducted and strain data and temperature distributions were taken at a set of steady state temperatures at two sound pressure levels (Table V). The reference temperature (Table V) was defined as the temperature at the center of the specimen. Many details relating to the instrumentation, the test procedures, and the test results are in Appendix B.

Considerable strain data were obtained during the test program, and the data supported the hypothesis that the presence and degree of thermal buckling of panels in acoustic environments may greatly affect the stress history, oil canning (if any), and the acoustic fatigue life of the panels.

The following trends were noted in the rms strains that were obtained in the thermal-acoustic panel tests. (The strains were obtained as a function of steady-state temperature while maintaining the sound pressure level.) As the steady-state temperature of the panels was raised from room temperature, the measured rms strains increased with increasing steady-state temperature prior to the detection of oil canning. As the steady-state temperature was further increased, the rms strains peaked out in the temperature range in which oil canning was detected. When the steady-state temperature was above the temperature range for which oil canning occurred, the measured rms strains had decreased substantially from the peak rms strains detected during oil canning. The rationale for the substantial decline in rms strain at temperatures above the oil canning temperature range is that the amplitude of thermal buckling had become so great that a dynamically stable curved configuration had been achieved and prevented further oil canning. Large thermal buckling had thus stiffened the panel and, in effect, caused a reduction in the dynamic response of the panel. (For details of the relation of temperature, strain, and oil canning of panel A-3-1, see subsection III.8.)

The relationship of rms strain to steady-state temperature that has just been described is shown in Figure 3. From this rms strain-temperature relation, one may estimate the relation between the panel acoustic fatigue life and the temperature (Figure 4). As the temperature is increased during the pre-oil-canning temperature range, the acoustic fatigue life is expected to decrease, principally because of the increasing rms strains. At temperatures for which oil canning is significant, the acoustic fatigue life is expected to decrease substantially because of the large stress reversals during the intermittent snapping through the original position. Above the oil canning temperature range, initially the acoustic fatigue life is expected to increase substantially because of the substantial decrease in rms strain. However if the steady-state temperature is significantly raised in the post oil canning range, then the material strength degradation may become the controlling factor and may cause a reduction in panel acoustic fatigue life. In the

TABLE V. TARGET THERMAL-ACOUSTIC TEST TEMPERATURES AND SPL'S

Test Condition A-1, A-2		Test Condition A-3		Test Condition A-4		Test Condition A-5	
SPL (db)	Temperature (F)	SPL (db)	Temperature F	SPL (db)	Temperature (F)	SPL (db)	Temperature (F)
Ambient	70	Ambient	70	Ambient	70	Ambient	70
↕	100	↕	100	↕	200	↕	300
	150		200		400		600
	200	Ambient	300	Ambient	600	Ambient	1000
	250	139	70	139	70	139	70
Ambient	300	↕	100	↕	200	↕	300
139	70		200		400		600
↕	100	139	300	139	600	139	1000
	200	160	70	160	70	160	70
139	300	↕	100	↕	200	↕	300
160	70		200		400		600
↕	100	160	300	160	600	160	1000
	200						
160	300						

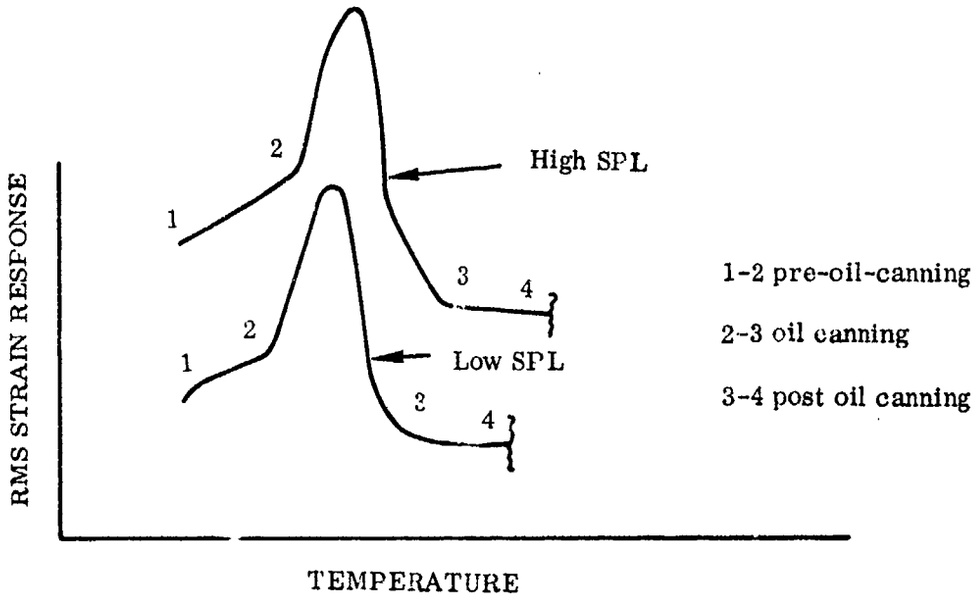

FIGURE 3. EFFECT OF TEMPERATURE AND SPL ON DYNAMIC STRAIN RESPONSE

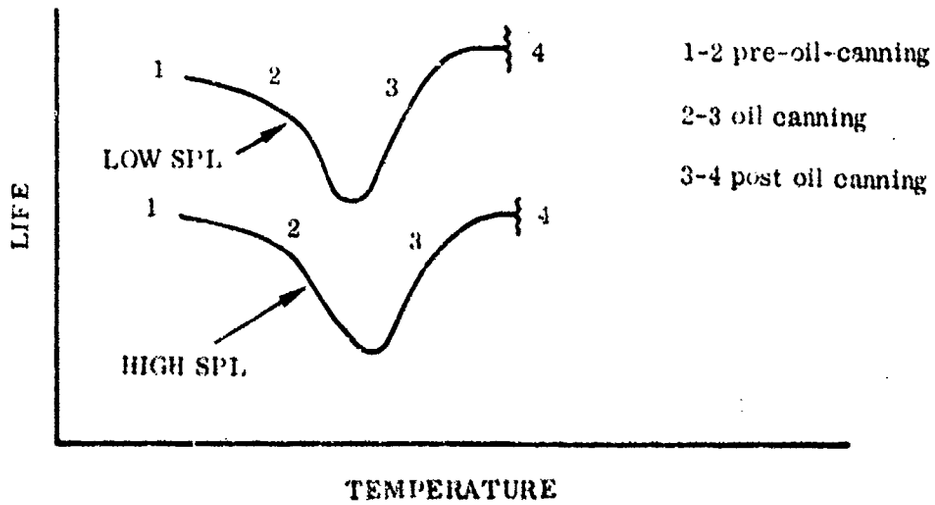

FIGURE 4. PREDICTED EFFECT OF TEMPERATURE AND SPL ON ACOUSTIC FATIGUE LIFE

thermal-acoustic test program, panels were not tested to an acoustic fatigue failure to verify the predictions of acoustic fatigue life that are shown in Figure 4.

III.5 TEST FACILITY

A schematic of the thermal-acoustic test facility is shown in Figure 5. A general view of the acoustic test facility is shown in Figure 6. The specimen module (in Figure 6) was rotated 90 degrees and lowered from its position during elevated temperature tests to show the heating module lamp-bank assembly. The assembly contains 32 3000 watt quartz lamps (at rated voltage) for tests to 600F and 45 of these lamps for tests to 1000F and is protected to some degree from the high acoustic environment by a 3/8 inch thick fused silica window. The assembly requires cooling air and water and exhaust ducting to minimize the temperature within the heating module. The quartz lamp assemblies are driven by a 376 kw ignitron power controller manufactured by Research Inc.

The heating module and specimen module were attached to a stainless steel frame and duct to form a progressive wave test section 8 inches wide by 24 inches high. This section was terminated in a test cell by a flared horn and absorptive material to minimize reflections of the acoustic energy.

The specimen module was designed to provide thermal isolation between the specimen and its mounting edges as well as isolation of the module from the radiant heat source. The specimen was clamped between layers of sheet transite and asbestos 5/16 inch thick. Additionally the front face of the module was covered with sheet asbestos and stainless steel to minimize conductive heat loss. To minimize radiation heat loss from the back side of the specimen, gold plated stainless steel reflectors were installed on the back cover of the module.

III.6 ANALYSIS – LINEAR THEORY

The analytical effort to determine the thermal effects on dynamic stress response was divided into two tasks. In the first task, linear dynamic response theory was used. In the second task, nonlinear dynamic response theory was used.

The attempt to use linear dynamic response theory was aborted when it became apparent that nonlinear theory offered the most potential for obtaining general results that would be the most useful to designers. However, the linear analytical work produced useful results, which are reviewed below.

Sample computer runs were made with the STARDYNE-DYNRE3 computer program to obtain analytical predictions (based on linear theory) of the natural frequencies, stress, and deflection of unstiffened and stiffened plates subjected to white noise acoustic excitation. The results from STARDYNE-DYNRE3 were compared with the analytical results obtained with the REDYN computer program that were reported in Reference 13. Close agreement was obtained between the results from STARDYNE-DYNRE3 and REDYN. The close agreement produces confidence in the results that may be obtained from either of those two computer programs when linear theory is applicable. The STARDYNE computer program is available only at Control Data Corporation Cybernet centers, whereas REDYN is a Northrop proprietary computer program.

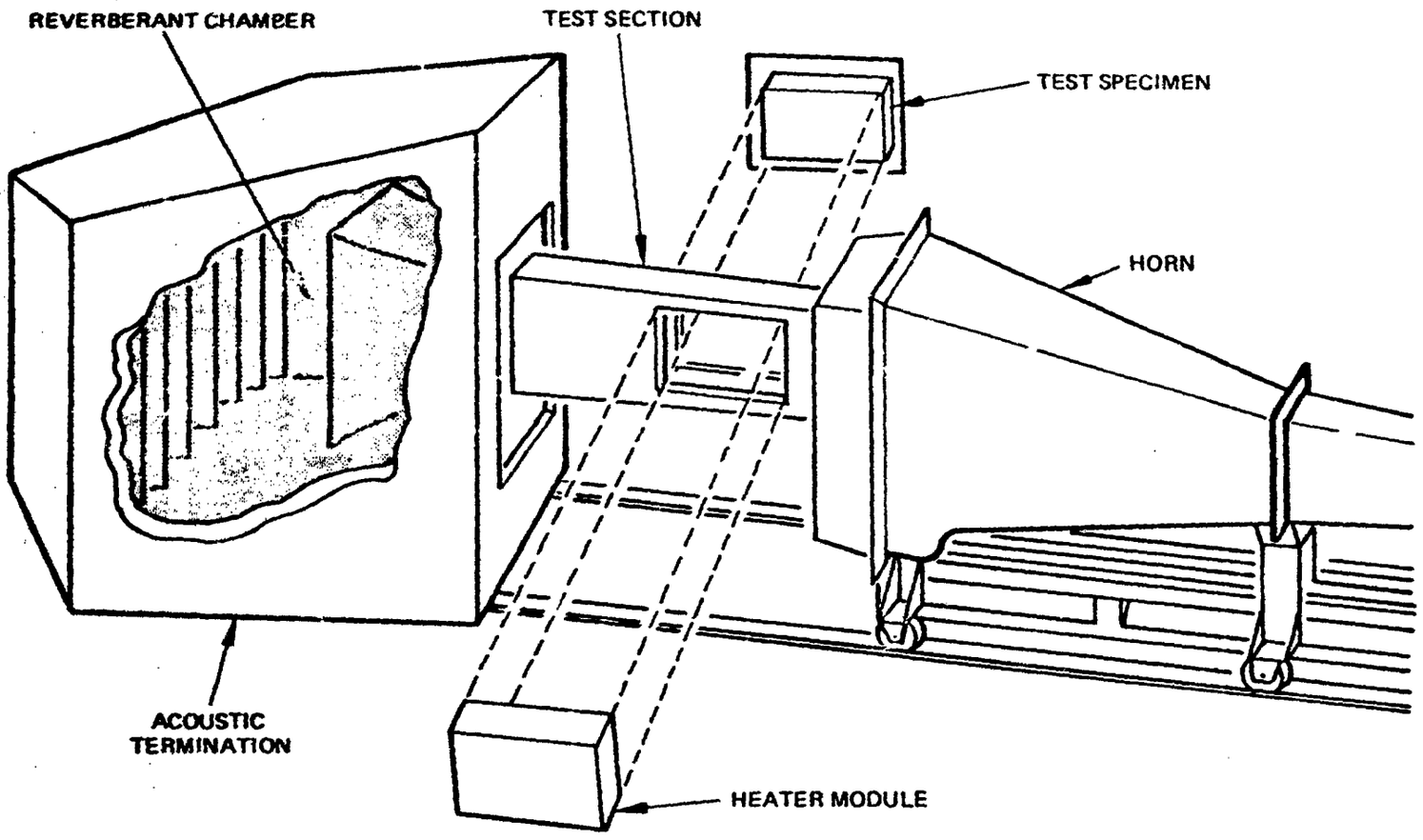

FIGURE 5. SCHEMATIC OF THERMAL-ACOUSTIC TEST FACILITY

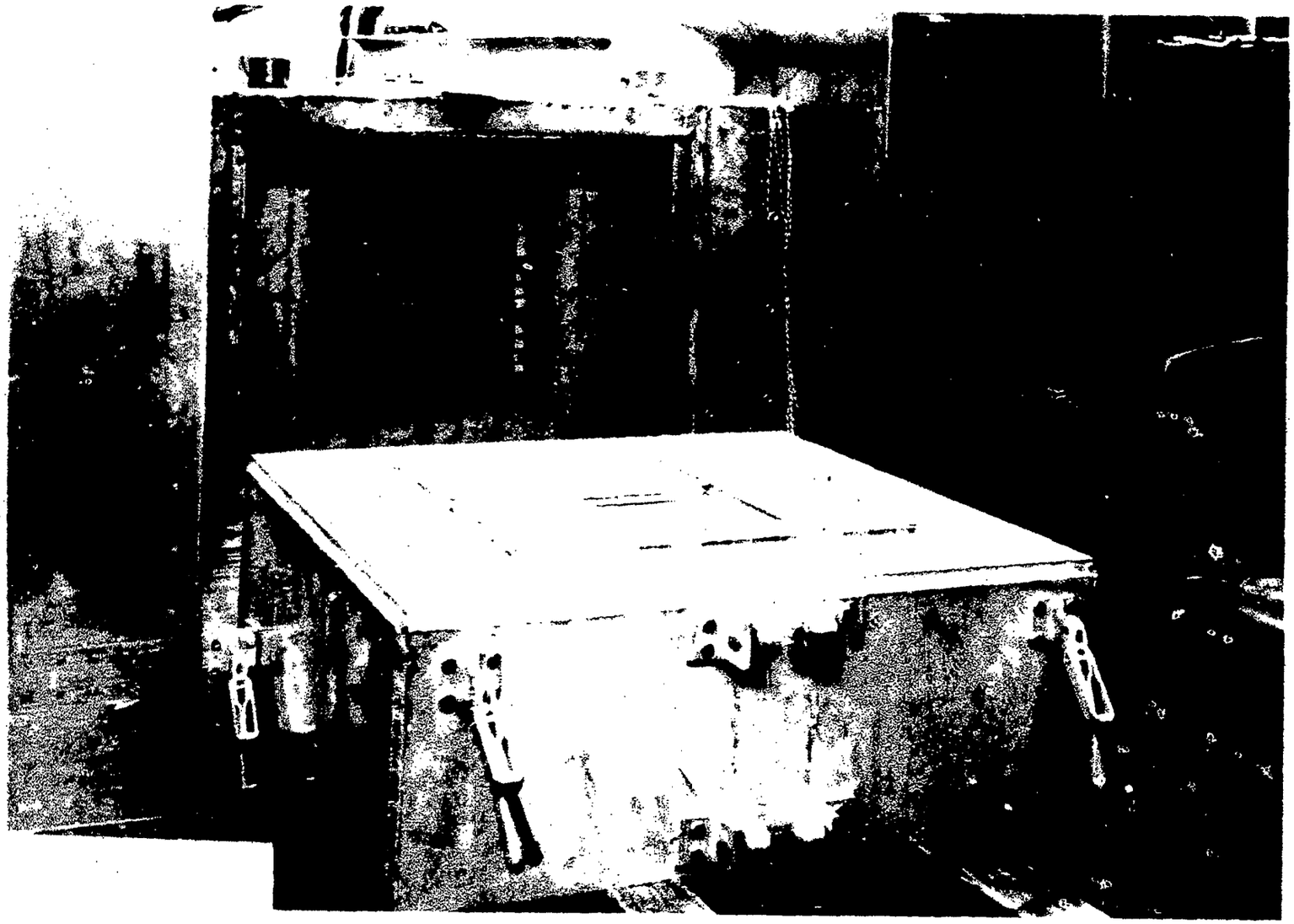

FIGURE 6. THERMAL-ACOUSTIC TEST FACILITY

III.7 PREDICTING OIL CANNING OF PANELS IN THERMAL-ACOUSTIC ENVIRONMENTS

A semi-analytical (or alternately, semi-empirical) method of predicting oil canning was developed and is reported on in this subsection. A completely rigorous theoretical investigation was not undertaken because of the analytical complexities and the uncertainty associated with the reliability and applicability of the results from such an investigation. In fact, very little theoretical work has been published on the effect of temperature on the dynamic characteristics of plates since Shulman's work in 1958 (Reference 20).

III.7.(a) Assumptions

The analytical study of oil canning was based on an investigation of (1) the nonlinear dynamic response of uniformly thin, isotropic, homogenous plates that are simply supported on all four edges and are subjected to random acoustic excitation and (2) the deflection at the center of the aforementioned simply supported plate because of thermal buckling.

The rationale for extending the results of the aforementioned dynamic analysis of simply supported plates to the dynamic analysis of multi-bay, thin-skinned panels is that in many situations, the predominant mode and response of multi-bay panels to acoustic excitation is characterized by adjacent bays being out-of-phase and separated by stiffeners that have little translational motion. Therefore, the individual bays can be expected to behave in many respects as though they are simply supported on all four edges. Consequently, insofar as the predictions of oil canning of a thin-skinned multi-bay panel is concerned, each bay is considered to be a simply supported plate with the same geometry as the nominal dimensions of the bay.

The accuracy of the predictions of oil canning that will be obtained with this method depend on several factors, such as the geometry of the stiffeners, and the degree of the geometrical likeness of adjacent bays. It is believed that the prediction of oil canning will be considerably more accurate than the intermediate predictions. (Predictions of resonant frequencies and deflections are intermediate steps in the process of predicting oil canning).

The prediction of oil canning is part of a three step process and is based on the assumptions that (1) the response of the fundamental mode of the plate predominates (as was demonstrated with linear analysis for many situations in Reference 21) and (2) the plate is not allowed to expand as its temperature is increased. The analysis for predicting the unimodal dynamic response (Reference 22) at ambient temperature is based on nonlinear differential equations that account for the interaction of membrane and bending strains. A sample problem is worked out at the end of this subsection to demonstrate the method of predicting the rms deflection ($\bar{w}$) at the plate center, the fundamental frequency (f) which depends on that deflection, the amplitude (A_o) of the thermal buckle, and the presence (or absence) of oil canning.

III.7.(b) Development of Equations

The appropriate equations for obtaining $\bar{w}$ and f are given below and can be solved iteratively with slide rule calculations.

$$f = \frac{1}{2\pi}\left(\frac{K}{M}\right)^{\frac{1}{2}} \tag{1}$$

and

$$\bar{w} = \frac{4}{\pi^2}\,\frac{\Gamma}{K}\left(\frac{\pi f S}{4\zeta}\right)^{\frac{1}{2}} \tag{2}$$

where

$$K = \left[\, D\pi^4\left(\frac{1}{a^2}+\frac{1}{b^2}\right)^2 + \frac{Eh\pi^4}{4}\left(\frac{1}{a^4}+\frac{1}{b^4}\right)\bar{w}^2\,\right] \tag{3}$$

and

$$M = \rho h \tag{4}$$

The symbols are defined on page xi. The calculation of $\bar{w}$ is the first step of the three-step process for predicting oil canning.

In the second step of the three step process, hand calculations based on geometrical considerations are performed to determine A_o, the deflection amplitude of the thermally buckled plate. The plate is assumed to be at a uniform temperature T and to have a buckled configuration given by

$$w = A_o \sin\frac{\pi x}{a} \sin\frac{\pi y}{b} \tag{5}$$

The amplitude is assumed small relative to the plate width and is calculated from shallow strip theory as

$$A_o \approx 0.707b\,(\alpha\Delta T)^{\frac{1}{2}} \tag{6}$$

with α being the thermal coefficient of expansion and ΔT being the temperature rise from ambient temperature to the plate temperature, T.

In the third step of the three-step process, the ratios $\frac{A_o}{\bar{w}}$ and $\frac{\bar{w}}{h}$ are computed. Test data that have been obtained and reported in Figure 7, indicate that oil canning can be expected if

$$A < \frac{A_o}{\bar{w}} < B, \qquad \frac{\bar{w}}{h} > C$$

where

$A \approx 1.5$

$B \approx 6.0$

$C \approx 0.3$

III.7.(c) Comparison of Predictions of Oil Canning with Experimental Data

Predictions of $\frac{A_o}{\bar{w}}$ and $\frac{\bar{w}}{h}$ for the 3-bay panels tested in this program (Appendix B) at 139 db and 160 db at temperatures for which inspections were taken are displayed in Figure 7. Whether or not oil canning was detected in the test (e.g., 160 db at 200F) is also displayed in Figure 7. The values of $A \approx 1.5$, $B \approx 6.0$, and $C \approx 0.3$ are consistent with the data displayed in Figure 7. More test data are needed to permit more confidence to be placed in the numerical values of A,B, and C.

Heuristically, a case can be developed for choosing A = 1.5., B = 6.0, and C = 0.3. For example, $A < 1.5$ implies that there is no stable curved configuration in the thermal-acoustic environment, because instantaneous dynamic deflections occur repeatedly whose amplitudes are greater than that corresponding to thermal buckling.

$B > 6.0$ implies that the dynamic deflection during the acoustic response will be less than the thermal buckle. Consequently, the peaks of the acoustic excitation and acoustic response will not cause the panel curvature to change from concave to convex or vice versa. In a sense, B is a measure of the instantaneous strain peak to the rms strain. The probability of B exceeding 6.0 is small for distributions such as the Rayleigh distribution which may be expected under conditions of unimodal, linear response to Gaussian excitation.

When $C < 0.3$, the dynamic deflection is usually less than the panel thickness. Oil canning was not detected in the tests corresponding to situations when $C < 0.3$ was predicted. Even if oil canning were to occur with $C < 0.3$, in most practical situations the stress may be low enough to prevent an acoustic fatigue failure from occurring.

III.7.(d) Proposed Criterion for Oil Canning

On the basis of the discussion under subsection III.7.(c) and until further test data or analyses are available, it is recommended that the criterion for oil canning be

$$1.5 \leq \frac{A_o}{\bar{w}} \leq 6, \quad \frac{\bar{w}}{h} \geq 0.3 \qquad (7)$$

III.7.(e) Sample Problem

The method of predicting the presence or absence of oil canning will be demonstrated with this sample problem. Consider an aluminum alloy plate that was heated from 80F to 100F and the edges were not permitted to translate. The plate is simply supported on all four edges, with the following geometrical and physical properties at 100F.

a = 16.0 inch (length)
b = 8.0 inch (width)
h = 0.04 inch (thickness)

γ = 0.10 lb/in^3 (weight density)
ζ = 0.03 (viscous damping factor)
α = 12.7 x 10^{-6} in/in/F (thermal coefficient of expansion)

Three-Bay Panels		
Material	SPL	
	139 db	160 db
2024-T81	△	▽
Ti-6Al-4V	▷	◁
Rene' 41	○	□

When a symbol is filled in, such as ▲ in contrast with △, oil canning was observed at that test condition.

The oil canning criterion is that oil canning will not occur above the upper solid line, below the lower solid line, and to the left of the vertical solid line of Figure 7.

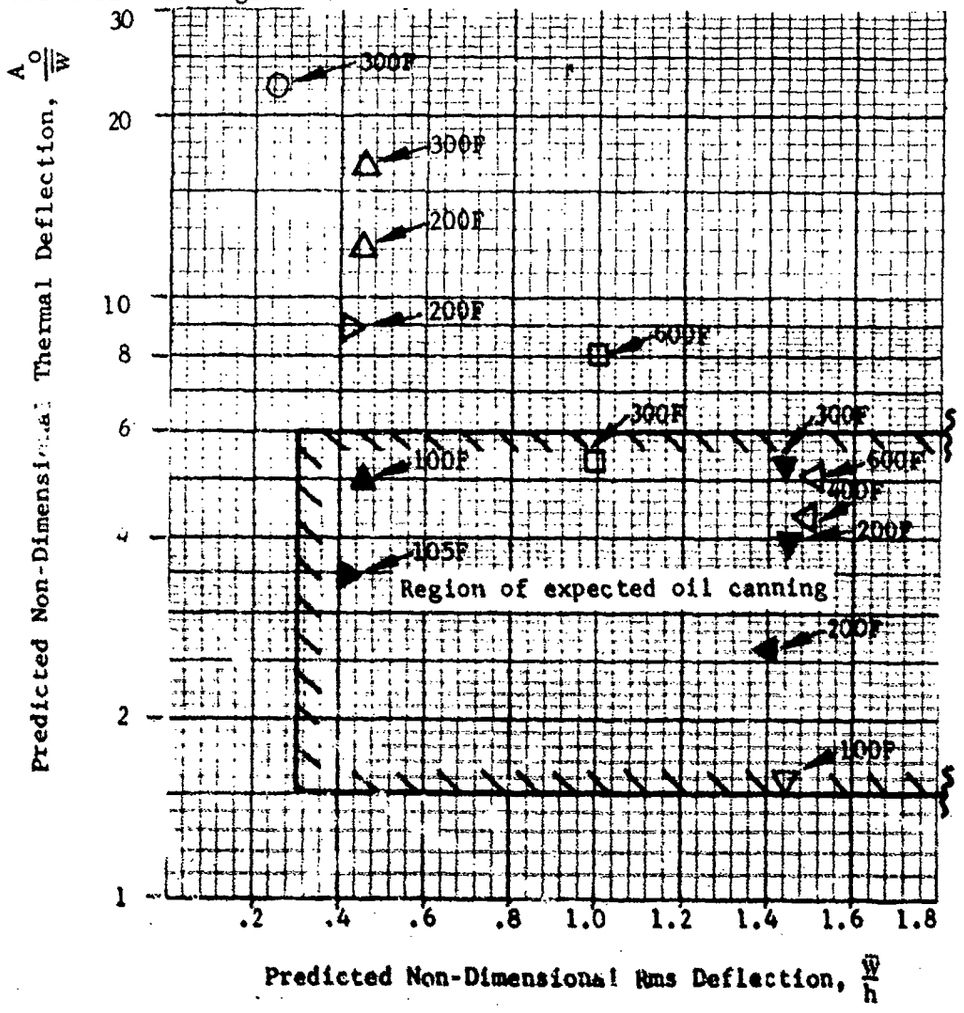

FIGURE 7. CORRELATION OF TEST DATA WITH THE PROPOSED CRITERION FOR OIL CANNING

$E = 10.5 \times 10^6$ psi (Young's modulus)
$\nu = 0.33$ (Poisson's ratio)

The PSD of the acoustic loading is taken as $S = 3.0 \times 10^{-6}$ psi ^{2}/Hz, which was the "average" PSD in the frequency range of the predominant response near ambient temperature in the 139 db SPL tests. The bending rigidity $D = Eh^3/[12(1-\nu^2)] = 62.84$ lb in.

In the calculations that follow, the subscripts to $\bar{w}$ and f indicate the iteration number in the calculations for $\bar{w}$ and f from Equations (1) and (2).

First Iteration

Assume $\bar{w}_1 = \frac{h}{2} = 0.020$ in-rms. ($\bar{w}_1$ is one-half the plate thickness)

From Equation (3), calculate $K_1 = 3.31$ lb/in^3.

From Equation (4), calculate $M = 10.36 \times 10^{-6}$ lb sec^2/in^3. (M is constant throughout the iterative process).

From Equation (1), calculate $f_1 = 90$ Hz.

From Equation (2), calculate $\bar{w}_1 = .017$ in-rms.

The calculated $\bar{w}_1$ is lower than the assumed $\bar{w}_1$.

Second Iteration

Since the assumed $\bar{w}_1$ was too high, assume $\bar{w}_2 = 0.018$ in-rms

From Equation (3) calculate $K_2 = 3.12$ lb/in^3.

From Equation (1), calculate $f_2 = 87.4$ Hz.

From Equation (2), calculate $\bar{w}_2 = .018$ in-rms.

Therefore, the calculated $\bar{w}_2$ equals the assumed $\bar{w}_2$ and no more iterations are required.

With a temperature rise of $\Delta T = 20$F from the ambient temperature to the test temperature, $A_o = 0.089$ inch from Equation (6).

Prediction of Oil Canning

In order to apply the criterion listed in Equations 7, the following items are calculated

$$\frac{A_o}{\bar{w}} = \frac{89}{18} = 4.9$$

and

$$\frac{\bar{w}}{h} = \frac{18}{40} = 0.45$$

An examination of $\frac{A_o}{\bar{w}}$ and $\frac{\bar{w}}{h}$ in view of the criterion for oil canning from Equation (7) results in the prediction that oil canning will occur at 100F and 139 db for the test panels A-3-1 and A-3-2. Those panels did oil can, as predicted, at 100F and 139 db.

III.7.(f) Other Calculations for Figure 7

Numerical values that were used in the calculations for Figure 7 are given in this subsection.

In all the calculations, the following geometrical properties were used:

a = 16.0 inch
b = 8.0 inch
h = 0.04 inch

For all the calculations, the PSD of the acoustic pressure was 3.0×10^{-4} psi^2/Hz at 139 db and 2.0×10^{-4} psi^2/Hz at 160 db; and the viscous damping factor was 0.03 for the 2024-T81 plates and 0.015 for the Ti-6Al-4V and Rene' 41 plates. The difference in viscous damping factors reflected differences in clamping rather than inherent differences among the different alloyed test specimens themselves.

The lb/in^3 densities were 0.10 for the 2024-T81 plates, 0.16 for the Ti-6Al-4V plates, and 0.30 for the Rene' 41 plates. Ambient temperature was 80F for all calculations except 85F for the Ti-6Al-4V specimens.

The values of Young's modulus and the coefficient of thermal expansion are in Table VI.

TABLE VI. PHYSICAL PROPERTIES

Material	Temperature	Young's Modulus	Coefficient of thermal expansion
	(F)	(psi)	(in/in/F)
2024-T81	100	10.5×10^6	12.7×10^{-6}
2024-T81	200	10.3×10^6	12.9×10^{-6}
2024-T81	300	10.0×10^6	13.1×10^{-6}
Ti-6Al-4V	105	15.8×10^6	5.3×10^{-6}
Ti-6Al-4V	205	15.4×10^6	5.8×10^{-6}
Ti-6Al-4V	400	14.0×10^6	5.8×10^{-6}
Ti-6Al-4V	600	13.0×10^6	5.8×10^{-6}
Rene' 41	300	30.0×10^6	6.8×10^{-6}
Rene' 41	600	28.6×10^6	7.0×10^{-6}

III.8 EFFECT OF OIL CANNING ON STRAIN FOR PANEL A-3-1

A detailed examination of the effect of temperature on the strain history and the strain spectral density at the panel center was performed during the thermal-acoustic test of panel A-3-1 under broad band excitation at sound pressure levels of 139 db and 160 db and at 79F (i.e., room temperature), 100F, 200F, and 300F.

The strain spectral densities at the panel center at room temperature, 100F, 200F, and 300F are in Figures 8 for the 139 db run and are in Figures 9 for the 160 db run. The spectral density of the broad band acoustic pressure at ambient temperature is in Figure 10 for the 139 db and 160 db runs.

During the 139 db run, oil canning was detected only at the 100F observation of strains. The oil canning was detected by (1) monitoring the strain signal on an oscilloscope and observing that the strain fluctuated successively about each of two distinct (average) strains, (2) noting the significantly higher percentage of strain spectral density below 50 Hz during the 100F run, and (3) noting the sharp decrease in rms strain as the temperature was increased above 100F. (The measured rms strains at various panel locations had in general increased as the panel temperature was raised from room temperature to 100F.)

As the temperature was increased from 100F to 300F during the 139 db run, the increasing thermal stresses produced a sufficiently curved (and hence stiffened) structure to eliminate the oil canning at 139 db. Additional evidence of the significant thermal bending at 200F and 300F was the significant increase (as a function of temperature) in the measured average tensile and average compressive strains at various panel locations.

During the 160 db run, oil canning was detected only during strain observations at 200F and 300F. The increasing amount of strain with low frequency content as the temperature increases is evident in Figure 9. In particular, at 300F which was the temperature at which the oil canning was the most severe, the response in a bandwidth of a few Hz centered at approximately 10 Hz was the bandwidth of the predominate response (Figure 9).

In summary, the major difference in the response characteristics of panel A-3-1 at 139 db and at 160 db, was that at 139 db the panel assumed a stable, stiffened configuration between 100F and 200F and further increases of temperature resulted in the disappearance of oil canning and a reduction of rms dynamic strains from their peak level during oil canning. However, at 160 db, once oil canning was observed during the 200F run, further increases in temperature did not produce a stable curved configuration which would have been deduced by a reduction of rms strains from their peak level in the 200F run. In fact, the rms dynamic strains and the average tensile and compressive strains at various panel locations were in general much higher with oil canning at 300F than with oil canning at 200F.

Strain Gage No. 11, Panel A-3-1
3.2 Hz Analyzer Bandwidth

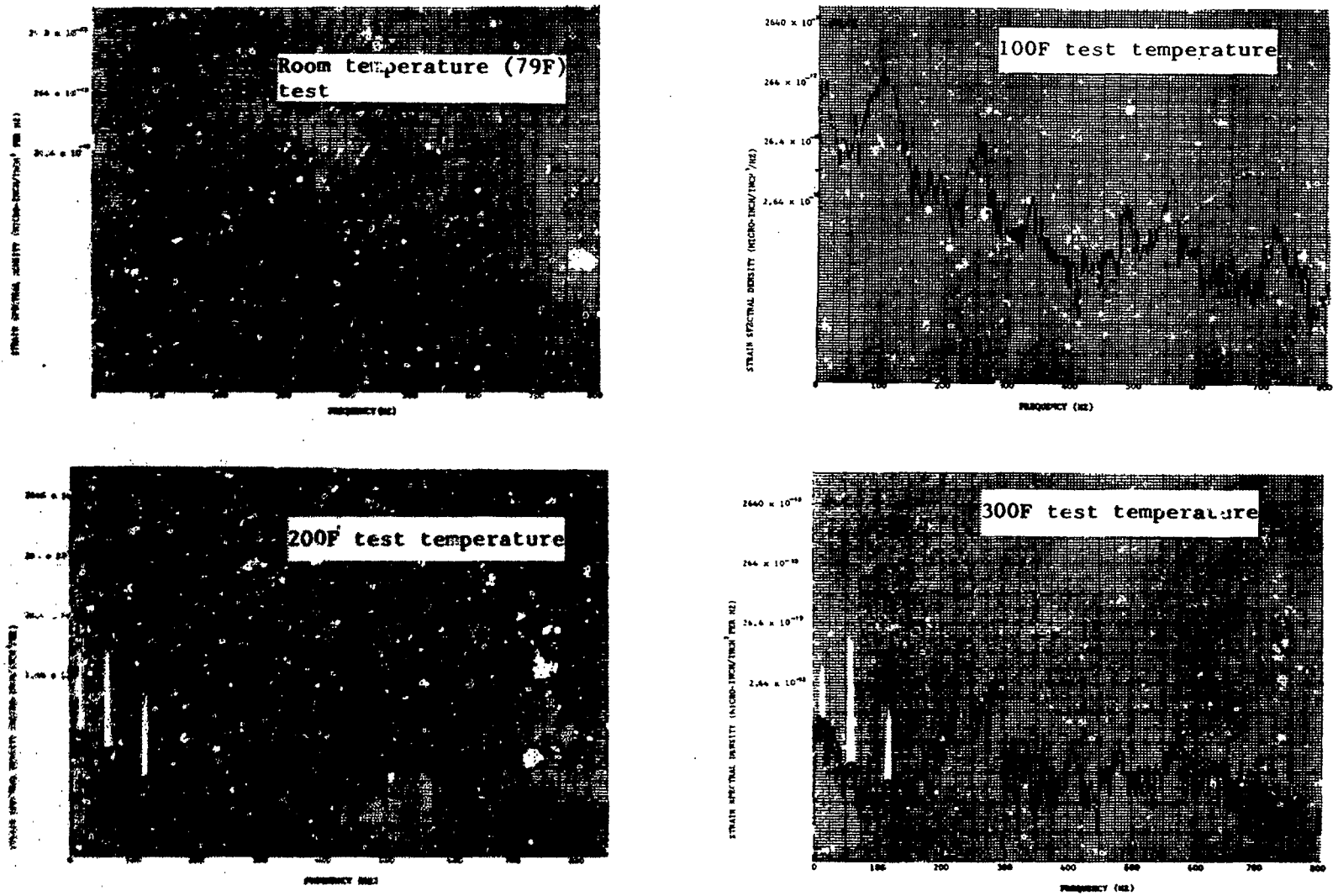

Figure 8. Strain Spectral Density of Panel A-3-1 at 139 DB SPL

Strain Gage No. 11, Panel A-3-1
3.2 Hz Analyzer Bandwidth

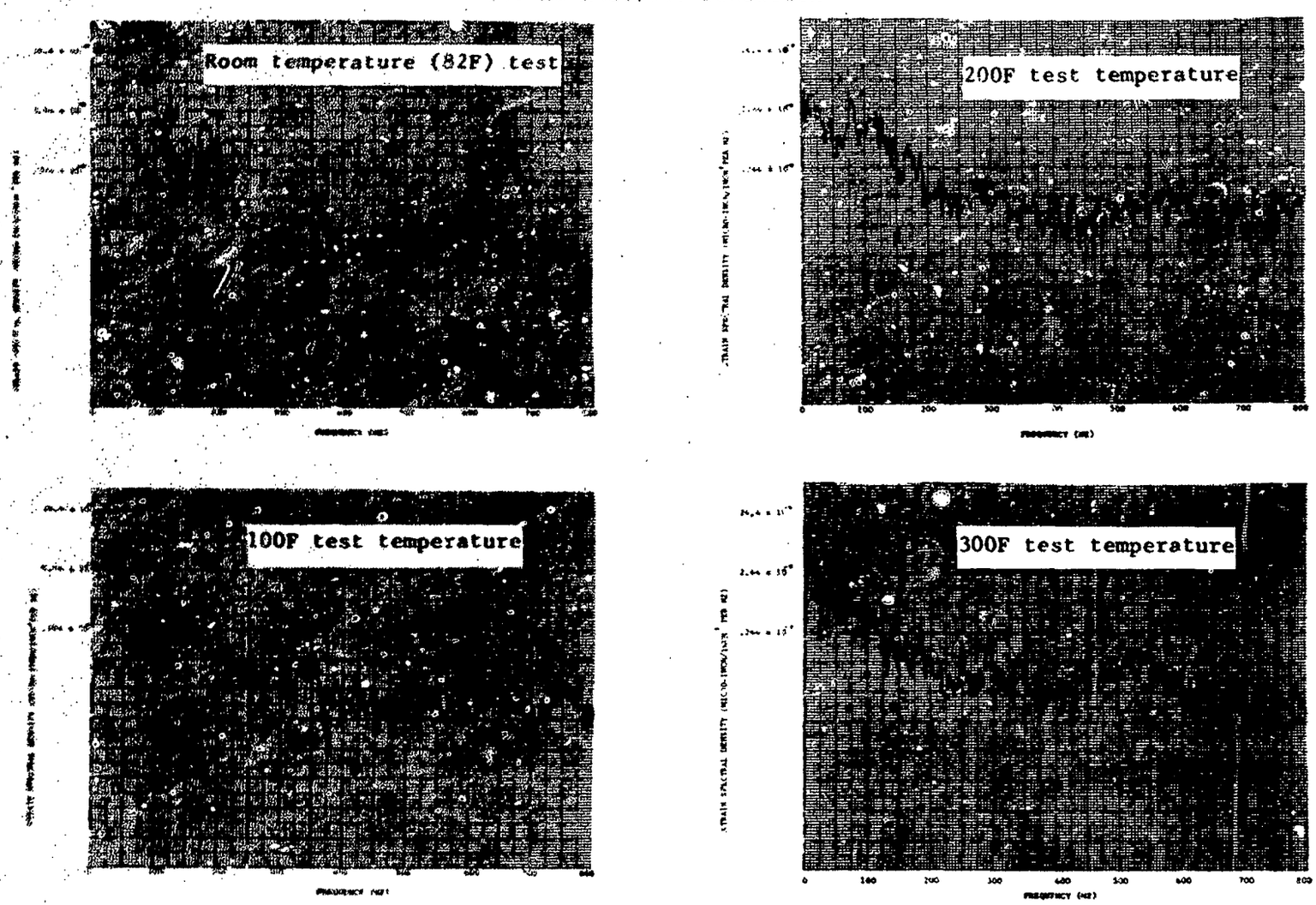

Figure 9. Strain Spectral Density of Panel A-3-1 at 160 DB SPL

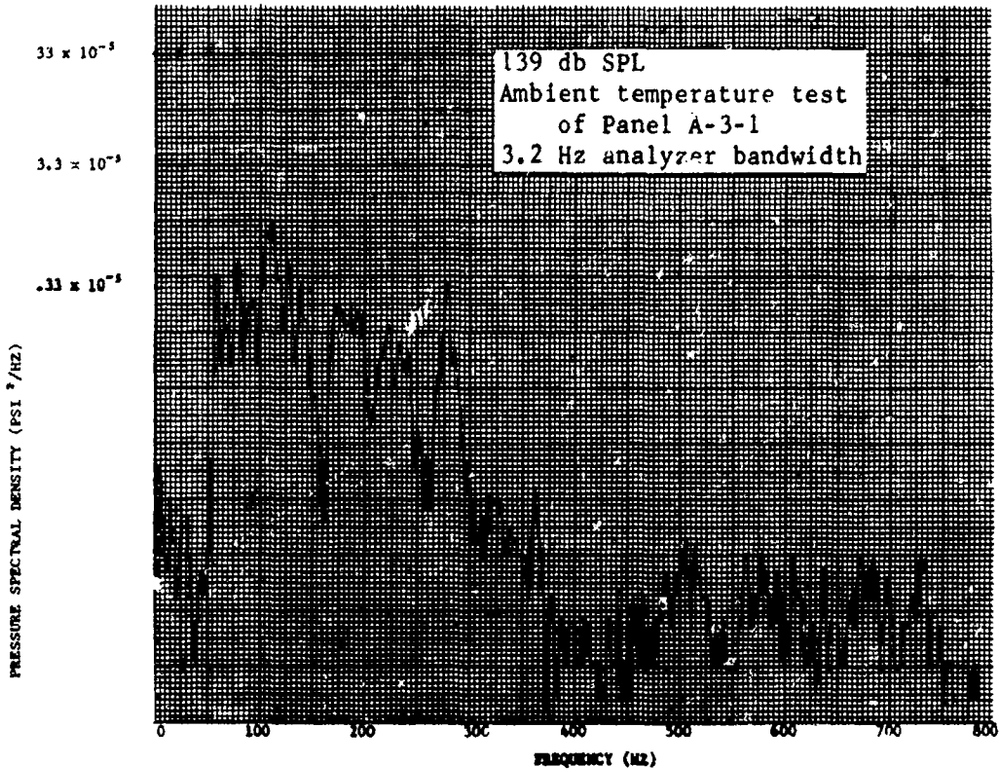

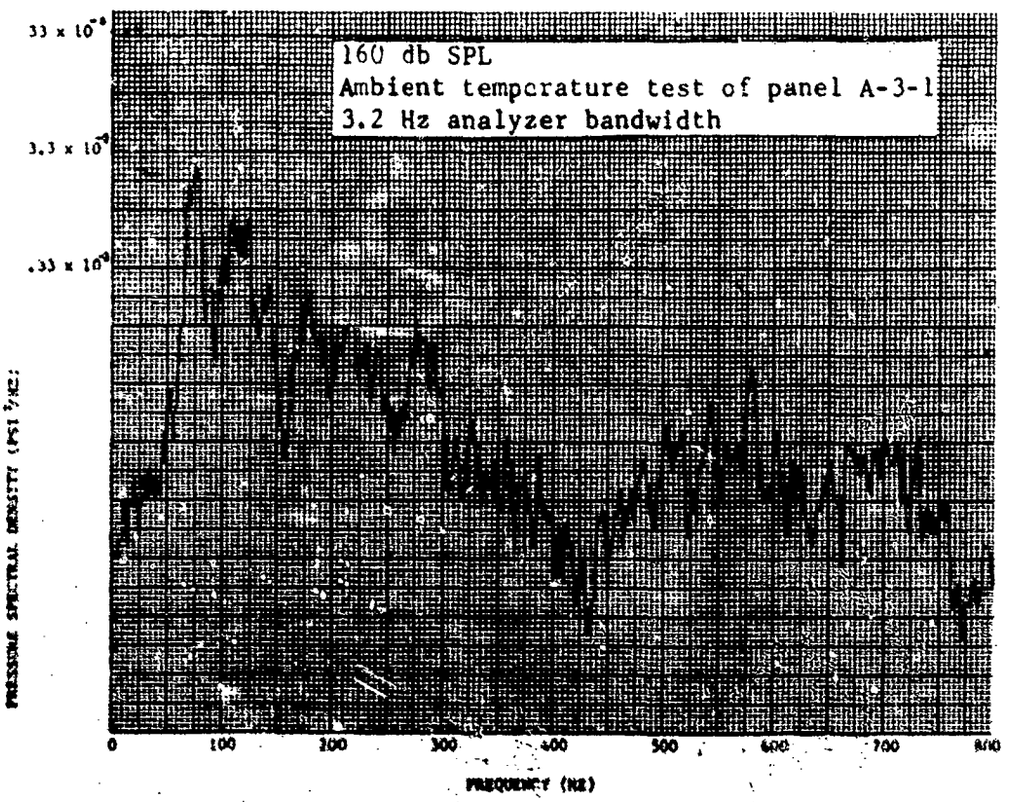

Figure 10. Representative Acoustic Pressures During Room Temperature Tests of Panel A-3-1

IV. THERMAL EFFECTS ON FATIGUE

IV.1 OBJECTIVES

The primary objectives of the thermal-shaker test program were to determine the effects of thermal cycling superimposed on acoustic loading, the effects of alternate applications of thermal stressing and acoustic loading, and the effects of the simultaneous application succeeded by an alternate application of the acoustic and thermal loading. Another objective of the thermal-shaker test program was to obtain fatigue data that were influenced by effects of heating. (In implementing the plan to obtain the objectives, the acoustic loading was simulated by shaker excitation).

IV.2 TEST FACILITY AND TEST SETUP

The thermal-acoustic test facility (Figure 5) was the test facility used in the thermal-shaker test program. A schematic of the test installation for shaker excitation is shown in Figure 11; a photograph of the shaker test set-up is shown in Figure 12; a front view of a shaker test specimen that was installed for tests is shown in Figure 13; and a view of the specimen, specimen clamps, and shaker rod prior to the assembly for testing is shown in Figure 14. In Figures 15 and 16 are shown a front and back view of a sample fatigue specimen that had been used in establishing the final test configuration and boundary conditions for the shaker test program.

There were some preliminary shaker-fatigue tests to finalize the specimen design. In the preliminary tests, the axial restraint was sought with a friction clamp (without the dowel pins near the ends of the specimens). However, the friction was not sufficient to prevent the specimen from slipping in the edge clamps at elevated temperatures and high levels of shaker excitation. In turn, the slipping prevented the oil canning which was being investigated in the fatigue tests. Therefore, it was necessary to install the dowel pins to attach the specimens to the test fixture to achieve the test objectives. Figures 15 and 16 are photographs of the last sample specimen that was tested to finalize the configuration and boundary conditions for the shaker tests.

IV.3 TEST CONDITIONS AND SPECIMEN DESCRIPTION

The specimens are identified by three hyphenated alpha-numeric characters. The first two characters denoted the test condition and the third character denoted the specimen number for that test condition. For example, specimen S-8-1 was the first specimen tested in the S-8 test condition. A brief description of the test conditions is in Table VII.

For the thermal-shaker tests, one configuration (Figure 17) and three materials (Table VIII) were used. The material was the 2024-T81 aluminum alloy in all the test conditions except S-5 and S-6. The configuration was a 10.00 by 2.00 by 0.063 or 0.040 inch beam specimen with an angle clip riveted at the center of the specimen to simulate a stiffener of a multi-bay panel expected to see service in a thermal-acoustic environment. There were three specimens for each test condition. The specimen length was chosen to permit the use of the fixturing that was used in portions of the thermal-acoustic test program.

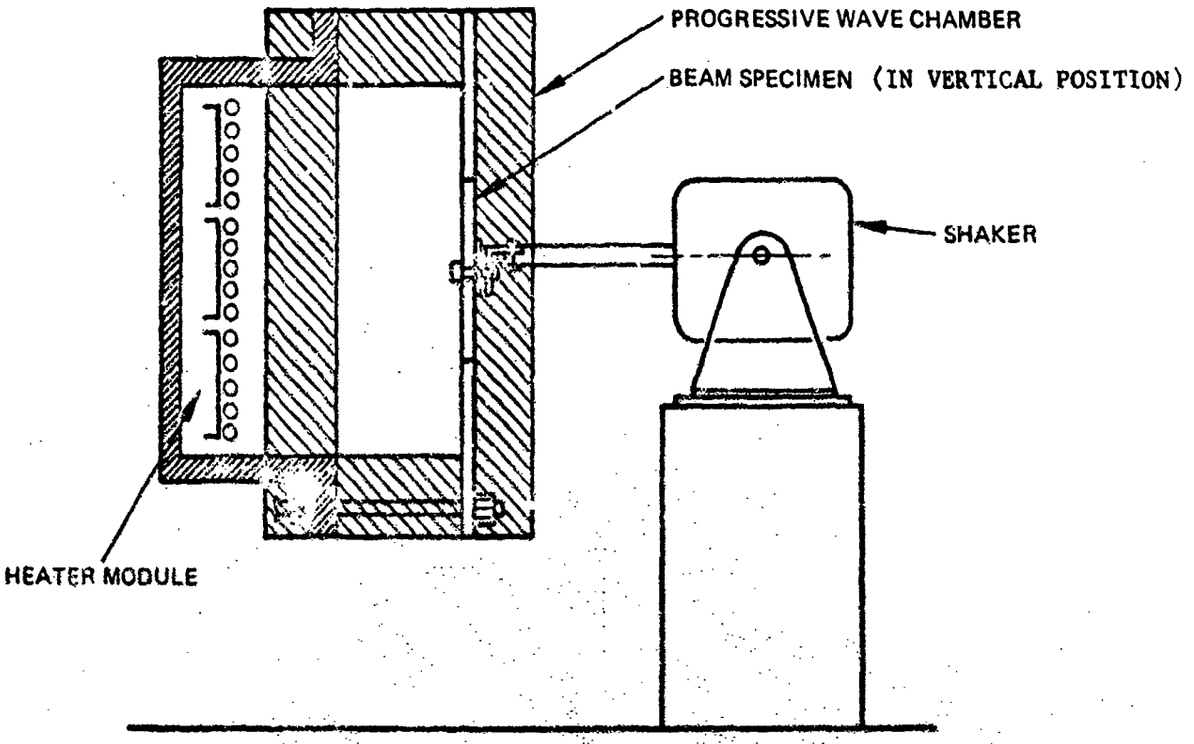

FIGURE 11 SHAKER INSTALLATION FOR ELEVATED TEMPERATURE TESTING.

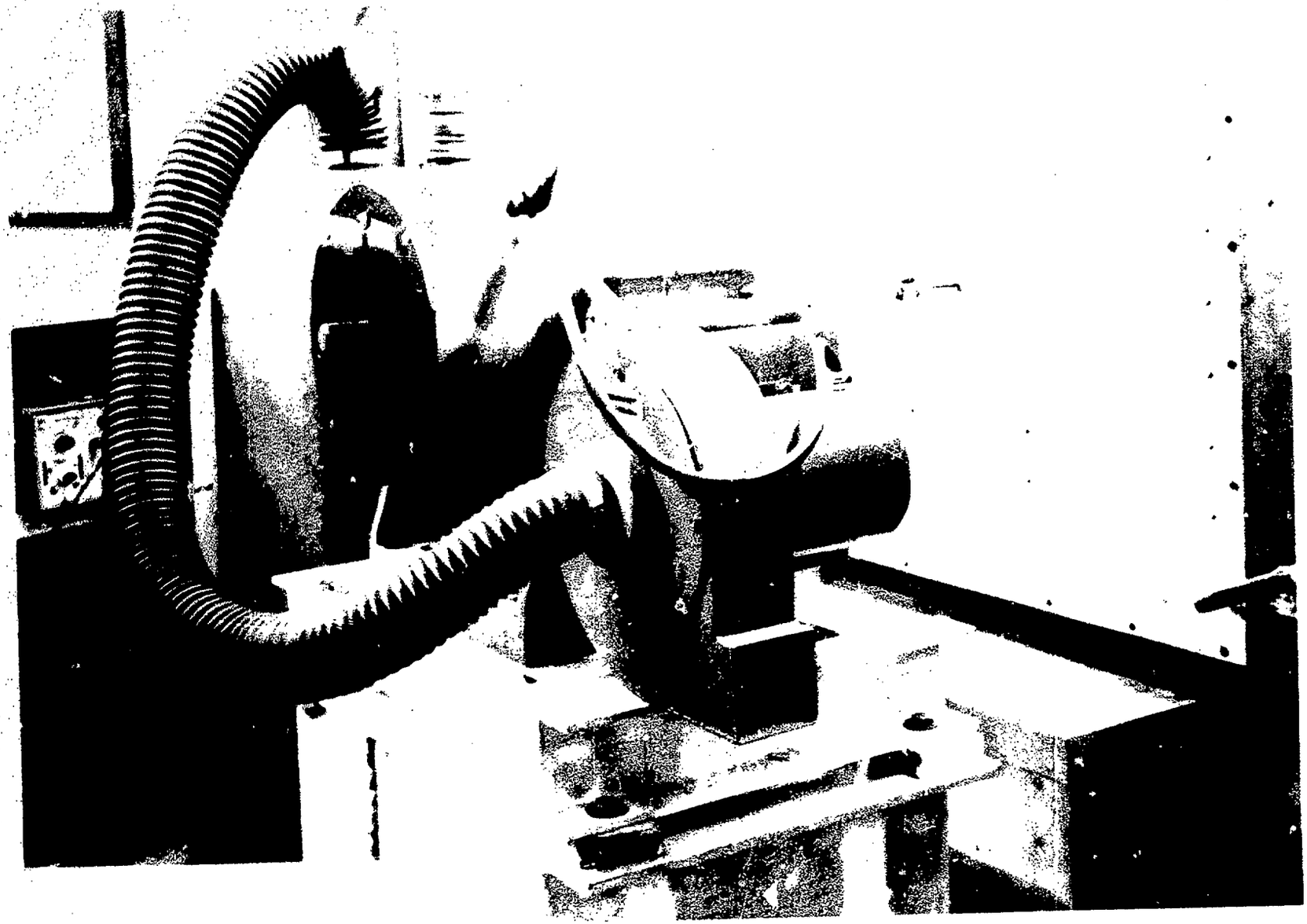

FIGURE 12. SHAKER TEST SETUP

FIGURE 13. FRONT VIEW OF SHAKER TEST SPECIMEN

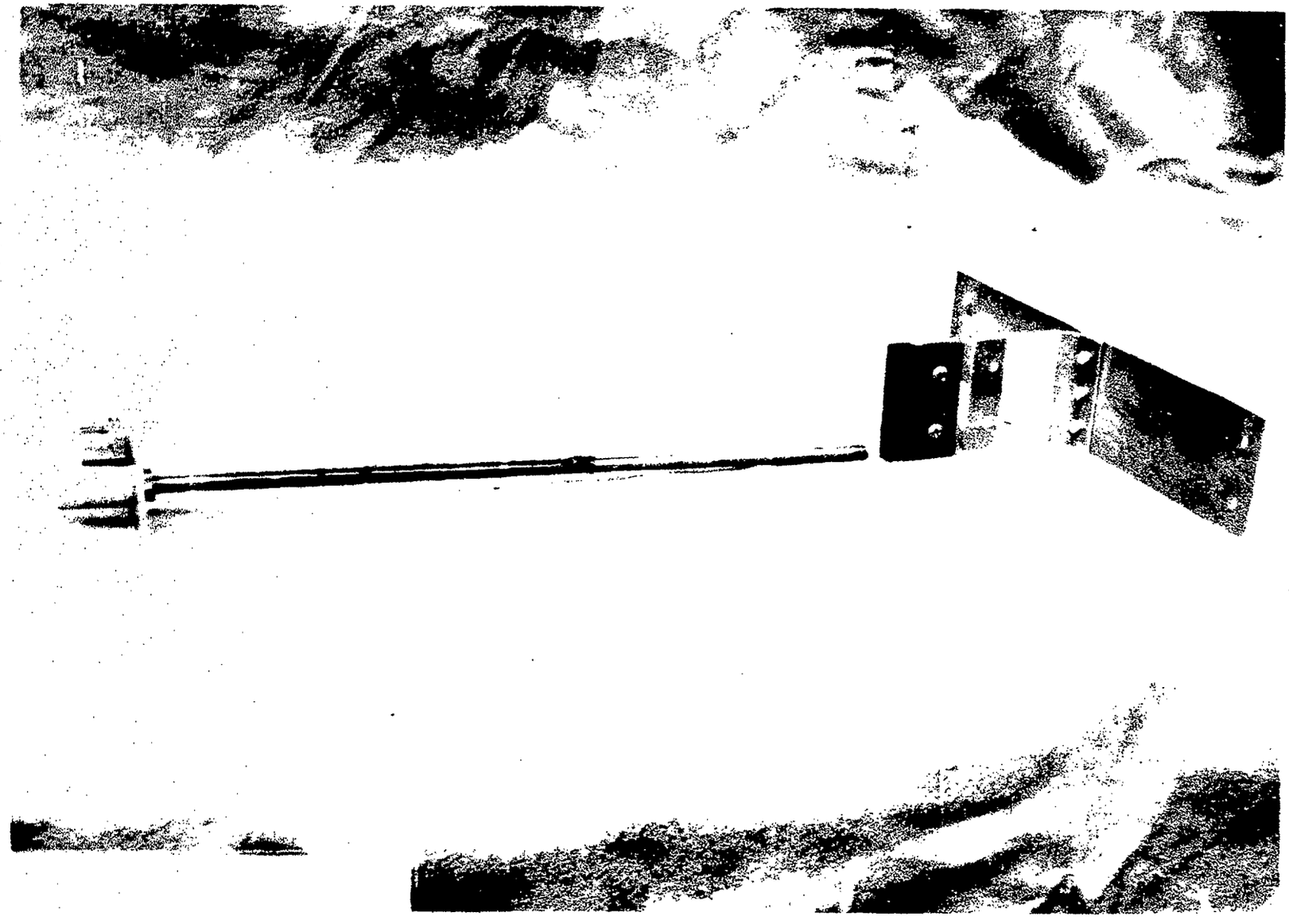

FIGURE 14. SHAKER SPECIMEN, CLAMP, AND ROD BEFORE ASSEMBLY

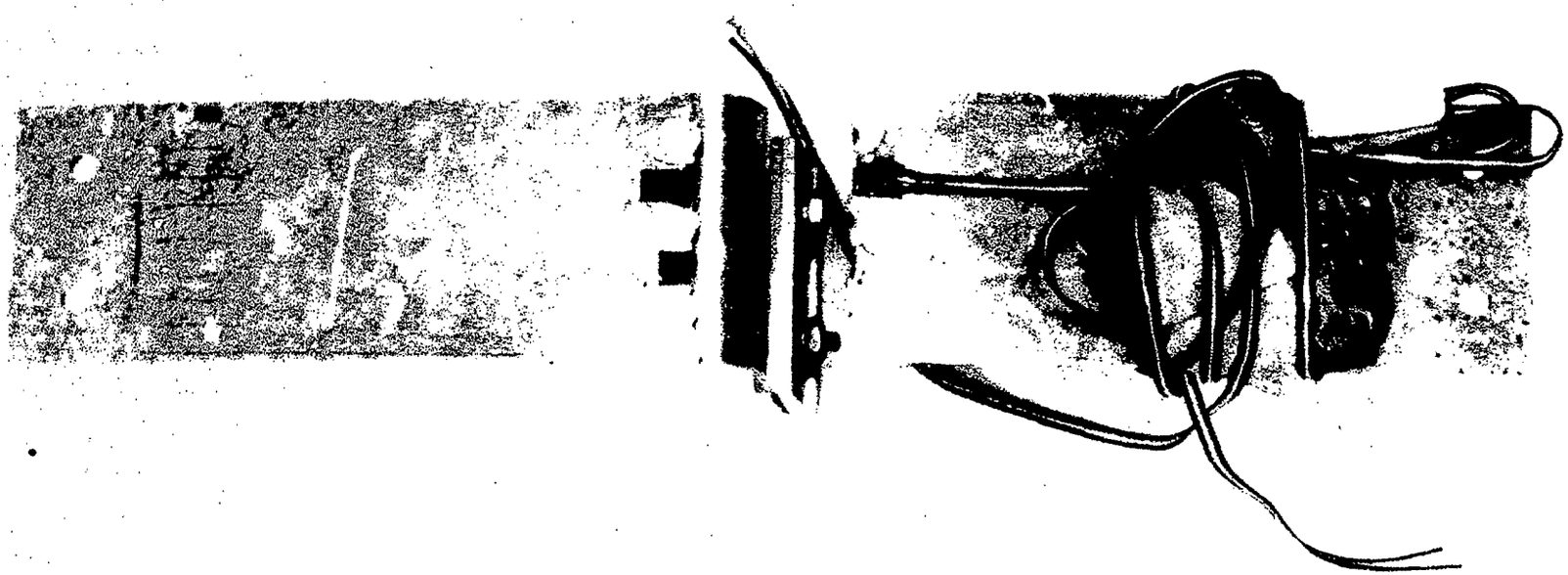

FIGURE 15. FRONT SURFACE OF SAMPLE SHAKER TEST SPECIMEN AFTER FATIGUE FAILURE

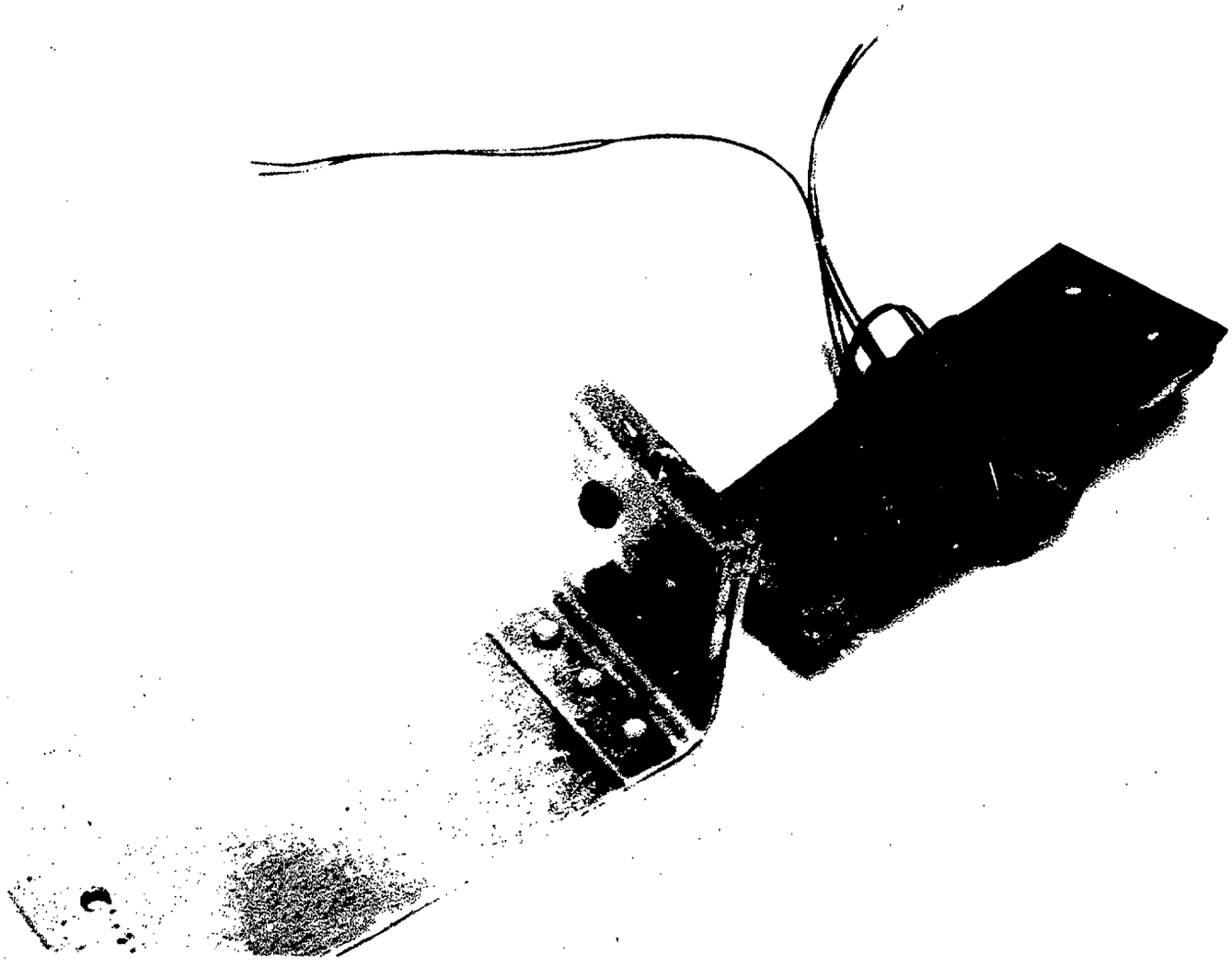

FIGURE 16. BACK SURFACE OF SAMPLE SHAKER TEST SPECIMEN AFTER FATIGUE FAILURE

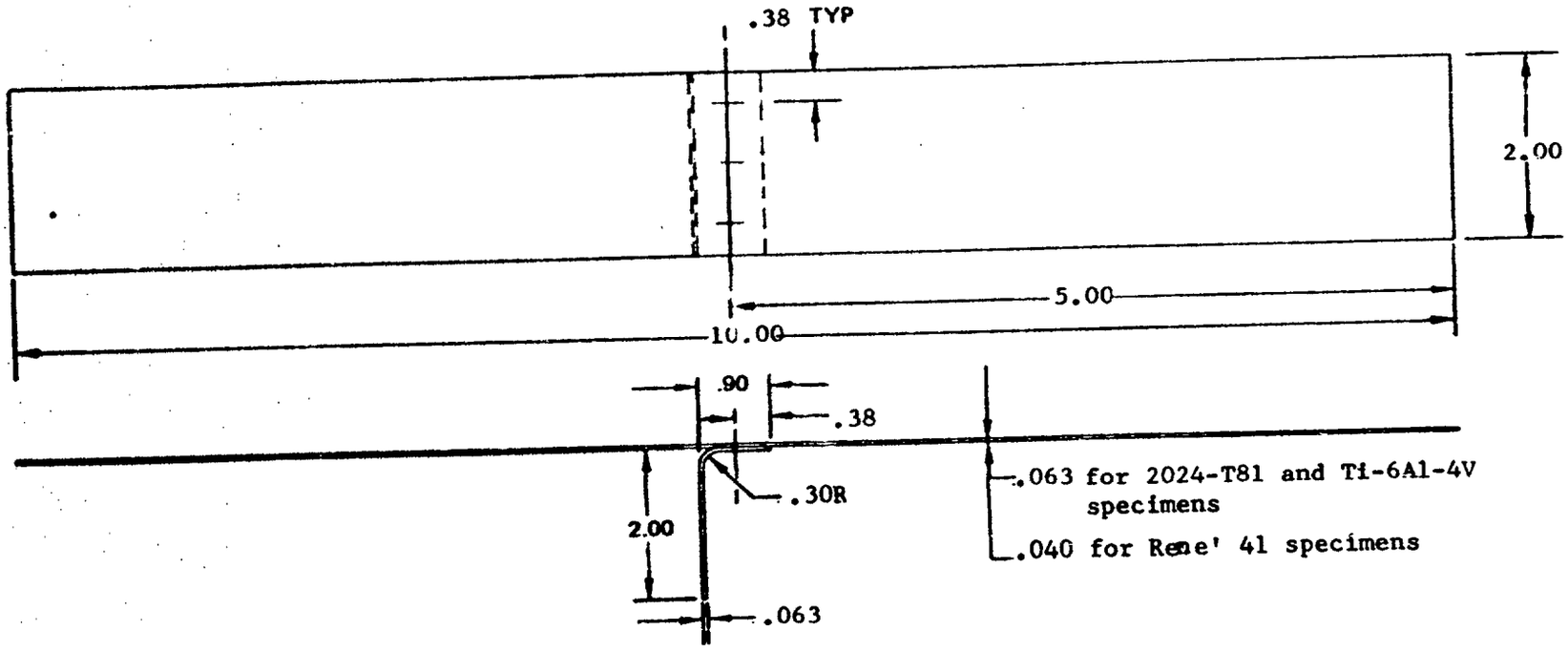

BEAM SPECIMENS		
SKIN	ANGLE	See Table IV for Rivets
2024-T81	2024-T81	
Ti-6AL-4V	Ti-6AL-4V	
RENE 41	RENE 41	

FIGURE 17 THERMAL-SHAKER TEST BEAM

TABLE VII TYPES OF SHAKER TESTS

TEST (1) CONDITION	MATERIAL	INVESTIGATION	TARGET MAX. TEMPERATURE	CONSTRAINT	IN PLANE THERMAL STRESS
S-1	2024-T81	Effect of random (shaker) loading at room temperature	Room	No	No
S-2	2024-T81	Effects of cyclic thermal stress in cases of random (shaker) loading	300F	Yes	Yes
S-3	2024-T81	Effects of alternate application of random (shaker) loading and cyclic thermal stress	300F	Yes	Yes
S-4	2024-T81	Effect of alternately applying test conditions S-2 and S-3	300F	Yes	Yes
S-5	Ti-6Al-4V	Same as S-7 except at 600F	600F	Yes	Yes
S-6	Rene' 41	Same as S-7 except at 1000F	1000F	Yes	Yes
S-7	2024-T81	Effect of random (shaker) loading and thermal stress at steady state temperature of 300F	300F	Yes	Yes
S-8	2024-T81	Effect of random (shaker) loading without thermal stress at steady state temperature of 300F	300F	No	No
S-9	2024-T81	Effect of axial constraint on life at ambient temperature with the same rms strain response as in Test Cond. S-1	Room	Yes	No
S-10	2024-T81	Effect of axial constraint on life at ambient temperature with the same rms target strain as in Test Conditions S-2, S-4, and S-7	Room	Yes	No

(1) Three specimens were tested at each test condition

TABLE VIII THERMAL-SHAKER TEST SPECIMENS

Quantity	Material	Overall Specimen Dimensions (inch)	Unsupported Specimen Dimensions (inch)
15	2024-T81	10.00 x 2.00 x .063	8.4 x 2.00 x .063
3	Ti-6Al-4V	10.00 x 2.00 x .063	8.4 x 2.00 x .063
3	Rene' 41	10.00 x 2.00 x .040	8.4 x 2.00 x .040

The maximum test temperatures were 300F for the 2024-T81 aluminum alloy, 600F for the Ti-6Al-4V titanium alloy, and 1000F for the Rene' 41 nickel base alloy.

There were a sufficient number of 2024-T81 aluminum alloy shaker specimens to obtain data under all of the sequential type loadings planned in the thermal-shaker test program. The effect of material on the fatigue characteristics were obtained by using Ti-6Al-4V and Rene' 41 test specimens for one type loading condition. Thus, Test Conditions S-5, S-6, and S-7 represented the same type of tests (i.e., steady-state, narrow-band random rms strain response at a constant elevated temperature and with axial restraint) but for three different materials.

Test Condition S-1 was to obtain base line random fatigue data in the absence of both thermal effects and axial restraint at ambient temperature, whereas Test Condition S-8 was to obtain the same type fatigue data but at 300F.

Test Conditions S-9 (at the rms strain response level of Test Condition S-1) and S-10 (at the rms strain response level of Test Condition S-2) were to determine the effect of axial restraints on the random fatigue data obtained at ambient temperature.

Test Condition S-2 was to determine the effect of thermal cycling superimposed on the steady rms strain response with the axial restraint of Test Condition S-10.

Test Condition S-3 (with axial restraint) was to determine the effect of alternately applying steady state shaker excitation and the thermal cycling.

Test Conditions S-4 (with axial restraint) was a combination of the Test Conditions S-2 and S-3.

A sample thermal cycle is in Figure 18. A sample cycle of Test Condition S-4 is in Figure 19. In Figure 19, time periods 1 and 2 correspond to a cycle in Test Condition S-2, whereas time periods 3 and 4 correspond to a cycle in Test Conditions S-3.

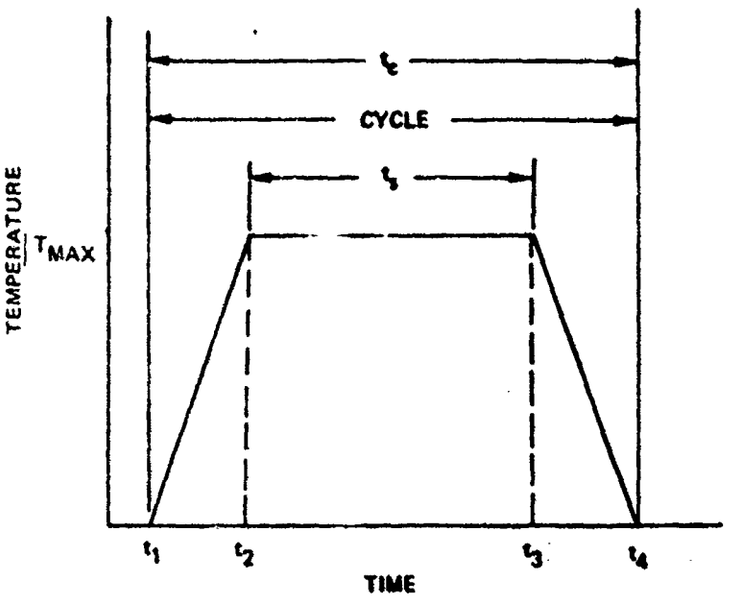

FIGURE 18 - SAMPLE THERMAL CYCLE

(1) Combines shaker excitation with heating from ambient temperature to 300F and temperature dwell at 300F.

(2) Cooldown to ambient temperature with no shaker excitation.

(3) Shaker excitation at ambient temperature.

(4) A complete thermal cycle (without shaker excitation) beginning at ambient temperature.

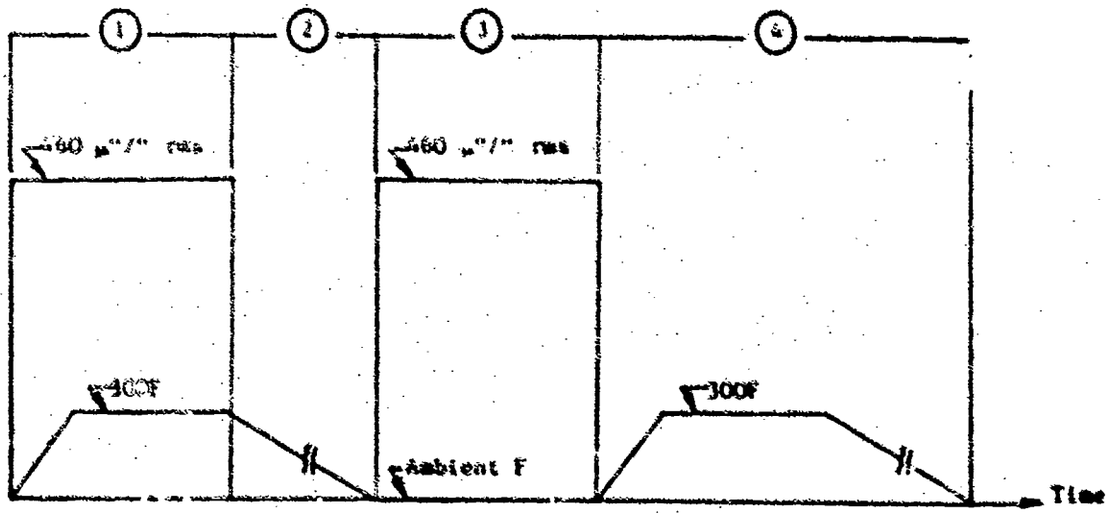

FIGURE 19 ONE COMPLETE CYCLE IN THE S-4 TEST CONDITION

IV.4 INSTRUMENTATION, TEST SETUP, AND TEST PROCEDURE

Strain gages and thermocouples were installed on the fatigue test specimens to obtain strain and temperature data at the line of rivets. The thermal-shaker instrumentation (and test) procedures had many items that were similar to the corresponding procedures of the thermal-acoustic test program and those items are not repeated in this review. The principal difference in the instrumentation and test procedures of the two test programs was because the acoustic excitation was replaced by shaker excitation.

Each test beam was coupled to a small vibration exciter with a short rod to help isolate the shaker from the thermal environment. An accelerometer mounted between the shaker and the push rod provided the control signal to an amplitude servomonitor to maintain the shaker excitation level throughout a test. Each test specimen was oriented for tests such that the length direction of the specimen was horizontal. In all the shaker tests, there was one-third octave narrow band excitation centered at 31.5 Hz.

Axial restraint of specimens, when required, was obtained by inserting two dowel pins through each end of the specimen and edge clamp and then clamping the specimen tightly in the test fixture.

IV.5 SHAKER TEST RESULTS

IV.5.(a) Life as a Function of Loading Conditions

The principal objective of the shaker tests was to determine the effects of different sequences and combinations of heating and shaker excitation. The detailed data that were obtained are in Appendix C. Much of the detailed data are summarized in Table IX and are discussed below.

In the S-2 test condition, the target rms strain at 300F was 460 micro-inch/inch. This level (460 micro-inch/inch) of strain represented the threshold at which oil canning was detected. In the S-4 test condition (see Figure 19) the rms strain at 300F and at ambient temperature was also 460 micro-inch/inch. An examination (Tables IX and C-1) of the cumulative dwell time (i. e., the life) at 300F in test conditions S-2 and S-4 indicates that the time to failure of the S-4 series of specimens was not significantly affected by the heating cycle without shaker excitation and by the shaker excitation at ambient temperature.

There was a fear that in Test Condition S-3, the time to failure would have been prohibitive if the target rms strain was 460 micro-inch/inch in the (ambient temperature) shaker excitation phase of a cycle. Consequently, in the S-3 test condition, the target rms strain was set at 766 micro-inch/inch as was the case in test conditions S-1 and S-9. (Recall that the test specimens had axial restraint in the S-3 and S-9 test conditions). Upon comparing the results

obtained in the S-3, S-9, and S-1 test conditions, it is concluded that failures occurred somewhat sooner in the S-3 test condition than in the S-9 test condition because in the portion of the S-3 test condition at ambient temperature there were residual in-plane stresses from the thermal cycle.

Fatigue failures occurred much sooner in the S-3 and S-9 test conditions than in the S-1 test condition. The earlier fatigue failures are attributed to higher peak stresses that were induced during the shaker excitation of the dowel pinned S-3 and S-9 test specimens, which stored more strain energy than the unpinned S-1 test specimens.

The average time to failure at 300F in the S-2 and the S-7 test conditions were about the same, which indicates that the thermal cycles in the S-2 test condition did not significantly affect the fatigue life.

Upon examining the S-4 and S-10 test results it is concluded that if the target strain at ambient temperature is to be 460 micro-inch/inch in the S-3 test condition, in some future test program the dwell time with the shaker excitation at ambient temperature should be 20 or 30 minutes to prevent many costly waiting periods for the specimen to cool to room temperature after the heating to 300F.

TABLE IX. FATIGUE LIFE DATA

TEST CONDITION	MAXIMUM TEMPERATURE	AXIAL CONSTRAINT	TARGET STRAIN	LIFE(1)	OIL CANNING
	(F)		(μ"/" - rms)	(Min)	
S-1	R.T.	No	766	170; 210; 202	No
S-9	R.T.	Yes	766	9; 6; 11	No
S-10	R.T.	Yes	460	62; 200, 253	No
S-2	300	Yes	460	18; 17; 18	Yes
S-3	300	Yes	766	4; 6; 9	No
S-4	300	Yes	460	26; 20; 16	Yes
S-7	300	Yes	460	14; 9; 25	Yes
S-8	300	No	820	130; 140; 138	No
S-5	600	Yes	460	117; 231; 133	Yes
S-6	1000	Yes	---	58	Yes

(1) The life of each of the three specimens for each test condition is recorded, except for the S-6 test condition, for which only one specimen life is recorded.

IV.5.(b) Effect of Oil Canning on Life

In Table C-1 are the average strains that were detected prior to and following the snap through the original flat positions of the test specimens that were experiencing oil canning during the shaker tests. The strain reversals during snap through were large and apparently were the principal factor that led to fatigue failures of the specimens.

In Table X are the data that support the hypothesis that the fatigue failures of the oil canning specimens were controlled by the stress reversals that occurred during the oil canning. The method of obtaining the entries in Table X are described below.

Fifty percent of the algebraic difference of the average strains of Table C-1 is shown as the single amplitude of the strain reversals in Table X. Fifty percent of the algebraic sum of the average strains is shown as the mean strain in Table X. The mean strains are absolute values and may represent either tensile or compressive strains. The strains were converted to stress (Table X) by multiplying by Young's modulus with values of 10.5×10^6 psi for 2024-T81 at ambient temperature; of 10.0×10^6 psi for 2024-T81 at 300F; of 14.9×10^6 psi for Ti-6Al-4V at 600F; and 25.7×10^6 psi for Rene' 41 at 1000F. The time to an observed failure is also given in Table X. Time to failure was converted to approximate cycles to failure by noting that snap-throughs were occurring at approximately 5 cycles per minute (i. e., 10 snap-throughs per minute).

The stress ratios in Table X were defined as the single amplitude stress divided by ultimate tensile strength. The stress ratio was computed to obtain a nondimensional comparison of the fatigue behavior of the three different materials used in the test program.

The values of ultimate tensile strength that were chosen for these calculations were 71.0 ksi for 2024-T81 at ambient temperature; 56.5 ksi for 2024-T81 at 300F; 103 ksi for Ti-6Al-4V at 600F; and 186 ksi for Rene' 41 at 1000F. Except for the Rene' 41 alloy, these ultimate strengths were obtained from the coupon test program. Because the Rene' 41 coupon tests at 1000F were with improperly aged material, an ultimate tensile strength was calculated for the Rene' 41 alloy. In Reference 23, it is recommended that the ultimate strength at 1000F of Rene' 41 be calculated as 90 percent of the ultimate strength at room temperature. That recommendation was followed and resulted in a calculated ultimate tensile strength of 186 ksi for the Rene' 41 alloy.

The average strains and mean strain of specimen S-6-2 were not recorded in Table X, because of uncertainty associated with the accuracy of those data.

The strains and stresses in Tables C-1 and X are indicative of the stress and strain in the specimens. However, it is to be noted that the strain gages in the tests of the Ti-6Al-4V and the Rene' 41 shaker specimens failed early in the fatigue tests. Therefore, the strain data for the Ti-6Al-4V and Rene' 41 specimens must be viewed with more caution than the strain data obtained in the 2024-T81 specimen tests. The strain gages in the 2024-T81 shaker specimen tests often survived approximately eighty to ninety percent of the fatigue test duration.

TABLE X. S-N DATA FOR OIL CANNING FATIGUE SPECIMENS

Specimen	Temperature	Single Amplitudes		Means (1)		Ultimate Tensile Strength	Life	Cycles to Failure	Stress(2) Ratio
		Strain	Stress	Strain	Stress				
	(F)	(μ"/")	(ksi)	(μ"/")	(ksi)	(ksi	(min)		Percent
S-2-1	300	2690	27	1280	13	56	13	~100	48
S-2-2	300	3700	37	2420	24	56	16	~100	65
S-2-3	300	3450	35	1660	17	56	16	~100	62
S-7-1	300	2560	26	1320	14	56	14	~100	46
S-7-2	300	3320	33	1790	19	56	9	~100	58
S-7-3	300	3320	33	1790	19	56	25	~100	58
S-5-1	600	2650	38	0	0	103	117	~1000	37
S-5-2	600	2050	31	250	4	103	231	~6000	30
S-5-3	600	2050	31	1150	17	103	133	~1000	29
S-6-2(3)	1000	2620	67	-	-	186	58	~100	36

(1) These mean strains are absolute values and may be either tensile or compressive.

(2) $\text{Stress Ratio} = \frac{\text{Single Amplitude Stress}}{\text{Ultimate Tensile Strength}}$

(3) Specimens S-6-1 and S-6-3 are not included in this Table because the material was not aged at 1400F for 16 hours. The mean strains of specimen S-6-2 are not reported because the accuracy in those data was much less than the accuracy of the mean strains in this table.

The S-N data in Table X were not expected to deviate significantly from S-N data in References 23 and 24, that were obtained in constant amplitude tests, because the random vibrations in this shaker-test program were considered to be of secondary importance relative to the stress reversals taking place during snap-throughs. A comparison of the test data in Table X with the test data in References 23 and 24 supports the hypothesis that the steady-state, random vibratory stresses were of secondary importance relative to the stress reversals occurring during snap-through.

IV.5.(c) Effect of Axial Constraint on Life of Non Oil Canning Specimens

In Table XI are tabulated the random S-N fatigue data that were obtained in the absence of oil canning. It is concluded from an examination of fatigue lives for Test Conditions S-1, S-8, and S-9 in Table XI that the axial restraint (in Test Condition S-9) had a much greater effect than the temperature rise to 300F (the test temperature in the S-8 test condition) on the fatigue life of specimens tested at 8.1 and 8.2 ksi-rms.

IV.5.(d) Spectral Densities of Acceleration Input and Specimen Response

A representative spectral density of acceleration input to a shaker test specimen is shown in Figure 20. Typical responses of strain spectral density are shown in Figures 21 and 22.

Figure 21 was obtained during the shaker excitation of specimen S-4-1 at ambient temperature whereas Figure 22 was obtained during the 300F test of specimen S-4-1. Figure 21 is a typical strain spectral analysis when snap through did not occur during an ambient temperature or an elevated temperature test condition. Figure 22 is a strain spectral analysis of an oil canning fatigue test specimen. In the spectral analyses shown in Figures 21 and 22, the analysis bandwidth was 0.32 Hz and the sample being analyzed was of 20 seconds duration.

TABLE XI. S-N DATA FOR FATIGUE SPECIMENS THAT DID NOT OIL CAN.

Specimen	Temperature	Axial Restraint	Strain	Stress	Ultimate Tensile Strength	Life	Cycles to Failure (2)	Stress Ratio (3)
	(F)		(μ"/"-rms)	(ksi-rms)	(ksi)	(min)		
S-1-1	R.T.	No	766	8.1	71.0	170	3.2×10^5	0.11
S-1-2	R.T.	No	766	8.1	71.0	210	4.0×10^5	0.11
S-1-3	R.T.	No	766	8.1	71.0	202	3.8×10^5	0.11
S-9-1	R.T.	Yes	766	8.1	71.0	9	1.7×10^4	0.11
S-9-1	R.T.	Yes	766	8.1	71.0	6	1.1×10^4	0.11
S-9-3	R.T.	Yes	766	8.1	71.0	11	2.1×10^4	0.11
S-10-1	R.T.	Yes	460	4.8	71.0	62	1.2×10^5	0.07
S-10-2	R.T.	Yes	460	4.8	71.0	200	3.8×10^5	0.07
S-10-3	R.T.	Yes	460	4.8	71.0	253	4.8×10^5	0.07
S-8-1	300	No	820 (1)	8.2 (1)	56.5	130 (1)	2.5×10^5	0.15
S-8-2	300	No	820	8.2	56.5	140	2.6×10^5	0.15
S-8-3	300	No	820	8.2	56.5	138	2.6×10^5	0.15

(1) Specimen S-8-1 was tested 120 minutes with the rms strain fluctuating between 560 and 650 micro-inch/inch. The strain was then raised to 820 micro-inch/inch for the final 10 minutes of the test.

(2) The cycles to failure were computed by assuming that the cycles were accumulated at the rate of 31.5 Hz.

(3) Stress ratio = stress/ultimate tensile strength

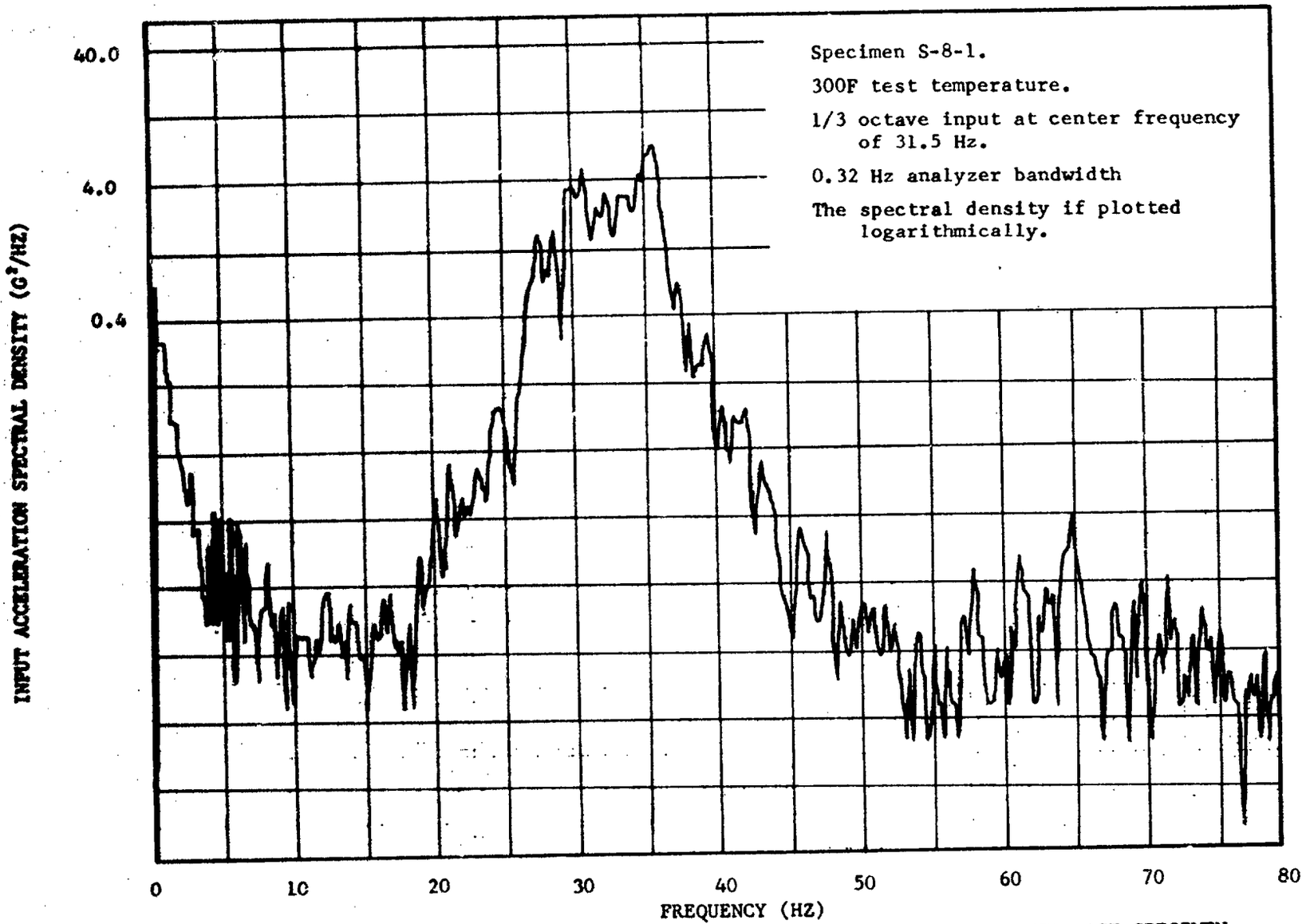

Figure 20 - SPECTRAL DENSITY OF REPRESENTATIVE ACCELERATION INPUT TO SHAKER TEST SPECIMEN

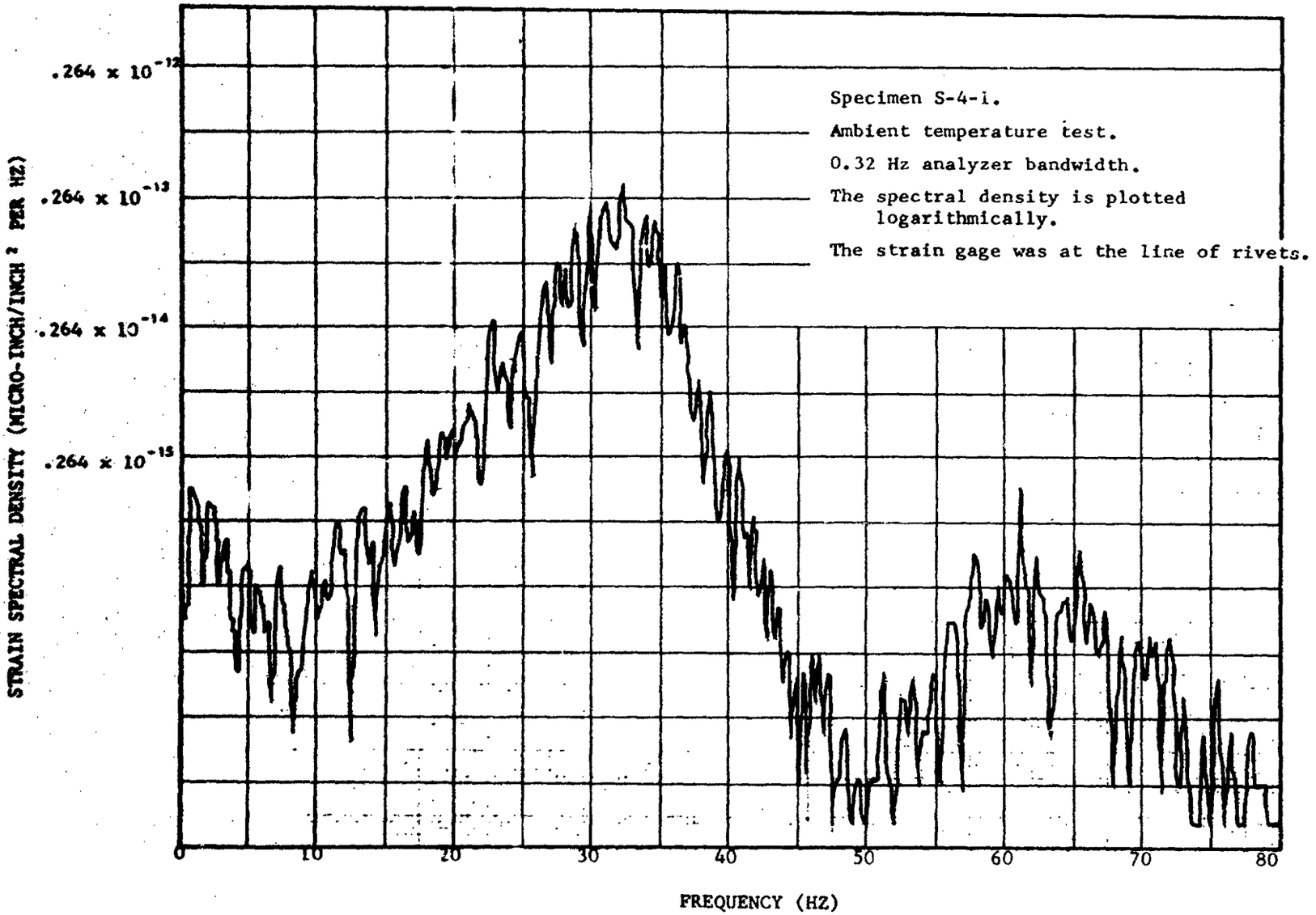

Figure 21. STRAIN SPECTRAL DENSITY IN THE ABSENCE OF OIL CANNING

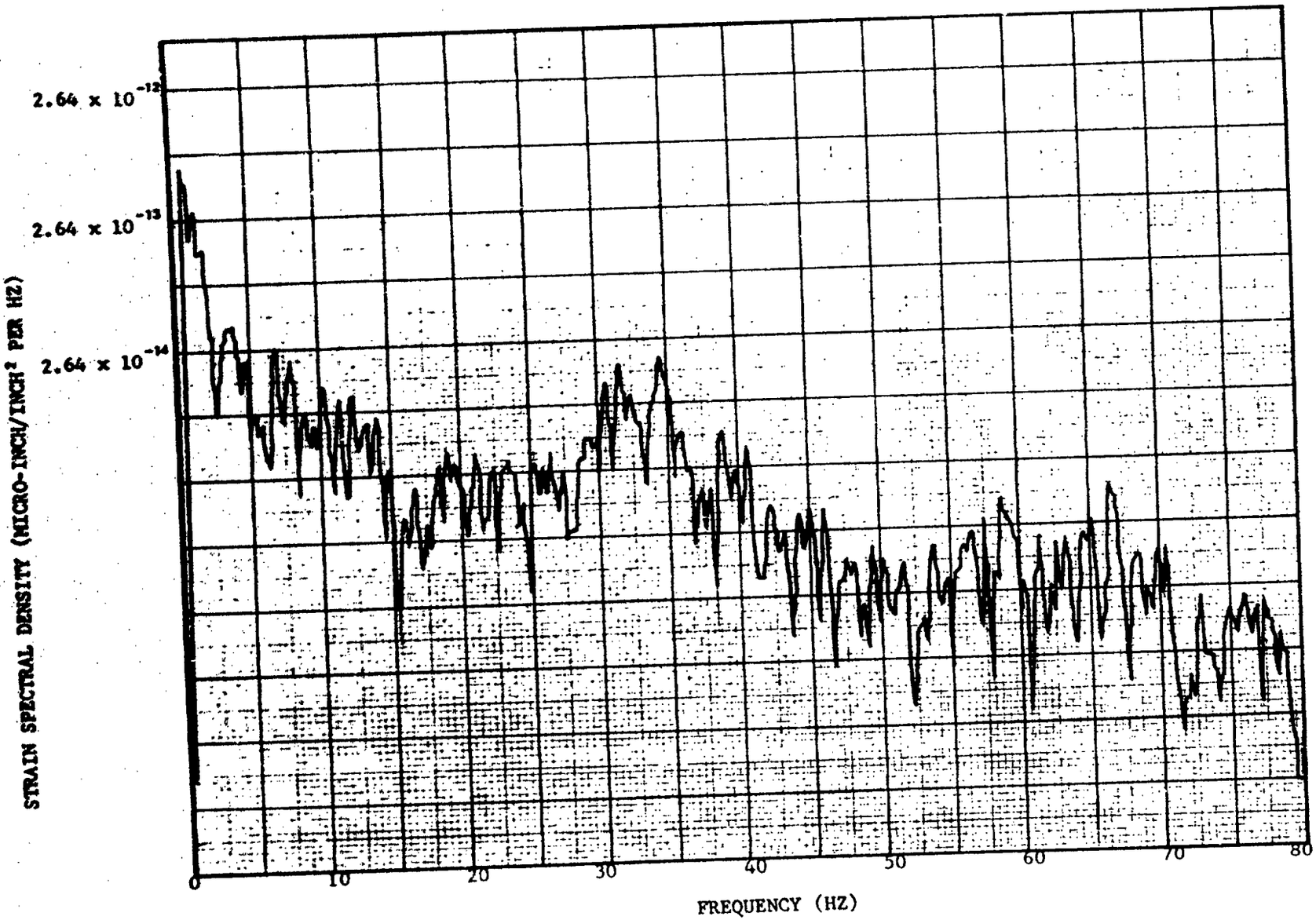

FIGURE 22. STRAIN SPECTRAL DENSITY IN THE PRESENCE OF OIL CANNING

V. CONCLUSIONS

Early fatigue failures are likely to occur if there is oil canning of thin-skinned aircraft structure under steady state loading conditions in combined thermal-acoustic environments. The predominant factor in the early fatigue failures is the continual, although intermittent, large stress reversals that are characteristic of oil canning.

In subsection III.7 is developed the criterion

$$1.5 \leq \frac{A_o}{\bar{w}} \leq 6, \quad \frac{\bar{w}}{h} \geq 0.3 \qquad (7)$$

for predicting the presence of oil canning of multi-bay metallic panels in steady-state thermal-acoustic environments. The criterion has the merit of (1) being easy to apply and (2) having resulted in predictions of the presence and absence of oil canning that agreed satisfactorily with the experimentally obtained data (Figure 7). Since the only multi-bay panels that were fabricated and tested in the experimental program were three-bay panels, there is still a need for further test data to verify the accuracy of the oil canning predictions for other sets of parameters (i.e., the temperature rise, sound pressure level and spectrum, and panel geometry and materials).

There is no generally accepted method of predicting either the magnitude of the stress reversals or the life of panels that continually experience oil canning in combined thermal-acoustic environments. However, there is much evidence that the life is not long under steady-state loading conditions that produce oil canning in the combined thermal-acoustic environments. Therefore, it is considered a conservative design practice to reject aircraft panel designs that violate the criteria in equations 7 or, alternately, fall outside of the bounds of Figure 7 since these rejected panel designs are expected to result in oil canning (and early fatigue failures) in steady-state thermal-acoustic environments.

Fatigue data were obtained from shaker tests under (1) the simultaneous application of thermal and shaker loading that produced oil canning and (2) the alternate application of the thermal and shaker loading (for which oil canning did not occur). Specimen fatigue life was a function of oil canning. It was concluded that the alternate application of thermal and shaker loading is not an acceptable method of simulating the simultaneous application of those loadings in tests to determine fatigue life, when oil canning occurs in the tests.

The principal factor affecting the fatigue damage and life of the oil canning shaker test specimens was the number of cycles of oil canning through the original flat position of the specimens. Other factors such as (i) the number of thermal cycles, (ii) the rms and peak response in the frequency range of the random excitation, and (iii) the rapidity of heating the specimens (the test specimens were heated up to 300F/minute) were of secondary importance in causing fatigue damage. It is expected that the relative importance of the factors affecting the fatigue life of the oil canning shaker specimens and of oil canning multi-bay panels in thermal-acoustic environments is the

same. Therefore, Goodman diagrams and/or constant amplitude-constant frequency S-N data at the required steady-state temperature may be used as a first estimate of the life of the oil canning panels if the number of cycles of panel snap-through and the stress extremes of the stress reversal in snap-through (i.e., oil canning) can be estimated.

REFERENCES

1. J. R. Ballentine, H. E. Plumblee, and C. W. Schneider, Sonic Fatigue in Combined Environment, Technical Report AFFDL-TR-66-7, May 1966.

2. P. P. Plant, I. F. Sakata, G. W. Davis, and C. C. Richie, Hypersonic Cruise Vehicle Wing Structure Evaluation, NASA CR-1568, April 1970.

3. O. F. Maurer and R. M. Shimovetz. Combined Environmental Sonic Fatigue Test of the Aft Fuselage Panels for a Fighter Bomber Aircraft, Technical Report AFFDL-TR-70-144, pp. 557-576, 1970.

4. P. R. McGowan, Structural Design for Acoustic Fatigue, Technical Documentary Report No. ASD-TDR-63-820, October 1963.

5. J. R. Ballentine, et al, Refinement of Sonic Fatigue Structural Design Criteria, Technical Report AFFDL-TR-66-156, January 1968.

6. R. C. Stroud and J. Mayers, Dynamic Response of Rapidly Heated Plate Elements, AIAA J., Vol. 9, No. 1, Jan. 1971, pp. 76-83.

7. B. A. Boley and A. D. Barber, Dynamic Response of Beams and Plates to Rapid Heating, Journal of Applied Mechanics, Vol. 24, No. 3, September 1957, pp. 413-416.

8. B. A. Boley, Thermally Induced Vibrations of Beams, Journal of the Aeronautical Sciences, Vol. 23, No. 2, February 1956, pp. 179-181.

9. S. Timoshenko and J. M. Gere, Theory of Elastic Stability, McGraw Hill Book Co., 1961, pp. 411-417.

10. A. M. Freudenthal, The Inelastic Behavior of Engineering Materials and Structures, John Wiley and Sons, New York, 1950.

11. B. J. Lazan, Damping of Materials and Members in Structural Mechanics, Pergamon Press, Oxford, England, 1968.

12. J. Marin, Mechanical Behavior of Engineering Materials, Prentice-Hall, Inc., Englewood Cliffs, N. J., 1962.

13. M. J. Jacobson, Advanced Composite Joints, Design and Acoustic Fatigue Characteristics, Technical Report AFFDL-TR-71-126, April 1972.

14. C. C. Osgood, Fatigue Design, Wiley-Interscience, New York, 1970.

15. R. C. Juvinall, Engineering Consideration of Stress, Strain, and Strength, McGraw-Hill, New York, 1967.

16. Spera, D. A., Calculations of Thermal-Fatigue Life Based on Accumulated Creep Damage, NASA TN-D-5489, 1969.

17. Baldwin, E. E., et al, Cyclic Strain Fatigue Studies on AISI Type 347 Stainless Steel, ASTM, Vol. 57, 1957.

18. Clauss, Francis J., and Freeman, James W., Thermal Fatigue of Ductile Materials, I and II, NASA TN 4160 and 4165, 1958.

REFERENCES

19. M. J. Jacobson, Acoustic Fatigue Design Information for Skin-Stiffened Metallic Panels, Northrop Report No. NOR 69-111, August 1969.

20. Y. Shulman, On the Vibrations of Thermally Stressed Plates in the Pre-Buckling and Post-Buckling States, Massachusetts Institute of Technology, Report ASRL-TR-25-25, January 1958.

21. M. J. Jacobson, Stress and Deflection Response of Honeycomb Panels Loaded by Spatially Uniform White Noise, AIAA Journal, Vol. 6, No. 8, August 1968, pp. 1503-1510.

22. M. J. Jacobson and W. S. Pi, Nonlinear Response of Acoustically Loaded Panels, Northrop Report NOR 73-27, (in preparation).

23. Metallic Materials and Elements for Aerospace Vehicle Structures, MIL-HDBK-5A, Department of Defense, Washington, D. C., February 1966.

24. Aerospace Structural Metals Handbook, AFML-TR-68-115, 1970.

APPENDIX A. MATERIALS SELECTION, MANUFACTURING OF SPECIMENS, AND MATERIAL QUALIFICATION TESTS

A.1 MATERIALS SELECTION

The primary criteria that were considered for material selection in the test program were: (a) the materials should be representative of those that might be used in a significant load-carrying structural component that also has to withstand elevated temperatures; (b) there should be available an adequate amount of thermo-physical and -mechanical property data in the open literature for the selected materials so that significant funds would not be expended in testing for such data; and (c) the materials selected would not present any undue manufacturing difficulties so that excessive expenditures would not have to be incurred.

Although for tension-critical structures, titanium alloys, as characterized by the 6Al-4V alloy, are superior to the other classes of materials, cost considerations have usually led to the selection of aluminum alloys when operating temperatures are not greater than approximately 300F. When using aluminum in that general temperature regime, the "favored" alloy is 2024 in the -T4 and/or -T81 tempers because of superior mechanical properties in that regime. Other alloys are superior at lower temperatures. In specific applications, particularly near the upper temperature regime for aluminum alloys, consideration must also be given to effects such as: sustained elevated temperature exposure on short-time elevated temperature and room temperature properties, onset of metallurgical instability, creep, etc. However, the general conclusions indicated above will still be valid.

For tension-critical structures at elevated temperature, titanium alloys are superior to the stainless steels, as exemplified by the PH15-7Mo, 17-7 PH, AM-350 varieties. Titanium alloys are also superior to the so-called "super-alloys" (e.g., nickel-base alloys) up to temperatures of approximately 800F to 900F (short-time use). The nickel-base alloys, as exemplified by the Inconel 718, Rene' 41, etc., are designed specifically for structural use to 1200F to 1400F (and higher to about 1800F for very low loads).

For both tension-critical and compression-critical structures, except for a narrow range of temperatures and very high loading intensities, the aluminum alloys, titanium alloys, and nickel-base alloys are the principal materials to be expected in structural applications to about 1200F. Therefore, an aluminum alloy, a titanium alloy, and a nickel-base alloy were chosen for use in the test program.

The specific materials that were selected were the bare 2024-T81 aluminum alloy, the 6Al-4V titanium alloy, and the Rene' 41 nickel-base alloy.

Data on physical and mechanical properties and fatigue characteristics of the materials chosen are available from a variety of sources (such as Reference A-1). However, MIL-HDBK-5A (Reference A-2) is probably the most widely available source. Because of the easy availability of MIL-HDBK-5A, the figures of MIL-HDBK-5A that are referred to in Table A-1 are not reproduced for this report. In Table A-1 is a summary of figures and tables of MIL-HDBK-5A, ASD-TDR-63-820 (Reference A-3), and NASA TN-D-3075 (Reference A-4) that contain infor-

TABLE A-1 LOCATION OF MATERIAL DATA (IN MIL-HDBK-5A UNLESS STATED OTHERWISE)

TITLE	2024-T81 Aluminum Alloy	Annealed Ti-6Al-4V	Rene' 41 Sheet
Effect of Temperature on Physical Properties of Thermal Capacity (C), Thermal Conductivity (K), and Thermal Coefficient of Expansion (α)	Figure 3.2.3.0	Figure 5.4.6.1	Figure 6.3.5.1
Effect of Temperature on the Ultimate Tensile Strength	Figure 3.2.3.3.1(a)	Figure 5.4.6.2.1(a)	Figure 6.3.5.2.1(a)
Effect of Temperature on the Tensile Yield Strength	Figure 3.2.3.3.1(b)	Figure 5.4.6.2.1(b)	Figure 6.3.5.2.1(a)
Effect of Temperature on the Tensile and Compressive Modulus	Figure 3.2.3.1.4	Figure 5.4.6.2.4	Figure 6.3.5.2.5
Typical Stress-Strain Curves at Room and Elevated Temperatures	Figures 3.2.3.3.6(g) 3.2.3.3.6(a) 3.2.3.3.6(c)	Figure 5.4.6.2.6	Figure 6.3.5.2.5
Random Fatigue Life	Figure 28 of ASD-TDR-63-820	Figure 27 of ASD-TDR-63-820	Figures 8, 10, 11, 12 of NASA TN D-3075 for notched specimens
Typical Constant-Life Fatigue Diagram and/or Constant Amplitude Fatigue Data	Figure 3.3.1(i) for 2024-T4 alloy Figure 3.3.1(j) for 7075-T6 alloy Figure 3.2.3.1.7(f) for 2024-T3 alloy	Figure 5.4.6.2.8(a) for bar specimens	Figures 9, 10, 11, 12 of NASA TN D-3075 for notched specimens
Room Temperature Design Mechanical & Physical Properties	Table 3.2.3.0(b_2) for nonclad aluminum alloys. Table 3.2.3.0(d_1) for clad aluminum alloys.	Table 5.4.6.1(a)	Table 6.3.5.1(a)

mation pertinent to the description of the 2024-T81 aluminum alloy, the 6Al-4V titanium alloy, and the Rene' 41 nickel base alloy.

A.1.(a) 2024-T81 Aluminum Alloy

Various aluminum alloys were considered before the bare 2024-T81 alloy was selected. Items that were considered before that alloy was selected are stated below.

The strength properties of bare 2024 in various tempers are among the highest obtainable in aluminum alloys. Including clad 2024, the 2024 alloy is one of the most universally used high strength aluminum alloys. Cladding reduces the strength of 2024 by about 5%. The room temperature aged conditions (e.g., -T3) of this alloy should not be used where the temperature exceeds 150F and corrosive conditions exist. The artificially aged conditions (e.g., -T81) maintain their strength and corrosion resistance up to a temperature of 300F. The corrosion resistance of the 2024 aluminum alloy which contains 4.5% Cu is inferior to that of alloys free from or low in copper (e.g., the 7075 alumimum alloy with 1.6% Cu). Therefore, where high corrosion resistance is required, clad 2024 sheet and strip are preferred over the bare material. The alloy is readily formable in either the annealed or solution treated condition. Limited forming can also be performed in the T4 condition. The machinability of the heat treated conditions is very good. The alloy may be resistance welded, but fusion welded is not generally recommended.

In Figure A-1 (from Reference A-5) are stress-strain curves for 2024 aluminum alloy in various tempers. For this program, the T81 temper was obtained by inplant heat treatment of material that was procured in the T3 condition.

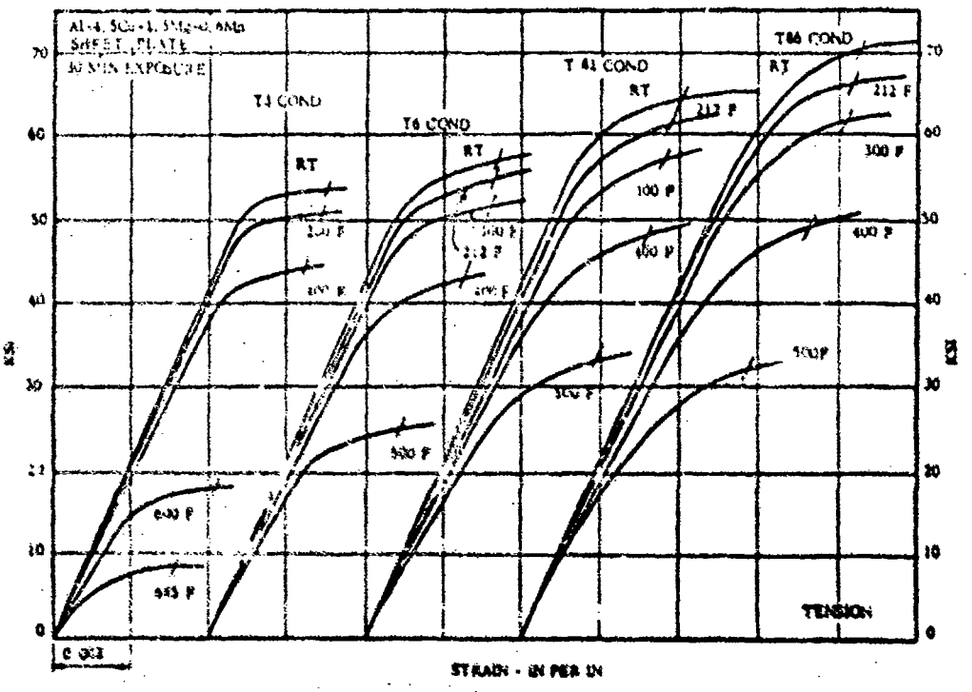

FIGURE A-1 - STRESS STRAIN CURVES FOR SHEET AND PLATE 2024 ALUMINUM ALLOY IN T3, T6, T81, AND T86 CONDITION (FROM CODE 3203, PAGE 9 OF REFERENCE A-5)

The choice of bare rather than clad aluminum alloy was made in view of the following considerations.

In Reference A-6, it is stated that while the effect of cladding on static mechanical properties may be calculated on a bulk or volumetric basis, the local nature of fatigue nucleation dictates that the fatigue strength of a clad alloy is significantly that of the weaker member of the core-clad combination; i.e., the clad material in all the aluminum alloy materials that were examined. This also predicts the fatigue strength reduction by cladding an alloy to be much greater than the reduction of static properties. The values in Table A-2 (from Reference A-6 with British specifications) confirm that cladding has appreciable effect on fatigue strength. Fatigue properties of clad 2024 and bare 2024 are in Table A-3, which was compiled from Reference A-5.

The 7075 aluminum alloy was not chosen because the unusually high static strength of 7075 at ambient temperature is not reflected in corresponding high fatigue resistance. Fatigue strengths are comparable to those of 2024 and 2014 which have lower static strength. At high temperatures, the 7075 alloy loses its strength advantage over 2024 even under static conditions.

A.1.(b) Ti-6Al-4V Titanium Alloy

Annealed rather than STA (solution treated and aged) Ti-6Al-4V was chosen for use in this program because the annealed material has better long life fatigue resistance and is used more often in designs of fatigue resistant structures. In Table A-4 is a summary from a recent titanium course (Reference A-7) of room temperature fatigue properties of Ti-6Al-4V. The advantage of the annealed condition over the STA condition at 10^6 and 10^7 cycles fatigue applications can be observed in Table A-4. Additional quantitative information on physical and mechanical properties of Ti-6Al-4V is available in Reference A-5 and the Ti-6Al-4V Handbook (Reference A-8).

Tensile tests and fatigue tests were conducted at room temperature to determine the effect of previous exposure up to three years at elevated temperatures up to 300F for clad 2024-T81 and 550F for annealed Ti-6Al-4V. These tests were reported in References A-9 and A-10. The results were that the tensile strengths and fatigue strengths after exposure were essentially as those before exposure.

A.1.(c) Rene' 41 Nickel-Base Alloy

The Rene' 41 alloy was chosen for the highest elevated temperature tests because of the availability of test data on the material and because Rene' 41 appeared to be a good candidate material for service applications at elevated temperatures.

In reference A-4, it was observed that, in the long life region such as 10^7 cycles, the fatigue strength tests of Rene' 41 at 700F are approximately the same as obtained in tests at 1400F. It was also observed that the absence of a progressive decrease in fatigue with increase in temperature had been noted previously for SAE 4340 steel and for PH15-7Mo stainless steel.

Additional fatigue data for Rene' 41 are on Page 44, Code 4205, of Reference A-5. The sharp knee at approximately 10^6 cycles of the 1400F Rene' 41 S-N curve of Figure 9 of Reference A-4 is not apparent in the 1600F Rene' 41 curve, but is apparent in the 800F curve.

TABLE A-2 EFFECTS OF CLADDING (FROM REFERENCE A-6)

Alloy(1)	Percentage Loss of Fatigue Strength (Because of Cladding) at	
	10^5 Cycles	10^8 Cycles
DTD.687	11.1	34.6
2024 S	8.3	39.7

(1) Note that British specifications were used in Reference 19 and DTD.687 is comparable to 7075-T6.

TABLE A-3 FATIGUE PROPERTIES OF 2024 ALUMINUM ALLOYS (FROM REFERENCE A-5)

Form	Sheet							
Condition	Temperature	Method	Stress Ratio, R	Fatigue Strength, ksi, at Cycles				
				10^5	10^6	10^7	10^8	5×10^8
T3-Clad	RT	Flexure	-1	32	20	15	13	12.5
T36-Clad	RT	Flexure	-1	32	20.5	16	13.5	13.5
T81-Clad	RT	Flexure	-1	27.5	17	14.5	13.5	13.5
T86-Clad	RT	Flexure	-1	32	19	14.5	13.5	13.0
T3-Bare	RT	Rotating beam	-1	34	26	21	18	18
T36-Bare	RT	Rotating beam	-1	37	29	22	19	19

TABLE A-4 FATIGUE PROPERTIES OF TITANIUM ALLOYS

ALLOY	FORM	MAXIMUM FATIGUE STRESS (ksi)					
		10^4	10^5 (CYCLES)	10^6	10^7	K_t	R
Ti-6Al-4V A	Sheet and plate	140	118	105	100	1.0	0.1
Ti-6Al-4V STA	Sheet and plate	155	107	80	75	1.0	0.1
Ti-6Al-4V A	Casting	--	~120	80	68	1.0	0.1
Ti-6Al-4V STA	Casting	--	125	103	88	1.0	0.1
Ti-6Al-4V A	Sheet and plate	80	60	54	52	3.0	0.1
Ti-6Al-4V STA	Sheet and plate	87	50	40	39	3.0	0.1
Ti-6Al-4V A	Casting	80	60	53	52	3.0	0.1

NOTE: A - Annealed
STA - Solution treated and aged

A.2 MANUFACTURING OF SPECIMENS

Because of the simple specimen configurations, manufacturing difficulties were not expected and did not occur.

A.2.(a) 2024-T81 Aluminum Alloy Specimens

All details were sheared and draw filed. The geometry of like details was held to within ± 0.030 inch. All of the angle details were formed on a power brake in the -T3 condition. All of the -T3 details were then heat treated to the -T81 condition, prior to drilling to produce riveted assemblies. A location tool was made and used to maintain a ± .020 inch location for the positioning of details on like specimens. A No. 20 drill was used to provide a $0.161 \begin{smallmatrix}+0.003\\-0.000\end{smallmatrix}$ inch hole size for AD5 rivets. The centerline location for all fasteners was held to ± 0.020 inch tolerance for all specimens. All rivets were squeeze riveted, while maintaining the normal upset head height and diameter per applicable process specifications. When flush rivets were installed, ± 0.002 inch from the flush condition was maintained.

A.2.(b) Ti-6Al-4V and Rene' 41 Alloy Specimens

Details were fabricated by square shearing the skin and angle parts to size. The edges were draw filed.

Pilot holes were punched under size in the detail points. Formed details were bent on the power brake. The skins and the formed details were assembled by clamping these items in position and opening the holes to $0.157 \begin{smallmatrix}+0.003\\-0.000\end{smallmatrix}$ inch diameter by drilling. The holes were de-burred. When flush rivets were to be installed, the skins were countersunk to fit the rivets. The rivets were inserted in the holes and the rivets were upset by the Drivmatic Riveter to comply with applicable specifications, completing the assembly. The Rene' 41 panels were heat treated at 1400F for 16 hours.

A.3 MATERIAL QUALIFICATION TESTS

Coupon tests were performed on the materials used in the test program to obtain ultimate tensile strength and Young's modulus and to guard against faulty material. The results are in Table A-5.

There was a marked reduction in the ultimate tensile strength of the 2024-T81 and Ti-6Al-4V specimens because of their increase in temperature, whereas the reduction of their Young's modulus was much less drastic.

The tests of the Rene' 41 coupons at 1000F are not reported in Table A-5 because the material, inadvertently, was not aged at 1400F for 16 hours before testing. However, as a matter of interest, it is noted that in the tests conducted on Rene' 41 coupons that were not aged at 1400F for 16 hours, there were two specimens that had an ultimate tensile strength of 90 ksi and 137 ksi, respectively, when tested at 1000F, and there were three specimens that each had an ultimate tensile strength of 144 ksi when tested at 75F. Young's modulus of the three unaged specimens that were tested at 75F were 29.0, 28.2, and 29.2 ksi, respectively. Young's modulus was not determined for the unaged specimens that were tested at 1000F.

TABLE A-5. COUPON TEST DATA

Material	Thick-ness (inch)	Speci-men No.	Tem-pera-ture (F)	Young's Modul-us psi	Ultimate Tensile Strength ksi	Speci-men No.	Tem-pera-ture (F)	Young's Modul-us psi	Ultimate Tensile Strength ksi
2024-T81	.040	1	75	10.2×10^6	70.2				
2024-T81	.040	2	75	10.5×10^6	71.2				
2024-T81	.040	3	75	10.3×10^6	71.5				
2024-T81	.040	average	75	10.3×10^6	71.0				
2024-T81	.063	4	75	10.8×10^6	70.5	7	300	10.5×10^6	56.8
2024-T81	.063	5	75	10.2×10^6	70.1	8	300	10.3×10^6	56.5
2024-T81	.063	6	75	10.6×10^6	71.3	9	300	10.5×10^6	56.3
2024-T81	.063	average	75	10.5×10^6	70.6	average	300	10.4×10^6	56.5
Ti-6Al-4V	.040	10	75	17.2×10^6	145.7				
Ti-6Al-4V	.040	11	75	17.0×10^6	146.4				
Ti-6Al-4V	.040	12	75	17.2×10^6	147.4				
Ti-6Al-4V	.040	average	75	17.1×10^6	146.5				
Ti-6Al-4V	.063	13	75	16.8×10^6	146.2	15	600	15.5×10^6	102.2
Ti-6Al-4V	.063	14	75	16.7×10^6	145.9	16	600	14.3×10^6	103.3
Ti-6Al-4V	.063	average	75	16.7×10^6	146.0	average	600	14.9×10^6	102.7
Rene' 41	.040	17	75	31.1×10^6	208.5				
Rene' 41	.040	18	75	30.7×10^6	203.7				
Rene' 41	.040	19	75	31.1×10^6	208.5				
Rene' 41(1)	.040	average		31.0×10^6	206.9				

(1) These Rene' 41 specimens were aged at 1400F for 16 hours before testing.

A.4 REFERENCES FOR APPENDIX A

A-1 G. Gerard, Thermostructural Efficiencies of Compression Elements and Materials, ASME Paper No. 56-AV-12.

A-2 Metallic Materials and Elements for Aerospace Vehicle Structures, MIL-HDBK-5A, Department of Defense, Washington, D.C. February 1966.

A-3 P. R. McGowan, Structural Design for Acoustic Fatigue, Technical Documentary Report No. ASD-TDR-63-820, October 1963.

A-4 E. P. Phillips, Fatigue of Rene' 41 Under Constant and Random Amplitude Loading at Room and Elevated Temperatures, NASA TN D-3075, 1965.

A-5 Aerospace Structural Metals Handbook, AFML-TR-68-115, 1970.

A-6 W. J. Harris, Fatigue Studies of Strucutral Sheet Aluminum Alloys, Ministry of Aviation S & T Memo 3164, May 1964.

A-7 W. J. Crichlow, Titanium Course, New York University, 1969.

A-8 D. J. Maykuth, R. J. Favor, and D. P. Moon, Ti-6Al-4V Handbook, Defense Metals Information Center, Columbus, Ohio 43201.

A-9 W. Illg and C. B. Castle, Fatigue of Four Stainless Steels and Three Titanium Alloys Before and After Exposure to 550 F (561 K) up to 8800 Hours, NASA TN D2899, 1965.

A-10 W. Illg, and L. A. Imig, Fatigue of Four Stainless Steels, Four Titanium Alloys, and Two Aluminum Alloys Before and After Exposure to Elevated Temperatures for up to Three Years, NASA TN D-6145.

APPENDIX B. TABULATION AND EVALUATION OF THERMAL-ACOUSTIC TEST DATA

B.1 INTRODUCTION AND SUMMARY

The number of tests and the amount and types of instrumentation in the thermal-acoustic test program, as well as the amount of data reduction following the tests, were established on the basis of obtaining sufficient test data to meet the overall program objectives. In this Appendix, many details are presented relating to the thermal-acoustic test program.

For all ten of the thermal-acoustic test specimens (static) strain and temperature data were recorded at the ambient sound pressure level; rms strains and temperature data were recorded at ambient and elevated temperatures at 139 db and 160 db SPL; average strains at a strain gage (i.e., the mean strain about which the rms strains were obtained) were recorded from oscilloscope observations at 139 db and 160 db SPL. The organization of these strain and temperature data is given in Table B-1. All of the Tables of this Appendix are at the end of this Appendix.

In the tables for average strain, when two strain entries are given for a specimen at a particular temperature, those two entries are indicative of the two relatively constant average strains during the oil canning.

The static strain entries for the aluminum alloy specimens in the Table are raw data and do not include corrections for temperature induced apparent strain. The temperature induced apparent strain for the WK series strain gages were taken from the strain gage manufacturer data sheets and are given in Tables B-2 and B-3. The corrections for temperature induced apparent strain are included in the tabulated average strains.

For the titanium alloy and Rene' 41 test specimens, temperature induced apparent strain is accounted for in all tabulated values of strain.

Membrane and bending strains were computed from the strain data that were obtained in the thermal tests at ambient sound pressure level. Membrane strains were obtained by adding algebraicly the static strains of the back-to-back gages whereas the bending strains were obtained by subtracting algebraicly those static strains. Damping factors and natural frequencies were also obtained. The organization of all these data is also given in Table B-1.

The following discussion outlines the test procedure that was the basis for the tests of the ten thermal-acoustic specimens.

The test specimens were instrumented with a set of high temperature strain gages. For the aluminum alloy and titanium alloy test specimens for the thermal-acoustic and thermal-shaker test program, WK strain gages (manufactured by Micro-Measurements) were used. These gages provide self-temperature-compensation and have been successfully applied to temperatures to 600F. High temperature epoxy adhesives were used for application of the gages to the specimen.

For the Rene' 41 test specimens in the thermal-acoustic and thermal-shaker test program, BLH Electronic Inc Type HT-1212-5B free grid gages were used. Because these gages are not temperature compensated and exhibit large static strains due to even moderate increases in temperature, it was necessary to develop experimentally a temperature induced apparent static strain curve for these gages. There was no temperature induced apparent strain correction needed for the dynamic strains. These strain gages were bonded to the test specimens with BLH "Rokide" CER-1000 ceramic adhesive.

Copper-constantan thermocouples and chromel-alumel thermocouples were installed on (by bonding with Mithra 200) the aluminum alloy thermal-acoustic and thermal-shaker test specimens. Chromel-alumel thermocouples were installed on the Ti-6Al-4V and Rene' 41 thermal-acoustic and thermal-shaker test specimens. The thermocouples were spot welded to the Rene' 41 test specimens, except at strain gage locations. At the strain gage locations, the thermocouples are part of the gage installation and were bonded with the "Rokide" ceramic adhesive without a spot radiant shield. The thermocouples were bonded to the Ti-6Al-4V test specimens with Mithra 200.

Instrumentation connections were made for the subsequent strain and temperature measurements. Each beam, plate, or three-bay panel was then installed in its fixture, (see, e.g., Figure 6 and Figure B-6) which provided the required boundary conditions. Clamped boundary conditions which applied a constraint against both normal motion (i.e., $w = 0$) and slope normal to the edge (i.e., $\partial w/\partial x = \partial w/\partial y = 0$) were sought in the test program.

The specimens were then tested at the ambient temperature to determine resonant frequencies, mode shapes and modal damping characteristics. Low level discrete frequency loudspeaker excitation was used for this determination. The damping factors were calculated with the logarithmic decrement from the strain decays that were obtained with a CEC oscillograph. Micro-miniature accelerometers (Endevco 2222B) provided the acceleration data, and the mode shape visualization was aided by observing polyvinylchloride pellet patterns.

Next the test specimen was mounted in the progressive wave acoustic test chamber opposite the radiant heating module. The initial thermal tests were at ambient sound pressure level. The thermal-acoustic tests were then conducted and strain data and temperature distributions were taken at a set of steady state temperatures at two sound pressure levels. The reference temperature was defined as the temperature at the center of the specimen. The location of the thermocouples and strain gages (in some cases, back to back) are given in Figures B-9, B-10, and B-11.

During the thermal tests with and without acoustic excitation, the specimens were heated to obtain a temperature rise of approximately 20F/minute. The temperature was held constant at the center of a specimen for approximately two minutes at the target temperature before strain and temperature readings for the entire panel were read.

During the thermal-acoustic tests, the heating supply was shut off, when necessary, during portions of data recording to prevent erroneous rms strain measurements induced by the ignitron power controller. It was not necessary to shut off the heating supply when oil canning was occurring, because the electrical pulses from the heating supply were masked by the electrical signals from the high level rms strain response. It was necessary to shut down the heating supply at elevated temperatures for which the test panel had achieved a stable thermally buckled condition, because the electrical signals from the low level rms strain response did not mask the electrical pulses from the power controller. However when the heating supply was shut down to avoid electrical pulses from the power controller, the rms strain response remained essentially unchanged (e.g., within ten percent) because the test panel remained in a thermally buckled stable configuration, even though the temperature was drifting down.

The sound pressure levels in the acoustic tests with broadband random excitation were at 139 db and at 160 db. Immediately after the SPL was set at 139 db, strain and temperature measurements were taken with the temperature at the specimen center at ambient and successively higher elevated temperatures. During the 139 db run, the temperature was increased from one reference level to the next highest reference level until the maximum reference temperature was reached.

In some cases following the 139 db run under random excitation, discrete frequency acoustic excitation at the fundamental frequency was applied to obtain damping factors at the ambient and elevated temperatures (see Table B-1).

The SPL was then raised to 160 db under broadband excitation and the tests to obtain strain response and the temperature distribution were then repeated in much the same manner as they had been conducted during the 139 db run. However, the SPL was not maintained at 160 db as the temperature was raised from ambient temperature to the various target test temperatures. The advantage sought in lowering the SPL was to prevent fatigue failures of the heat lamps. The effect of the temporary lowering of the SPL was believed to be of secondary importance on the strain data that were being obtained.

In some test cases there were back-to-back strain gages. In all instances when there were back-to-back strain gages, the strain signal from each gage was recorded.

When membrane strains are reported in the Tables of this Appendix, the membrane strain was obtained in thermal tests without acoustic excitation. If e_1 was the static strain of one of the back-to-back strain gages and e_2 was the static strain of the other strain gage, then the membrane strain was the average of the algebraic sum, i.e., $\frac{e_1 + e_2}{2}$. In dynamic cases, the strain signal from each strain gage was often decomposed into an average strain and an rms strain. In dynamic tests, the membrane rms strain (i.e., midway through the panel thickness)at locations of back-to-back strain gages was not computed.

In many instances when there were back-to-back strain gages, the rms strain of one gage of the pair equalled the rms strain of the other gage of the pair. When these two rms strains were unequal, the implication was that the neutral axis was not in the midplane between the two gages. (For back-to-back strain gages in the vicinity of a stiffener, the neutral axis may often not lie in the midplane between the gages.)

The method that is described in this paragraph was used for calibrating the DC shift on the oscilloscope during acoustic (and shaker) excitation. For the 2024-T8I and Ti-6Al-4V thermal-acoustic and thermal-shaker test specimens, each (single) active gage was calibrated to produce a voltage of 0.50 volts at 1280 micro-inch/inch of strain. For the Rene' 41 test specimens, the calibration ranged from 0.25 volts at 370 micro-inch/inch of strain at ambient temperature to 0.25 volts at 440 micro-inch/inch of strain at 1000F. These calibrations applied to both AC and DC response.

During the thermal-acoustic tests the outputs of the gages were recorded on an FM tape recorder. When these data were played back the signal was monitored by a True Rms Voltmeter with detection valid down to approximately 2 Hz and by an oscilloscope to interpret the data and to determine the DC offset about which the dynamic response was occurring. Since in most cases the offset was near the same order of magnitude or larger than the dynamic response, the measurement could easily be detected by observing the oscilloscope trace of the DC mode. As an example, a dynamic reading of 25 mv about a mean offset of 50 mv could be easily read on an oscilloscope scaled at 100 mv/cm. The fluctuating strain components with frequencies less than 2 Hz are not included in the recorded rms strain values, since the True Rms Voltmeter being used in the test did not interpret strain components with spectral content below 2 Hz.

The oscilloscope output was also used for determining the acceptability of data and for detecting the presence of oil canning. Oil canning produced a scope display that fluctuated from a positive DC offset to a negative DC offset in a random manner.

A 16-channel Brown recorder was used to monitor and record the temperatures of the specimen under test. The static strain data recorded as a function of temperature were read directly from an SR-4 strain indicator and 10-channel switching unit. During combined temperature and acoustic tests, the strain data were recorded on a 14-channel F-M tape recorder. Analysis of the strain data was performed on an SD301C real time spectrum analyzer and a B and K True Rms Voltmeter.

The acoustic environment was controlled and monitored by two photocon pressure transducers located within the test cell. During ambient temperature conditions one transducer was installed in the center of the test cell while the second transducer was located 24 inches upstream. During high temperature conditions the upstream pressure transducer was monitored to estimate the acoustic environment in the test cell. The microphone data were recorded on the F-M tape recorder during the conduct of the tests.

A Hewlett Packard Model 120 B oscilloscope was used to observe the strain response versus time for arbitrary strain gages during the tests.

All temperatures in the Tables are in (units of) degrees Fahrenheit; all sound pressure levels (SPL's) are in db relative to 20 $\mu N/m^2$; all static, average, membrane, and bending strains are in micro-inch/inch; and all random strains are in micro-inch/inch rms. Recall that rms strains do not include the average strain about which the random strains may fluctuate.

Typical photographs of the specimens are in Figures B-1 through B-7. Particular specimens that are illustrated are specimens A-2-2, A-3-2, A-4-1, A-5-1, and A-5-2. (Specimen A-1-1 is shown in Figure 6). A view of the thermal-acoustic section without the test fixture for the thermal-acoustic specimens is in Figure B-8; front and back views of Specimen A-5-2 installed in the test fixture are in Figures B-6 and B-7, respectively.

B.2 INSTRUMENTATION OF BEAM SPECIMENS A-1-1 AND A-1-2

The beam specimens A-1-1 and A-1-2 were tested to determine the effects of a one dimensional varying temperature distribution.

During the thermal acoustic-tests, beam specimens A-1-1 and A-1-2, which were tested separately, were oriented in the test fixture so that the air flow in the acoustic test chamber was parallel to the length direction of the specimens. Strain gages No. 1 and No. 2 were upstream and back-to-back; strain gages No. 3 and No. 4 were at the center of the beam and back-to-back; and strain gages No. 5 and No. 6 were downstream and back-to-back. The location of the strain gages (and thermocouples) is in Figure B-9.

Measurements from five thermocouples were taken in the test of specimen A-1-1 and measurements from three thermocouples were taken in the test of specimen A-1-2. The location of the thermocouples is in Figure B-1.

A picture of specimen A-1-1 installed in the test fixture is shown in Figure 6. The air gaps between specimen A-1-1 and the two thin acoustic reflector plates (that are clamped on three sides and free on the fourth side) that are part of the test fixture in the tests of specimens A-1-1 and A-1-2 are clearly visible in Figure 6. The two acoustic reflector plates also served as heat shields for the test fixture.

B.3 MODAL AND THERMAL TESTS OF SPECIMENS A-1-1 AND A-1-2

The fundamental frequency of specimen A-1-1 was 113 Hz under loudspeaker excitation at ambient temperature. At temperatures of 100F, 200F, and 300F, the fundamental frequency was obtained under discrete frequency acoustic excitation and was slightly lower (Table B-9) than the aforementioned 113 Hz. The fundamental frequency is influenced by the in-plane compressive stress which tends to reduce the fundamental frequency of a flat beam and by the increasing curvature (from the thermal buckling) which tends to increase the fundamental frequency. Apparently these two effects essentially cancelled each other, since the net change in fundamental frequency was small.

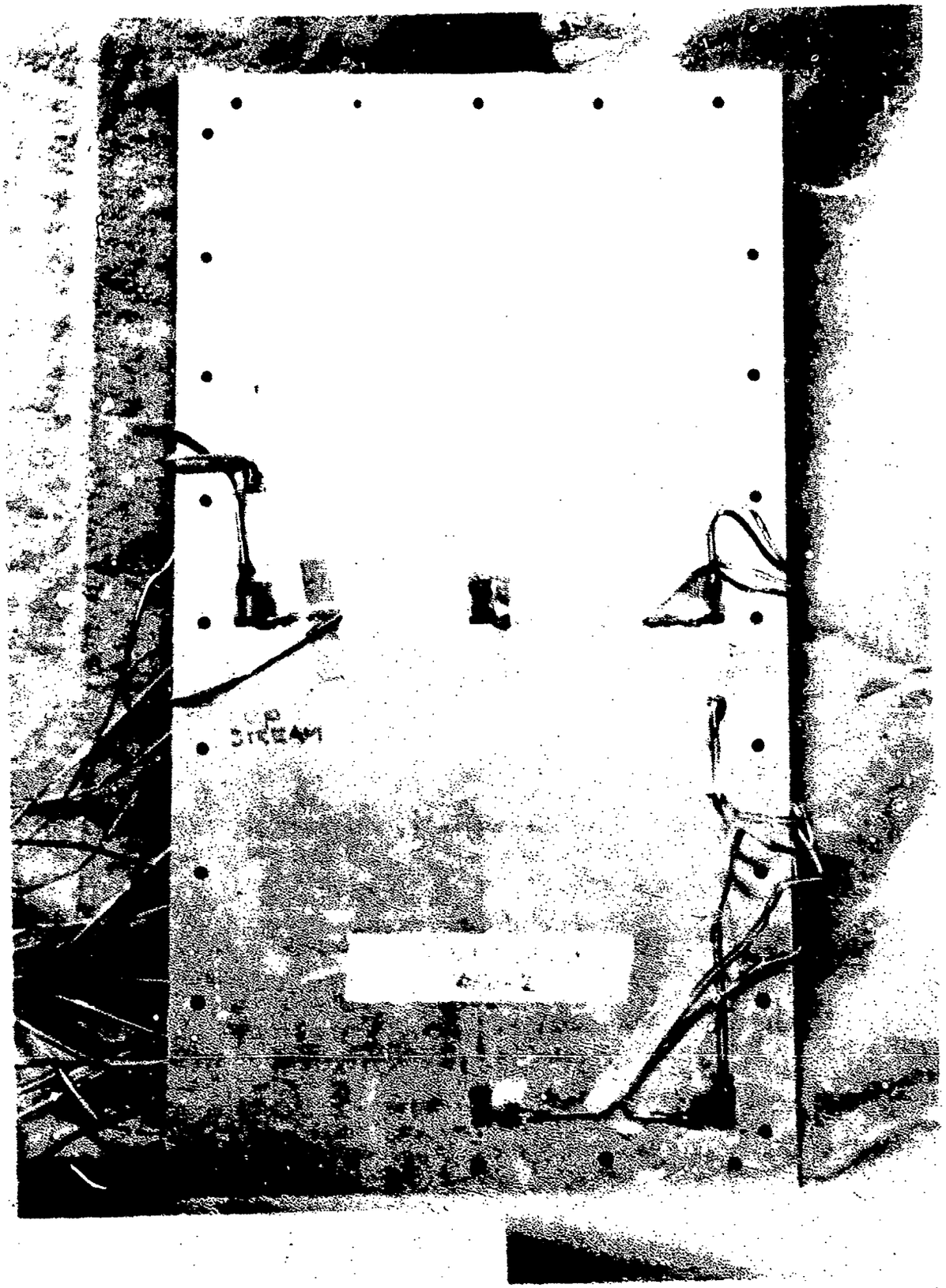

FIGURE B-1. FRONT VIEW OF SPECIMEN A-2-2

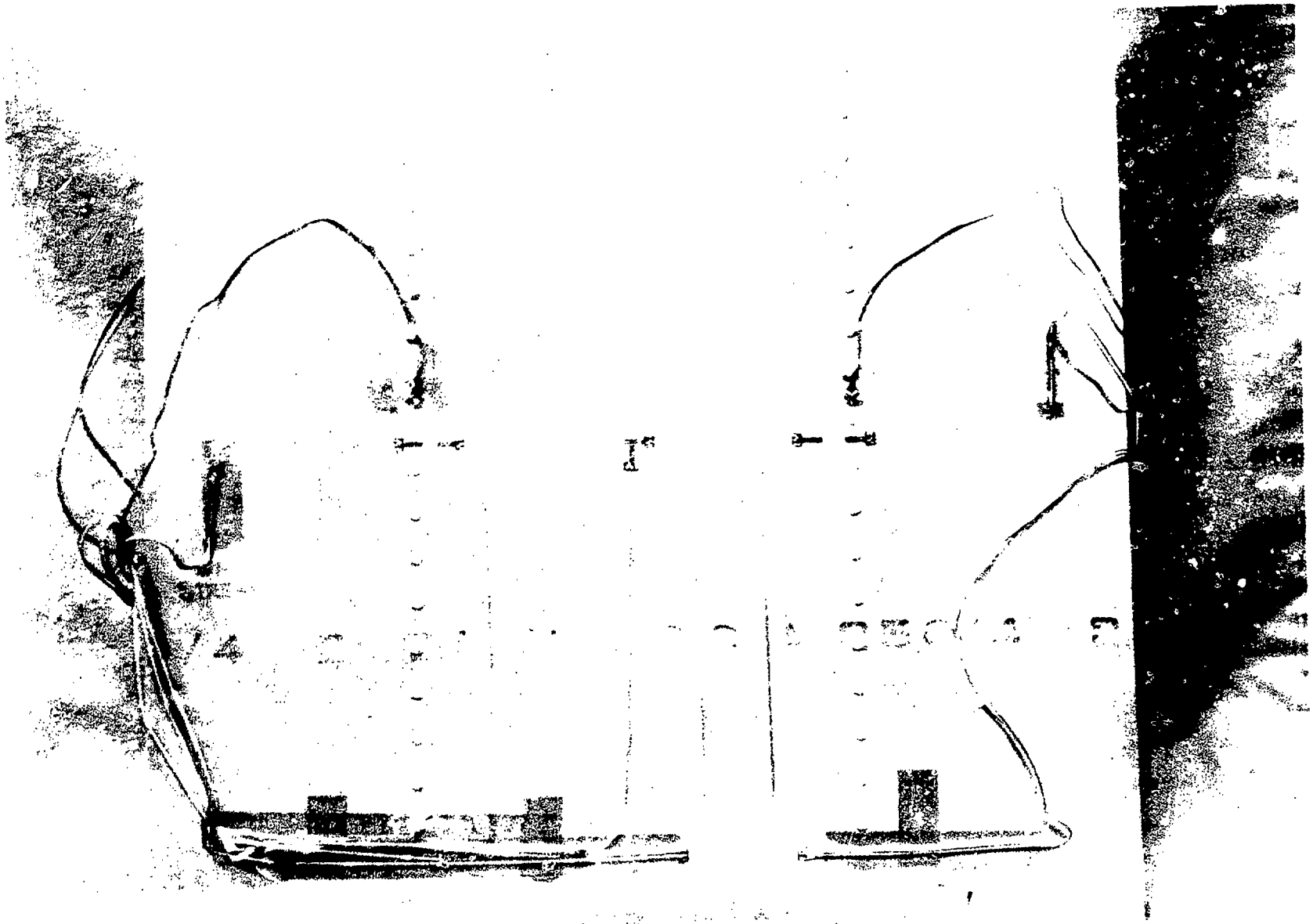

FIGURE B-2. FRONT VIEW OF SPECIMEN A-3-2

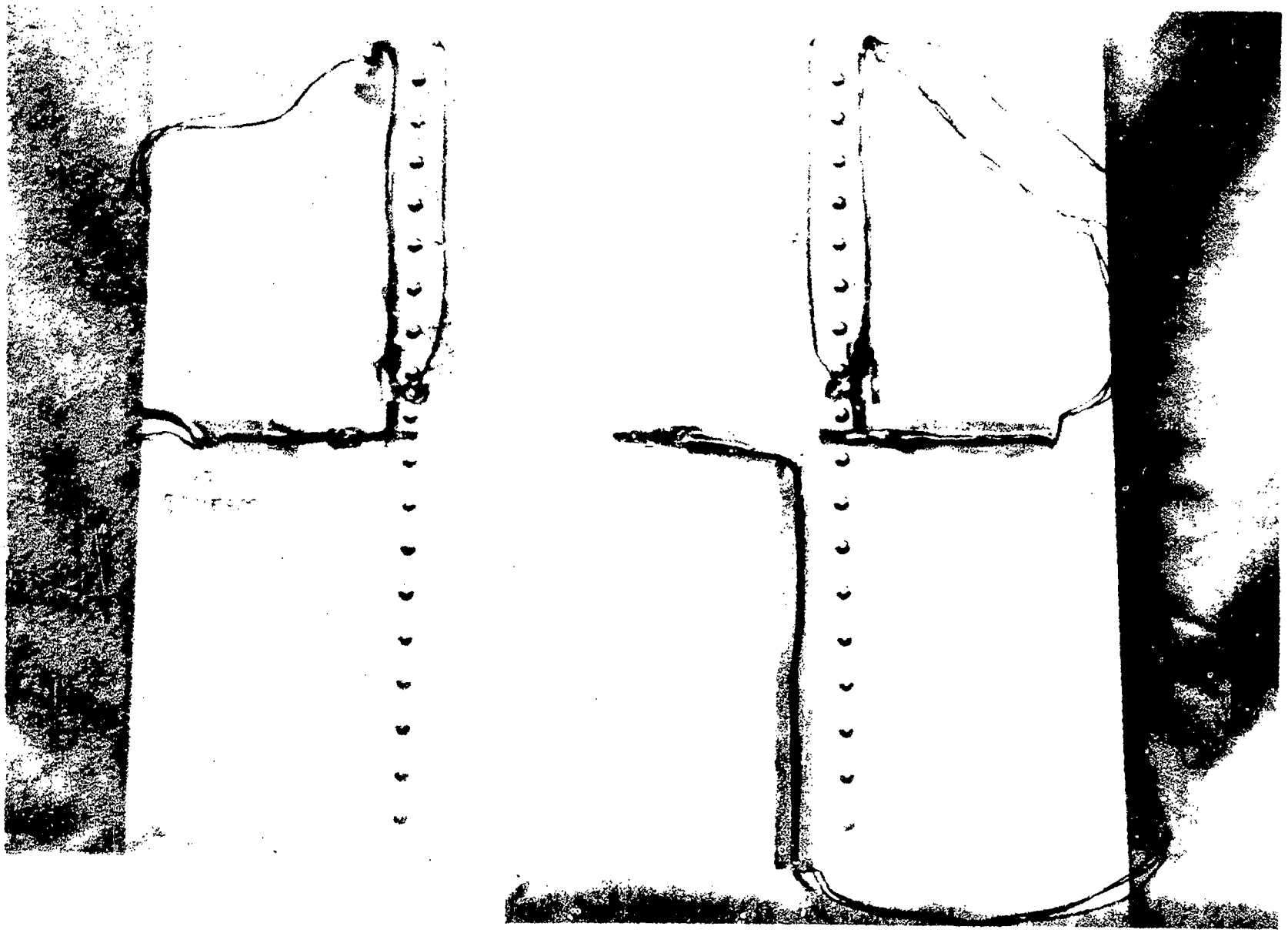

FIGURE B-3. FRONT VIEW OF SPECIMEN A-4-1

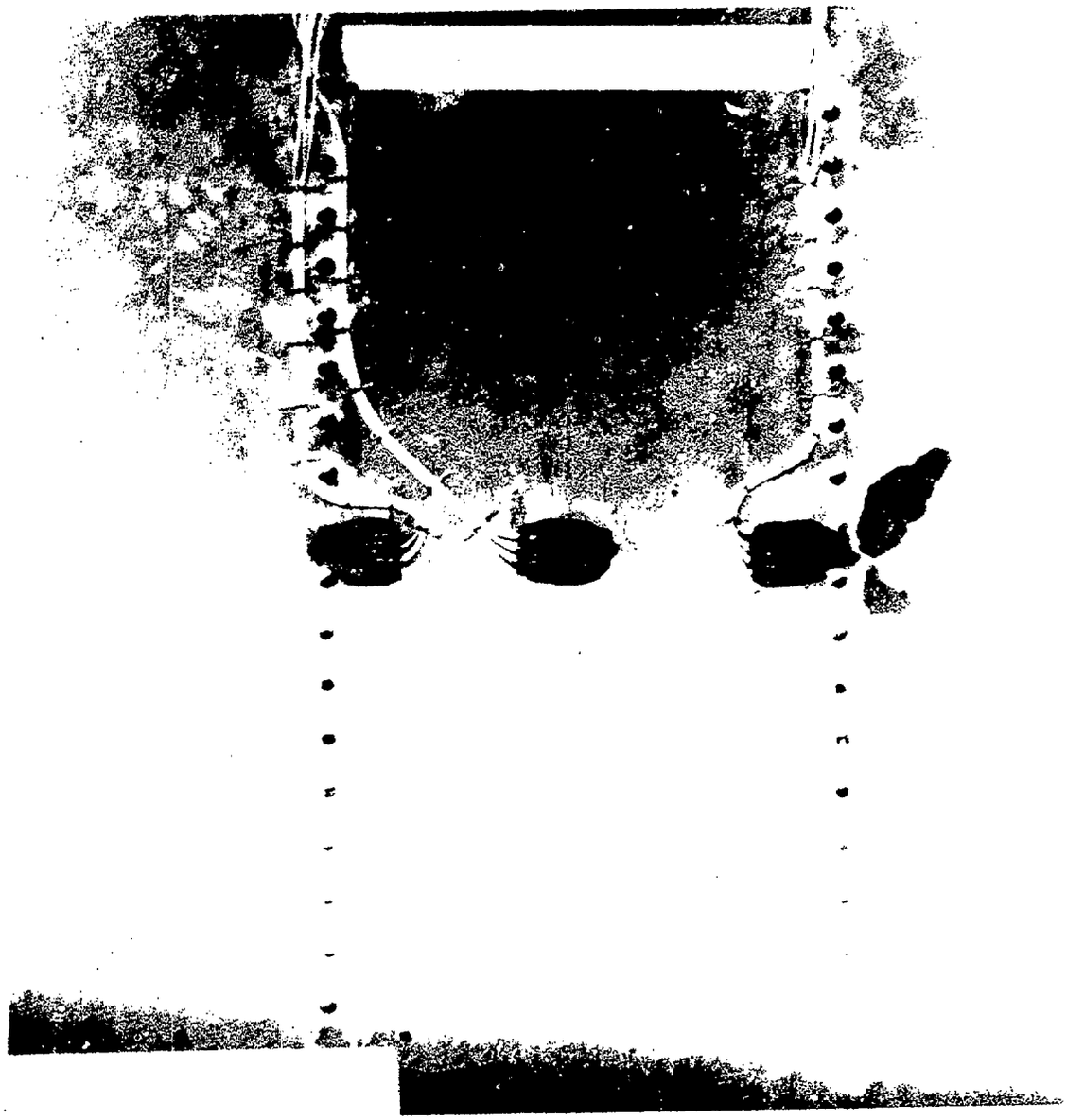

FIGURE B-4. FRONT VIEW OF SPECIMEN A-5-1

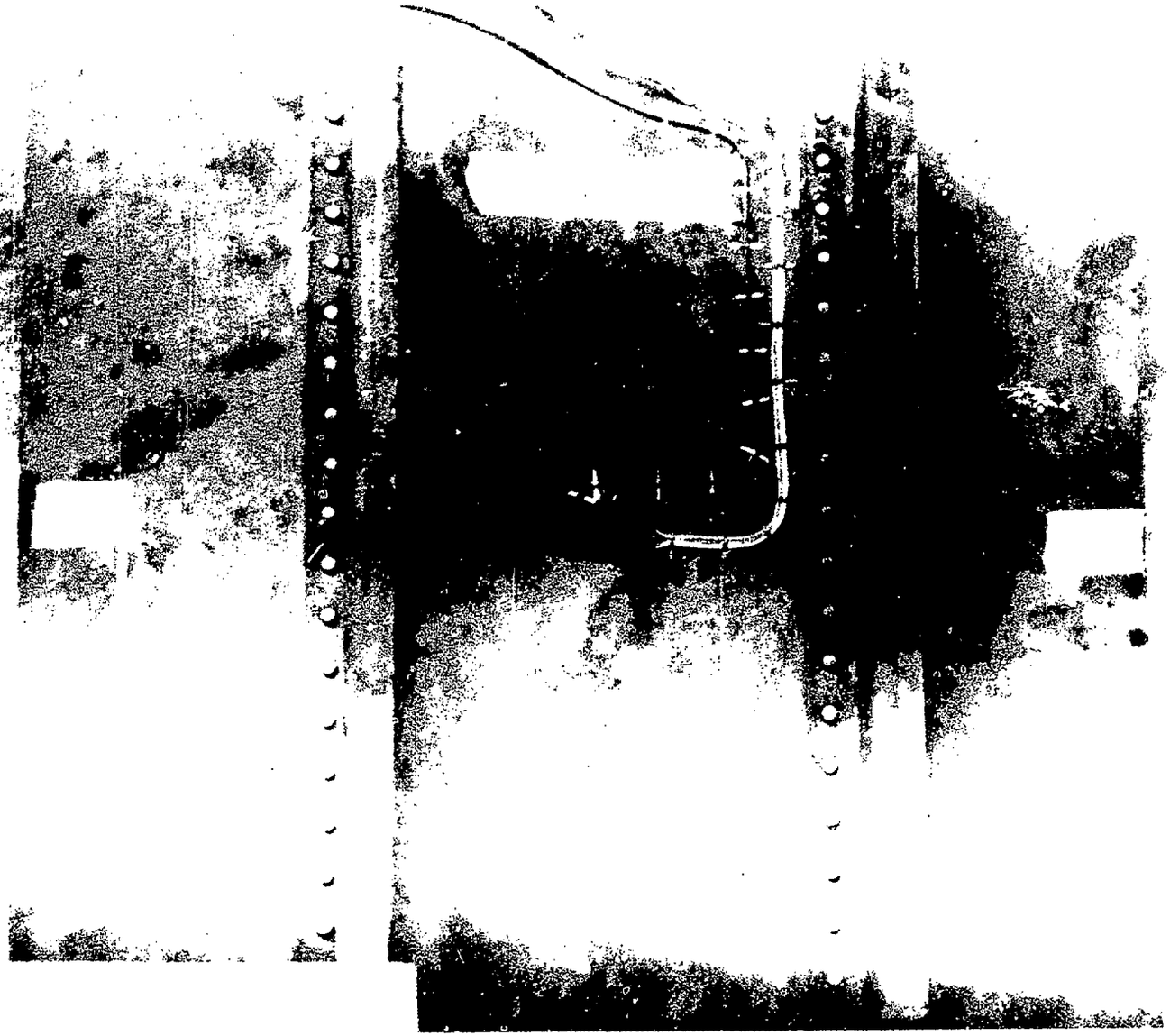

FIGURE B-5. BACK VIEW OF SPECIMEN A-5-1

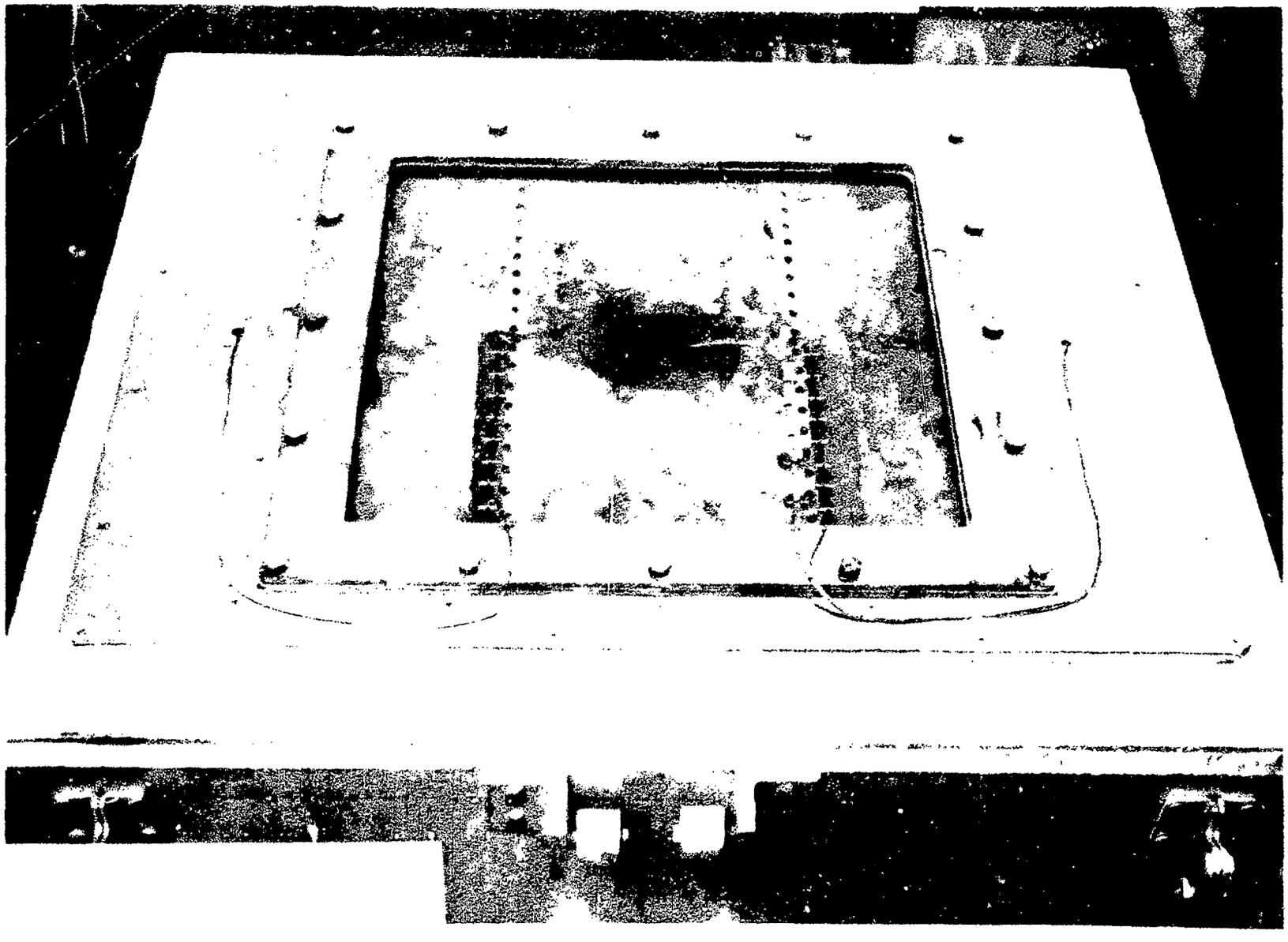

FIGURE B-6. FRONT VIEW OF PANEL A-5-2 INSTALLED IN THE TEST FIXTURE

FIGURE B-7. BACK VIEW OF PANEL A-5-2 INSTALLED IN THE TEST FIXTURE

FIGURE B-6. THERMAL-ACOUSTIC TEST CELL WITH TEST FIXTURE REMOVED

NOTES: 1. S denotes strain gage and T denotes thermocouple.
2. The portion of the specimen that is exterior to the continuous dashed lines is in contact with the test fixture.

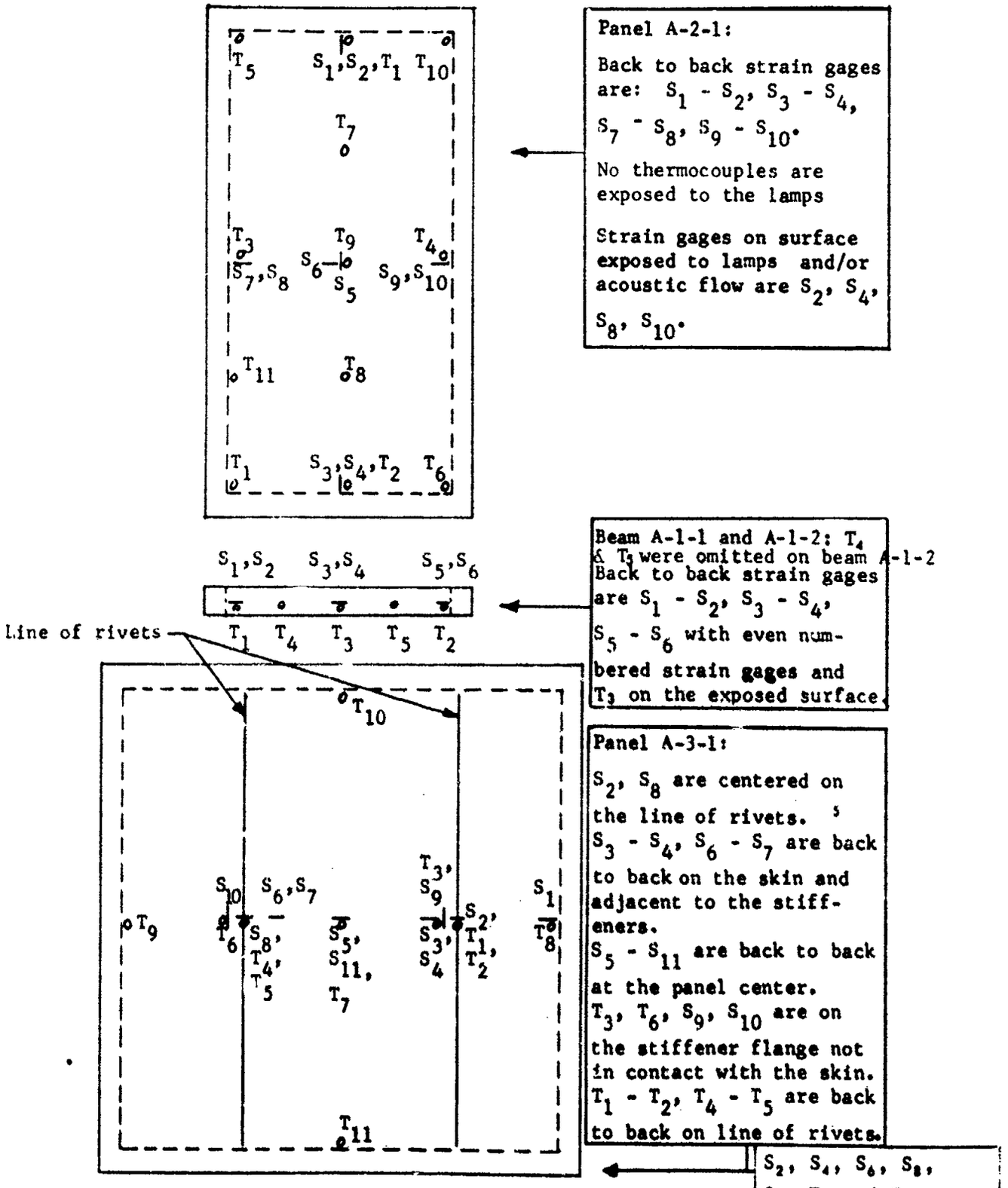

FIGURE B-9 LOCATIONS OF STRAIN GAGES AND THERMOCOUPLES OF SPECIMENS A-1-1, A-1-2, A-2-1, and A-3-1

The fundamental frequency of specimen A-1-2 that was obtained under loudspeaker excitation was 116 Hz before the thermal test at ambient SPL and was 111 Hz following the test. The implication is that the edge fixity was slightly changed because of the heating cycle.

The predicted fundamental frequency of the unstiffened beams, based on clamped edge conditions and a beam length of 8.4 inch, a thickness of 0.04 inch, Young's modulus of 10.5×10^6 psi, and a mass density of 0.100 lb/in^3, is 118 Hz. (Equations for calculating natural frequencies of homogenous, isotropic beams of uniform thickness with various end conditions are in Reference B-1.) The formula used in calculating the fundamental frequency was

$$f = \frac{1.03h}{a^2}\left(\frac{gE}{\gamma}\right)^{\frac{1}{2}} .$$

The conclusion reached after evaluating the test data obtained in the thermal tests at ambient sound pressure level is that specimen A-1-1 buckled when the temperature was increased from 78F to 100F and specimen A-1-2 buckled when the temperature was increased from 74F to 85F. This buckling was expected because the test setup tended to prevent motion of the ends of the specimen as the specimens were heated and the critical buckling stress was reached as the temperature was increasing towards 100F.

The critical buckling stress and strain of a clamped-clamped beam was calculated from

$$s_{cr} = \frac{4\pi^2 EI}{bh\,a^2} \qquad (B.1)$$

and

$$e_{cr} = \frac{s_{cr}}{E} . \qquad (B.2)$$

The aforementioned beam, for which the fundamental frequency was calculated to be 118 Hz, had a critical buckling stress of 770 psi and a critical buckling strain of 73 micro-inch/inch. For the beam, a uniform temperature increase of 6F produces 73 micro-inch/inch of thermal expansion ($e = \alpha\Delta T$, and $\alpha = 13 \times 10^{-6}$ micro-inch/inch for the aluminum alloy specimens at ambient temperature).

When the temperature was increased from 100F to 300F in the thermal tests at ambient SPL, the bending strains (Tables B-8 and B-13) increased considerably more than the average in-plane strains. Thus, in the postbuckling state up to 300F, there was considerable bending without a corresponding increase in the in-plane thermally induced membrane stress.

B.4 DYNAMIC TESTS OF SPECIMENS A-1-1 AND A-1-2

The rms dynamic strains in the thermal-acoustic tests of specimen A-1-1 are in Table B-5 and of specimen A-1-2 are in Table B-11. The average strains during the dynamic tests of specimen A-1-1 are in Table B-6 and of specimen A-1-2 are in Table B-11.

For specimen A-1-1, during the 139 db run the rms dynamic strains did not shift appreciably with increasing temperature, and the membrane strains at elevated temperatures did not significantly exceed the static buckling strains. However, during the 160 db run, the rms dynamic strain did shift significantly in going from 100F to 200F with the membrane strains not deviating too significantly from the critical buckling strain. (The membrane strains in the dynamic tests are not tabulated in this report).

For specimen A-1-1, during the 160 db run the increase in rms strain with increasing temperature occurred because there was no stable curved configuration and the combination of increasing temperature, restrained ends of the specimen, and the high intensity pressure resulted in rms strains that increased with increasing temperature.

The examination of the rms dynamic strains and average strains during dynamic tests of specimen A-1-2 (Table B-11) lead to the following conclusions. As the temperature was increased from ambient to 300F at 139 db SPL, the rms strains decreased as the midplane compressive strains and the curvature from bending increased. There was no evidence of oil canning during the 139 db SPL run.

During the 160 db SPL run of specimen A-1-2, there was evidence of oil canning when the data were taken at 200F and 300F. The reason that the rms strain was lower at 300F than at 200F is probably a result of increased curvature and stiffening because of heating. Until oil canning occurred in the 160 db run, the rms strains had increased only slightly with increasing temperature.

The principal difference between the thermal-acoustic test results of the beam specimens A-1-1 and A-1-2 was the presence of oil canning of specimen A-1-2 and the absence of oil canning of specimen A-1-1. The most probable explanation is that since the edge clamping of each of the two specimens depended on friction from the clamping, specimen A-1-1 was probably not clamped as tightly as specimen A-1-2. To avoid this problem on some of the specimens tested later in the program, dowel (shear) pins were inserted through the specimen ends and the edge clamps to prevent slipping. The friction is required to develop the thermal strains and the curvature that are required immediately prior to oil canning. The average strains of specimen A-1-2 (Table B-11) are much higher than the average strains of specimen A-1-1 (Table B-6). This comparison of strain data supports the premise that oil canning did not occur in the thermal-acoustic tests of specimen A-1-1 at 160 db SPL, because the edge clamp was not tight enough to develop the frictional force and the curvature that was necessary for the oil canning.

B.5 INSTRUMENTATION OF PLATE SPECIMENS A-2-1 AND A-2-2

Specimen A-2-1 was instrumented with ten strain gages and twelve thermocouples (Figure B-9). Specimen A-2-2 was instrumented with twenty strain gages and five thermocouples (Figure B-10). The strain gages of specimen A-2-2 were installed in sets of four. The four members of a set were back-to-back and parallel to both of the perpendicular edges in order to permit the calculation of stress in the biaxially loaded plates.

B.6 MODAL AND THERMAL TESTS OF SPECIMENS A-2-1 AND A-2-2

The fundamental frequency (under loudspeaker excitation at ambient temperature) of specimen A-2-1 was 119 Hz and of specimen A-2-2 was 129 Hz. The calculated fundamental frequency was 138 Hz for a plate clamped on all four edges and with geometrical properties of 16.4 inch length, 8.4 inch width, and 0.04 inch thickness, and with Poisson's ratio of 0.33 and Young's modulus of 10.5×10^6 psi. The clamped-clamped beam functions were used in obtaining the equation for calculating fundamental frequency that is in Equation (47) of Reference B-2. The discrepancies between the test and predicted fundamental frequencies are attributed principally to differences in edge fixity.

The thermal buckling stress can be calculated using Equation (9-11) on page 387 of Reference B-3. The equation is

$$\left(s_x + \left(\frac{a}{b}\right)^2 s_y\right)_{cr} = \frac{4}{3}\frac{\pi^2 D}{a^2 h}\left(3 + 3\frac{a^4}{b^4} + 2\frac{a^2}{b^2}\right) . \qquad (B.3)$$

The above equation was based on an assumed deflection shape

$$w = \frac{\delta}{4}\left(1 - \cos\frac{2\pi x}{a}\right)\left(1 - \cos\frac{2\pi y}{b}\right) . \qquad (B.4)$$

If there is uniform temperature throughout the plate and if there are equal restraints on all four edges against in-plane expansion, then in the absence of bending there will be a uniform biaxial stress state with $s_x = s_y$.

For a plate with a length of 16.4 in., a width of 8.4 in., a thickness of 0.04 in., Poisson's ratio of 0.33, and Young's modulus of 10.5×10^6 psi, one obtains from equation (B.3)

$$s_{cr} = s_x = s_y = 853 \text{ psi}$$

and from Hooke's law,

$$e_{x_{cr}} = \frac{1}{E}(s_x - \nu s_y) = 55 \text{ micro-inch/inch} .$$

NOTES:
1. A strain gage is denoted by a dash and S.
2. A thermocouple is denoted by a circle and T.
3. The portion of the specimen that is exterior to the continuous dashed lines is in contact with the test fixture.

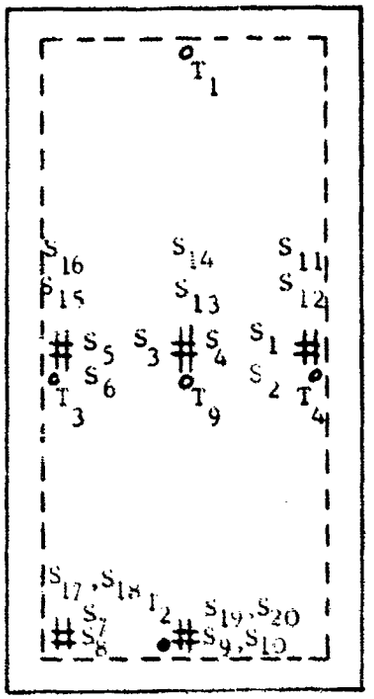

PANEL A-2-2

S_i and S_{i+1} are back to back strain gages if i is an odd number. The strain gage axis is in the panel width direction if i is less than 11; the strain gage is in the panel length direction if i is greater than 10. If i is even, S_i is on the surface exposed to the heating lamps.

Thermocouple T_9 is at the panel center.

The other four thermocouples are each near the intersection of a panel center line and a panel edge. No thermocouple is exposed to the heating lamps.

PANEL A-3-2

The thermocouple locations are defined in Figure B-9.

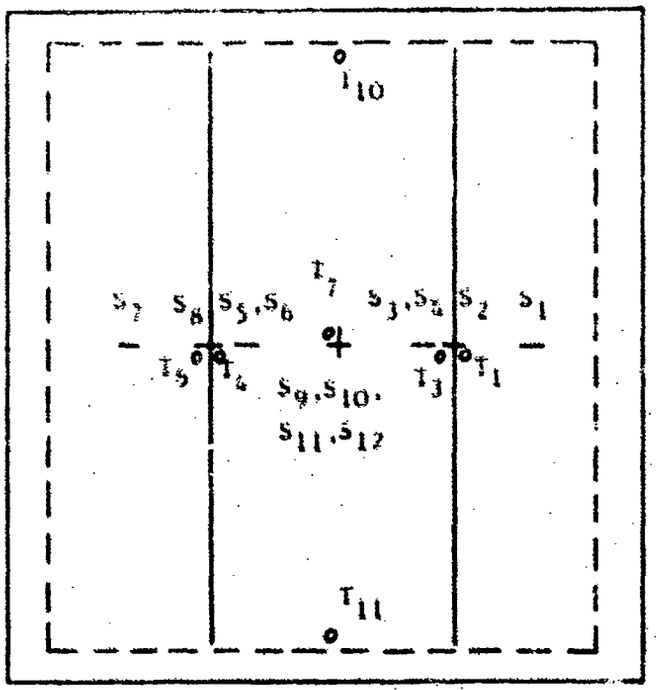

Strain gage pairs S_3-S_4, S_5-S_6 and S_9-S_{10} are back to back and in the width direction of the central bay; the pair S_{11}-S_{12} are back to back and parallel to the stiffeners. S_i is on the surface exposed to the heating lamps if i is even and is on the other surface of the skin if i is odd. S_2 and S_8 are at the line of rivets, and S_1 and S_7 are at the center of the outer bays.

FIGURE B-10 LOCATION OF STRAIN GAGES AND THERMOCOUPLES OF SPECIMENS A-2-2 AND A-3-2

Since an unrestrained isotropic panel will extend according to $e = \alpha\Delta T$ when the temperature is uniformly increased by ΔT, a temperature increase of only 4F will induce buckling of the restrained panels A-2-1 and A-2-2. From the thermal strain test data (Tables B-8 and B-19) it is verified that large bending strains have indeed occurred when the temperature was increased to 100F from ambient temperature.

The temperature distribution across the length of the panel A-2-1 was not uniform (Table B-17), and it was determined at the conclusion of the ambient SPL run that the cause was due to an electrical short in the lower lamp bank assembly. The test was not rerun, since maintaining a temperature at strain gages No. 1 through No. 5 along the length of the panel was not considered to be too significant in affecting the temperatures along the width of the panel at the important locations of strain gages No. 6 through No. 10.

The strain data obtained during the thermal test of specimen A-2-1 are in Table B-14 and during the test of specimen A-2-2 are in Table B-18. The membrane and bending strains during these tests at ambient SPL are in Tables B-9 and B-19.

Because there were not back-to-back gages in perpendicular directions on panel A-2-1, stresses could not be computed for panel A-2-1. In order to compute membrane and bending stresses for the two dimensionally thermally stressed unstiffened plates, specimen A-2-2 was instrumented with 20 strain gages that were in sets of four to obtain strains in perpendicular directions at back to back locations.

Static stresses were obtained upon using Hooke's law for two-dimensional stresses of biaxially stressed isotropic material,

$$s_x = \frac{E}{1-\mu^2}(e_x + \nu e_y)$$

$$s_y = \frac{E}{1-\mu^2}(e_y + \nu e_x) \qquad (B.5)$$

The strains were converted to nondimensional stress based on an assumption of one-third for Poisson's ratio. The nondimensional membrane and bending stresses are in Tables B-20 and B-21 and are based on the strain data in Table B-19.

An evaluation of the stresses in Table B-20 is now presented and the results are evaluated on the basis of the postbuckling behavior of biaxially stressed plates. The membrane stresses

$$\frac{s_{11} + s_{12}}{2}, \quad \frac{s_{13} + s_{14}}{2}, \text{ and } \frac{s_{15} + s_{16}}{2}$$

at the shorter center line indicate a distribution of extensional stresses in the panel direction with compression at the edges and tension at the plate center. The membrane stresses

$$\frac{s_3 + s_4}{2} \text{ and } \frac{s_9 + s_{10}}{2}$$

at the longer center line indicate a distribution of extensional stresses in the panel width direction with higher compressive stresses at the panel edge than at the panel center.

A comparison of membrane stresses

$$\frac{s_{17} + s_{18}}{2} \text{ and } \frac{s_{15} + s_{16}}{2}$$

shows that there is a smaller membrane stress at the panel corner than at the intersection of the panel edge and long center line.

A comparison of membrane stresses

$$\frac{s_7 + s_8}{2} \text{ and } \frac{s_9 + s_{10}}{2}$$

shows the same pattern of membrane stresses as was just noted for

$$\frac{s_{17} + s_{18}}{2} \text{ and } \frac{s_{15} + s_{16}}{2}$$

The aforementioned experimentally obtained membrane stress pattern of panel A-2-2 appears to be consistent with a pattern that can be theoretically obtained using the approach on pages 411-417 of Reference B-3 for the analysis of postbuckling stresses of isotropic plates.

The strains of Table B-18 were converted to nondimensional stress using Equations (B.3); the resulting nondimensional stresses are in Table B-22. Some of the high tensile stresses in Table B-22 can be of considerable importance in applications when there is high intensity acoustic excitation at the elevated temperatures, because the acoustic fatigue life is functionally dependent on both the average thermal stress (at a point) and the fluctuating stress, which in turn may be particularly sensitive to the presence of absence of oil canning.

The temperature data obtained in the thermal tests are in Table B-23. The strain corrections (that are included in Table B-19) for temperature induced apparent strain were based on the nominal temperatures in Table B-23.

B.7 DYNAMIC TESTS OF SPECIMENS A-2-1 AND A-2-2

The rms dynamic strains of specimen A-2-1 are in Table B-15 and of specimen A-2-2 are in Table B-24. The average strains during the dynamic tests of specimen A-2-1 are in Table B-16 and of specimen A-2-2 are in Table B-25.

Oil canning was not detected in the test of specimen of A-2-1. However, oil canning may have occurred without being detected since tests were conducted only at discrete combinations of sound pressure level and temperature. If oil canning actually did not occur, the most probable explanation is that the friction clamp was inadequate (there were no dowel pins connecting the specimen to the fixture) and permitted slippage, which in turn affected the curvature that would have been necessary for oil canning.

To avoid the problem of slippage in the friction clamps during the test of specimen A-2-2, dowel pins were installed along the periphery of the test specimen to join the specimen to the test fixrure during the tests.

The sequence of the dynamic testing of specimen A-2-2 that is reported in Tables B-24 and B-25 is now described. The first 139 db run was conducted and then the 160 db run was conducted. Following those tests, an examination of the back-to-back dynamic strain gage data from gages No. 3 through No. 6 indicated that the neutral axis of the dynamic strains was not midplane of the skin (because of the proximity of the stiffeners) during the 139 db run, since the back-to-back gages had considerably different dynamic strains. In exploring this further, the 139 db run was repeated after the conclusion of the 160 db run. During the second 139 db run, the back-to-back gages had much more nearly equal strain readings, possibly because of the intervening 160 db run.

During the first 139 db run, oil canning was detected at 100F (see Table B-25). Panel A-2-2 was much stiffer at 200F and 300F at 139 db (see the rms strain response in Table B-24), because the curvature from heating had led to a stable (i.e., no oil canning) curved configuration at 139 db.

Oil canning was not detected at 100F, 200F, or 300F during the second run at 139 db, but the considerable increase in stiffness that results in a decrease in rms response was again noted at 200F and 300F (Table B-24).

Oil canning was detected at 200F during the 160 db run (see Table B-25), and at 300F the dynamic response had decreased considerably.

B.8 INSTRUMENTATION OF PANEL SPECIMENS A-3-1 AND A-3-2

Specimen A-3-1 was instrumented with eleven strain gages and eleven thermocouples (Figure B-9). Specimen A-3-2 was instrumented with eleven strain gages and nine thermocouples (Figure B-10).

B.9 MODAL AND THERMAL TESTS OF SPECIMENS A-3-1 AND A-3-2

Under loud speaker excitation the fundamental frequency of specimen A-3-1 was 103 Hz (Table B-9) and of specimen A-3-2 was 131 Hz (Table B-36). The most probable explanation for the discrepancy in the natural frequencies is that there was less effective edge fixity obtained in the installation of specimen A-3-1 in the test fixture.

The observed strain data (before corrections for temperature induced apparent strain) in the thermal test at ambient SPL are in Table B-26 for specimen A-3-1 and in Table B-30 for specimen A-3-2. The membrane and bending strains during these ambient SPL tests are in Table B-27 for specimen A-3-1 and in Table B-31 for specimen A-3-2. The temperature distribution during these tests (and also during the dynamic tests) are in Table B-28 for specimen A-3-1 and in Table B-32 for specimen A-3-2.

Prior to the thermal-acoustic runs with specimen A-3-2, natural frequencies and strains at the center of the three bays were obtained under discrete frequency, loudspeaker excitation. Based on the strain amplitudes, the phase relations of the three bays are predicted in Table B-36, in which the strains are nondimensionalized.

In comparing the strains of various locations (e.g., the panel center) of specimens A-3-1 and A-3-2, the correspondence of strain gages is as given in Table B-34 (e.g., strain gage No. 7 of panel A-3-1 corresponds to strain gage No. 5 of panel A-3-2).

It is deduced from the strain data that were obtained in the tests of specimens A-3-1 and A-3-2 that there was an odd number (most probably one) of half waves in the center bay at the elevated temperatures in the test of panels A-3-1 and A-3-2. Most of the bending of the central bay occurred before 150F was reached in the test of each of the panels. The membrane compressive strains of all the back-to back strain gages increased until 300F was reached in the test of panel A-3-1 but only at the middle of the central bay of panel A-3-2 did the membrane compressive strain increase until 300F was reached.

The decrease in membrane strain at the higher elevated temperatures of panel A-3-2 was probably due to some slippage at the edge clamps which relieved the compressive strain and stress. However, the stress in the width direction of the bay cannot be calculated because there are no strain data for the length direction of the bay.

B.10 DYNAMIC TESTS OF SPECIMENS A-3-1 AND A-3-2

The rms dynamic strains of specimen A-3-1 are in Table B-29 and of specimen A-3-2 are in Table B-33. The average strains during the dynamic tests of specimen A-3-1 are in Table B-16and of specimen A-3-2 are in Table B-35.

B.10(a) Specimen A-3-1

A discussion of the dynamic tests of specimen A-3-1 is in subsection III.8. Natural frequencies obtained under acoustic excitation at ambient temperature (and at elevated temperatures) during the 139 db and 160 db run did not coincide with natural frequencies obtained under loudspeaker excitation. This was not investigated further since it is known that response nonlinearities caused by large deflections and in-plane stresses will cause shifts from natural frequencies that are obtained under linear response conditions.

B.10(b) Specimen A-3-2

Oil canning was not detected in the 139 db run, but there was a decrease in rms response at 100F, 200F, and 300F which indicates oil canning occurred between 76F (ambient) and 100F.

Oil canning was detected at 200F and 300F during the 160 db run. However, during the 160 db run, the rms strain response in general was significantly higher at 200F than at 300F. The implication is that the curvature (and stiffening) was increasing as 300F was being approached, and consequently the rms strains were decreasing. Another implication is that if the temperature were increased somewhat beyond 300F, the oil canning would have ceased at 160 db SPL.

B.11 INSTRUMENTATION OF SPECIMENS A-4-1 AND A-4-2

Specimen A-4-1 was instrumented with seven thermocouples and six strain gages (Figure B-11) and specimen A-4-2 was instrumented with seven thermocouples and four strain gages. The strain geges that were denoted as strain gages No. 4 and No. 6 on specimen A-4-1 were parallel to the line of rivets on the surface that was exposed to the heating lamps and were offset from the line of rivets by 0.3 inch. Strain gages No. 4 and No. 6 were installed to obtain data reflecting the thermal effect on strain in the stiffened portion of the skin and in the direction of the stiffeners.

Strain gage No. 2, 8, 9, and 10 were each oriented in the width direction of the central bay of specimens A-4-1 and A-4-2. Strain gage No. 9 and No. 10 were back-to-back at the center of the middle bay; strain gage No. 2 and No. 8 were at the upstream line of rivets, respectively. Stresses are not computed for specimens A-4-1 and A-4-2 because strain gage data were not taken with gages installed perpendicular to each other in the two-dimensional stress fields.

B.12 MODAL AND THERMAL TESTS OF SPECIMENS A-4-1 AND A-4-2

The strains that were obtained in the thermal tests at ambient SPL were corrected for temperature induced apparent strains (Table B-3) and are given in Table B-37. The strains of the back-to-back strain gages No. 9 and No. 10 were then added or subtracted to obtain the membrane or bending strain, respectively (Table B-38).

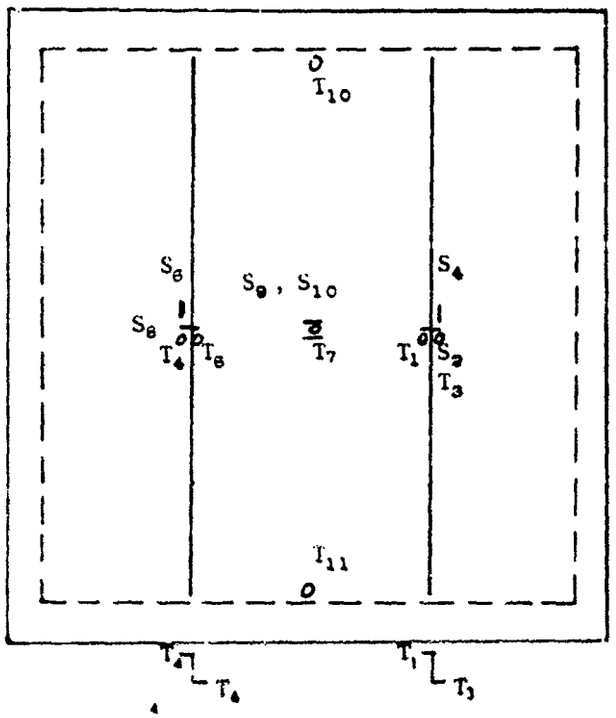

PANELS A-4-1 AND A-4-2

The thermocouple locations are defined in Figure B-9. The thermocouples are denoted by T_i.

All strain gages were exposed to the heating lamps except S_9. The strain gages are denoted by S_i.

S_9 and S_{10} are back to back at the middle of the central bay. S_2 and S_8 are at the line of rivets. S_4 and S_6 are parallel to the stiffeners.

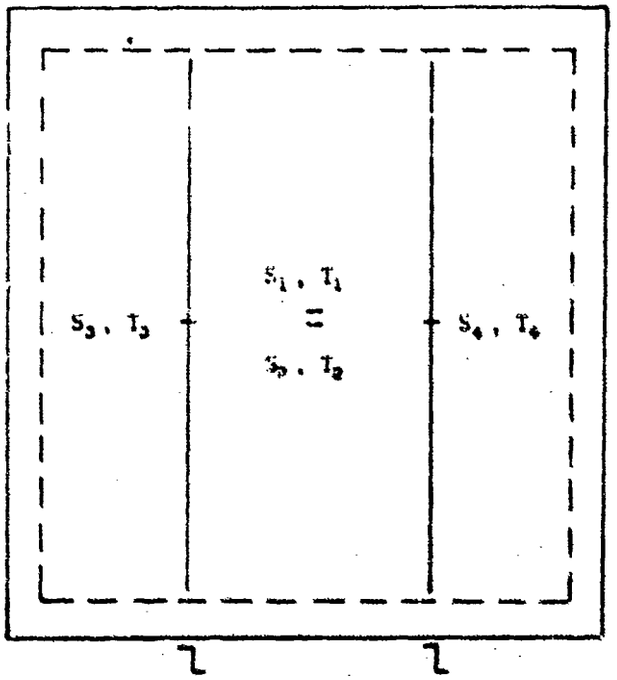

PANELS A-5-1 AND A-5-2

The strain gage and thermocouple locations of panel A-5-1 are shown in the schematic at the left. Strain gage No. 2 was the only strain gage not exposed to the heating lamps. Strain gages Numbers 1 and 2 are back to back at the panel center for both panels A-5-1 and A-5-2. For panel A-5-2, the thermocouple locations are shown in the 3-bay panel schematic drawing of panels A-4-1 and A-4-2 at the top of this page.

FIGURE B-11. LOCATION OF STRAIN GAGES AND THERMOCOUPLES OF PANELS A-4-1, A-4-2, A-5-1 AND A-5-2

An examination of the data in Table B-37 discloses the following items. Due to thermal buckling, the central bay of specimen A-4-1 bent towards the heating lamps whereas the central bay of specimen A-4-2 bent away from the heating lamps. The fact that the membrane stress peaked out in the 300F to 400F range indicates that the specimens were slipping in the edge fixture as the temperature was increased above 300F until the maximum temperature was reached.

Following the thermal runs at ambient SPL and prior to the thermal-acoustic runs, natural frequencies and accelerometer and strain data were obtained at room temperature at the center of the three bays under discrete frequency, loudspeaker excitation. Based on the accelerometer and strain data, the phase relations of the three bays were predicted and are given in Table B-39. The natural frequencies of the lowest four modes that were detected for the two panels were in relatively close agreement. The predominant response of mode number 1 was in the central bay; the predominant response of mode number 2 was in the outer bays.

The temperature data obtained in the thermal tests at ambient SPL are a part of Table B-40 (for specimen A-4-1) and Table B-41 (for specimen A-4-2).

B.13 DYNAMIC TESTS OF SPECIMENS A-4-1 AND A-4-2

The temperature data obtained in the thermal-acoustic tests are a part of Tables B-40 and B-41. The rms dynamic strains are in Table B-42 and the average strains at each strain gage during the dynamic runs are in Table B-43.

Oil canning was not observed at the scheduled inspections of strain signals at ambient temperature, 200F, 400F, and 600F during the 139 db and 160 db runs of specimen A-4-1. Oil canning of specimen A-4-2 was observed in the strain signal at 108F during the 139 db run, but the oil canning ceased when the temperature was increased past 110F during the 139 db run. In addition, oil canning of specimen A-4-2 was observed at 200F during the 160 db run.

The strain spectral density of strain gage No. 9 of specimen A-4-2 is shown in Figure B-12 for the thermal-acoustic combinations of 139 db and 160 db SPL and ambient temperature and 200F. The spectral density of the acoustic pressure was much the same as shown in Figure 10.

B.14 INSTRUMENTATION OF SPECIMENS A-5-1 AND A-5-2

Specimen A-5-1 was instrumented with four strain gages and four thermocouples and specimen A-5-2 was instrumented with two strain gages and seven thermocouples. This instrumentation (Figure B-11) survived the tests with combined temperatures and SPL's up to 1000F and 160 db respectively.

The accuracy in the strain readings of the Rene' panels A-5-1 and A-5-2 is significantly less than the accuracy in the strain readings of the aluminum alloy and titanium alloy panels. The corrections for temperature induced apparent strain at the high elevated temperatures was of the same order as the strain readings. There was a considerable reduction in the precision and

Strain Gage No. 9
4.2 Hz Analyzer Bandwidth

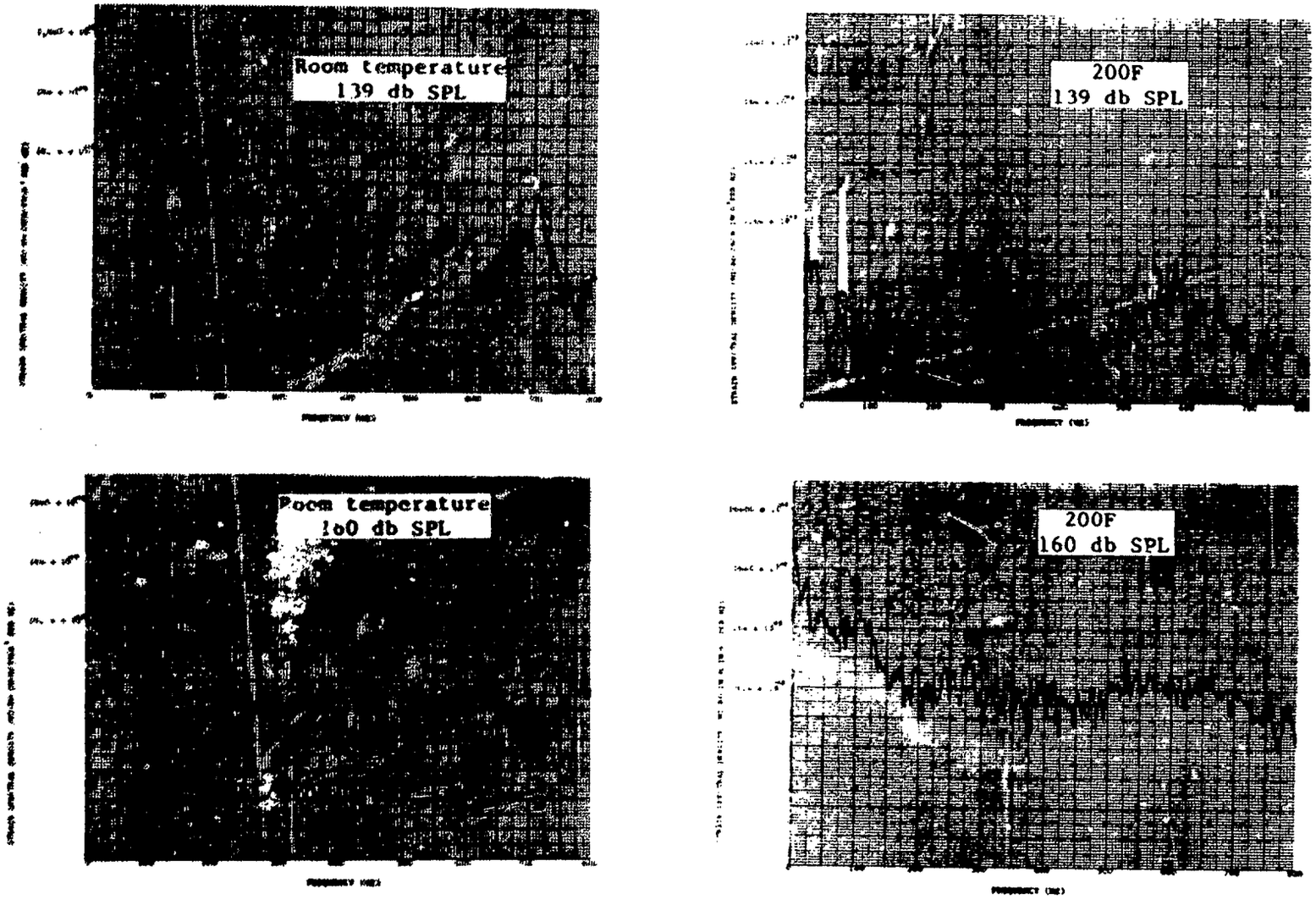

FIGURE B-12. STRAIN SPECTRAL DENSITY OF PANEL A-4-2

accuracy of the strains because they were computed as the difference of large numbers.

B.15 MODAL AND THERMAL TESTS OF SPECIMENS A-5-1 AND A-5-2

The strains that were obtained in the thermal tests at ambient SPL were corrected for temperature induced apparent strains and are given in Table B-44. The strains of the back-to-back gages No. 1 and No. 2 were then added or subtracted to obtain the membrane or bending strain, respectively (Table B-45). The behavior of the strains above approximately 600F indicates that the slipping of the panels in the frictional clamps of the test fixture may have occurred. Prior to the thermal tests at ambient SPL, natural frequencies and phase relations were obtained under loudspeaker excitation and are given in Table B-46.

The temperature data for specimens A-5-1 and A-5-2 at ambient SPL are in Tables B-47 and B-48, respectively.

B.16 DYNAMIC TESTS OF SPECIMENS A-5-1 AND A-5-2

The temperature data for specimens A-5-1 and A-5-2 during the dynamic tests are in Tables B-47 and B-48. The rms dynamic strains are in Table B-49 and the average strains at each strain gage during the dynamic runs are in Table B-50.

Oil canning was not observed at the scheduled inspections of strain signals at ambient temperature, 300F, 600F, and 1000F during the dynamic runs. However, it is quite likely that oil canning occurred as the temperature was increased from ambient temperature to 300F.

Oil canning was observed during the cooldown of panels A-5-1 and A-5-2 from the most severe test condition, i.e., the 160 db SPL test at 1000F. On the cooldown of panel A-5-1, at 150 db SPL and 95F oil canning began. The sound pressure level was immediately dropped to prevent strain gage failures on panel A-5-1.

Oil canning began to occur at 160 db SPL and 170F during the cooldown of panel A-5-2. The oil canning became increasingly more apparent as the temperature dropped to 125F at which time the SPL was dropped to prevent strain gage failures.

The strain spectral density of strain gage No. 1 of specimen A-5-1 is shown in Figure B-13 for the thermal-acoustic combinations of 139 db and 160 db SPL at ambient temperature. The spectral density of the acoustic pressure was much the same as shown in Figure 10.

Strain Gage No. 2
Room temperature
3.2 Hz Analyzer Bandwidth

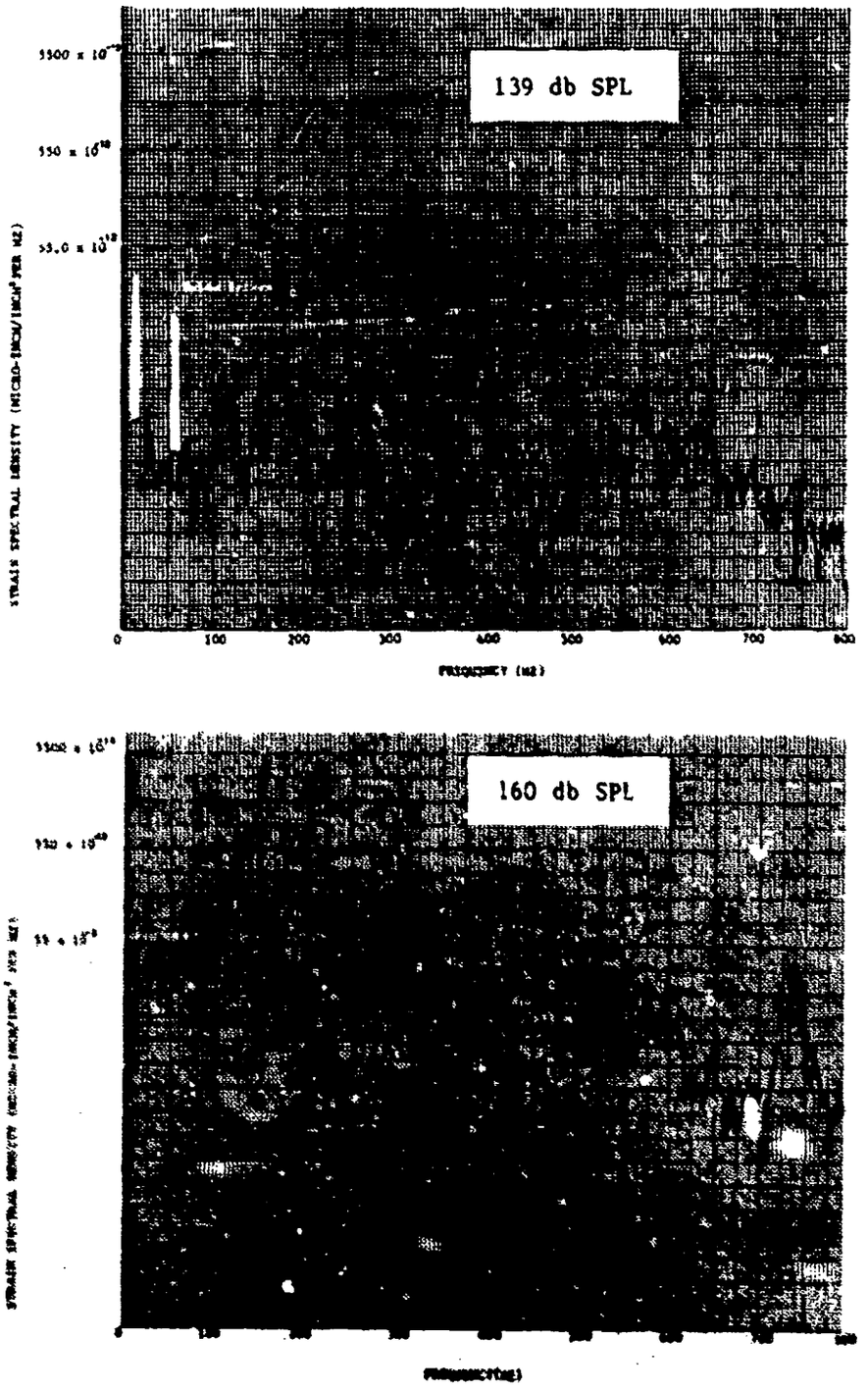

FIGURE B-13. STRAIN SPECTRAL DENSITY OF PANEL A-5-1

TABLE B-1 ORGANIZATION OF EXPERIMENTAL DATA IN APPENDIX B.

Specimen / Strains and Temperature	A-1-1	A-1-2	A-2-1	A-2-2	A-3-1	A-3-2	A-4-1	A-4-2	A-5-1	A-5-2
	Table	Table	Table	Table	Table	Table	Table	Table	Table	Table
Static Strains (Ambient SPL)	B-4	B-10	B-14	B-18	B-26	B-30	B-37	B-37	B-44	B-44
Rms Strains (Acoustic Tests)	B-5	B-11	B-15	B-24	B-29	B-33	B-42	B-42	B-49	B-49
Average Strains (Acoustic Tests)	B-6	B-11	B-16	B-25	B-16	B-35	B-43	B-43	B-50	B-50
Temperatures	B-7	B-12	B-17	B-23	B-28	B-32	B-40	B-41	B-47	B-48
Membrane and Bending Strains	B-8	B-13	B-8	B-19	B-27	B-31	B-38	B-38	B-45	B-45
Natural Frequencies and Damping Factors	B-9	None	B-9	None	B-9	B-36	B-39	B-39	B-46	B-46

TABLE B-2. TEMPERATURE INDUCED APPARENT STRAINS IN TESTS OF 2024-T81 SPECIMENS

Temperature F	Apparent Strain[1] (micro-inch/inch)
78	0
100	10
150	25
200	30
250	15
300	0

(1) Data supplied by Micro-Measurements for Type WK strain gages.

TABLE B-3. TEMPERATURE INDUCED APPARENT STRAINS IN TESTS OF Ti-6Al-4V SPECIMENS

Temperature F	Strain (micro-inch/inch)
75	0
100	40
150	80
200	90
250	80
300	60
350	20
400	-40
450	-120
500	-240
550	-330[1]
600	-516[1]

(1) This strain was obtained by the contractor; all other strains in this table were given by the manufacturer (Micro-Measurements) and confirmed with coupon tests by the contractor.

TABLE B-4 STRAIN RECORDS OF SPECIMEN A-1-1 AT AMBIENT SPL

Nominal Temperature	Strain[1]					
	e_1	e_2	e_5	e_6	e_3	e_4
(F)	(μ"/")	(μ"/")	(μ"/")	(μ"/")	(μ"/")	(μ"/")
78	-12	0	-20	-14	-63	48
100	60	-167	66	-24	-232	174
150	380	-492	424	-261	-594	526
200	582	-696	650	-491	-862	753
250	744	-861	818	-686	-1082	900
300	863	-1003	936	-848	-1267	1010
200	536	-618	542	-151	-790	656

(1) The strains are not corrected for temperature induced apparent strains. Those corrections can be made using the data in Table A-2.

TABLE6-5 DYNAMIC RMS STRAIN RECORDS OF SPECIMEN A-1-1

SPL	Nominal Temperature	Strains					
		e_1	e_2	e_5	e_6	e_3	e_4
(db)	(F)	(μ"/")	(μ"/")	(μ"/")	(μ"/")	(μ"/")	(μ"/")
139	83	82	84	82	69	77	74
139	100	72	77	77	72	58	64
139	200	77	84	72	69	64	64
139	300	82	87	77	72	67	69
160	79	460	480	520	530	410	-
160	100	450	460	480	520	410	-
160	200	565	520	640	720	-	-
160	300	-	-	640	720	-	-

TABLE B-6 AVERAGE STRAINS IN THERMAL-ACOUSTIC TESTS OF SPECIMEN A-1-1

SPL	Nominal Temp.	Strain[1]					
		e_1	e_2	e_5	e_6	e_3	e_4
(db)	(F)	(μ"/")	(μ"/")	(μ"/")	(μ"/")	(μ"/")	(μ"/")
139	Ambient	0	0	-102	0	26	-51
139	100	-36	16	-112	0	41	-61
139	200	-56	-132	-102	-81	-4	-107
139	300	-51	-205	-102	-102	0	-179
160	Ambient	0	0	-128	0	0	-
160	100	-10	-10	-138	-10	-10	-
160	200	-30	-30	-158	-30	-	-
160	300	-	-	-	-	-	-

(1) These strains are not corrected for temperature induced apparent strain.

TABLE B-7 TEMPERATURES OF SPECIMEN A-1-1

SPL	Nominal Temperature	Temperature[1]				
		T_1	T_2	T_4	T_5	T_3
(db)	(F)	(F)	(F)	(F)	(F)	(F)
Ambient	Ambient	78	78	78	78	78
Ambient	100	92	92	98	97	100
Ambient	150	132	130	148	144	152
Ambient	200	164	162	190	184	201
Ambient	250	202	202	237	230	253
Ambient	300	240	240	280	273	300
Ambient	200	186	184	194	188	300
139	Ambient	83	83	83	83	83
139	100	94	94	97	97	100
139	200	162	163	186	178	200
139	300	246	264	277	276	300
160	Ambient	79	79	79	79	79
160	100	93	95	99	100	100
160	200	143	157	-	-	200
160	300	212	262	-	-	298

(1) Note that the specimen center line is horizontal and parallel to the acoustic flow. T_1 and T_4 are downstream of the center of the specimen whereas T_2 and T_5 are upstream of the center of the specimen. T_6 is at the panel center.

TABLE B-8 MEMBRANE AND BENDING STRAINS OF SPECIMENS A-1-1 AND A-2-1

Specimen	Nominal Temperature	Strains					
		$\frac{e_2+e_1}{2}$	$\frac{e_2-e_1}{2}$	$\frac{e_6+e_5}{2}$	$\frac{e_6-e_5}{2}$	$\frac{e_4+e_3}{2}$	$\frac{e_4-e_3}{2}$
	(F)	(μ"/")	(μ"/")	(μ"/")	(μ"/")	(μ"/")	(μ"/")
A-1-1	Ambient	-6	6	-17	3	-7	55
	100	-63	-108	11	-45	-39	153
	150	-81	-436	57	-342	-59	560
	200	-87	-639	50	-570	-85	808
	250	-73	-792	51	-752	-106	991
	300	-70	-933	44	-803	-128	688
	200	-72	-577	65	-446	-97	723

Specimen	Nominal Temperature	Strains							
		$\frac{e_2+e_1}{2}$	$\frac{e_2-e_1}{2}$	$\frac{e_4+e_3}{2}$	$\frac{e_4-e_3}{2}$	$\frac{e_8+e_7}{2}$	$\frac{e_8-e_7}{2}$	$\frac{e_{10}+e_9}{2}$	$\frac{e_{10}-e_9}{2}$
	(F)	(μ"/")	(μ"/")	(μ"/")	(μ"/")	(μ"/")	(μ"/")	(μ"/")	(μ"/")
A-2-1	Ambient	-10	-1	-3	86	-88	-38	-12	-3
	100	-43	-51	-40	95	-13	58	-7	22
	150	-50	-6	-33	95	-15	74	-7	30
	200	-113	-123	-80	115	-38	133	-15	115
	250	-115	-186	-98	105	-33	152	-5	111
	300	-85	-240	-100	120	-45	166	-24	108
	200	-17	32	7	57	55	77	-10	0
	100	18	-20	2	48	66	66	24	-28

TABLE B-9 DAMPING FACTORS AND NATURAL FREQUENCIES OF SPECIMENS A-1-1, A-2-1, AND A-3-1

Specimen	Reference Temperature	Natural Frequency	Non-Dimensional Viscous Damping Factor	Fundamental Frequency
	(F)	(Hz)		(Hz)
A-1-1	83	113 (1)	-	Yes
A-1-1	100	110 (2)	.025 (2)	Yes
A-1-1	200	108 (2)	.033 (2)	Yes
A-1-1	300	106 (2)	.038 (2)	Yes
A-2-1	78	119 (1)	.030 (1)	Yes
A-3-1	79	108 (1)	-	Yes
A-3-1	79	254 (1)	-	No
A-3-1	79	337 (1)	-	No
A-3-1	200	103 (2)	.036 (2)	Yes

(1) Obtained under low level loudspeaker excitation

(2) Obtained under discrete frequency acoustic excitation (approximately 150 db)

TABLE B-10-STRAIN RECORDS OF SPECIMEN A-1-2

AT AMBIENT SPL

Nominal Temperature	Strain (1)					
	e_1	e_2	e_3	e_4	e_5	e_6
(F)	(μ"/")	(μ"/")	(μ"/")	(μ"/")	(μ"/")	(μ"/")
74	-48	18	-10	45	-14	45
80	-10	-78	-62	55	26	-46
85	34	-158	-114	86	82	-132
90	66	-202	-146	110	116	-181
95	130	-285	-211	165	190	-279
100	163	-325	-246	195	226	-323
125	330	-506	-412	346	404	-528
150	444	-627	-534	455	525	-668
200	664	-878	-794	664	754	-940
250	828	-1080	-1020	816	918	-1158
300	955	-1255	-1233	952	1046	-1343
200	621	-805	-822	686	680	-846
80	-23	97	-56	163	0	137

(1) These strains are not corrected for temperature induced apparent strains. Those corrections can be made using the data in Table A-2.

TABLE B-11-STRAIN DATA IN THERMAL - ACOUSTIC

TEST OF SPECIMEN A-1-2

SPL	Nominal Temperature	Static, Rms, and Average Dynamic Strains[4]						Type
		e_1	e_2	e_3	e_4	e_5	e_6	
(db)	(F)	(μ"/")	(μ"/")	(μ"/")	(μ"/")	(μ"/")	(μ"/")	
Amb	Amb	100	-110	-94	58	74	-104	Static
139	Amb	56	44	26	44	58	48	Rms (1)
139	Amb	-128	-128	-180	-102	-26	-26	Average (2)
139	100	44	44	18	34	46	28	Rms
139	100	52	-410	-358	-26	128	-384	Average
139	200	18	18	18	18	18	18	Rms
139	200	512	-1024	-870	384	640	-1024	Average
139	300	20	20	18	18	18	18	Rms
139	300	768	-1432	-1306	540	896	-1484	Average
Amb	Amb	110	-144	out	out	out	-64	Static
160	Amb	384	410	--	--	--	410	Rms
160	Amb	-204	0	--	--	--	0	Average
160	100	460	436	--	--	--	486	Rms
160	100	-256	0	--	--	--	-384	Average
160	200	484	460	--	--	--	358	Rms
160	200	384 -1024*	-640 1024*	--	--	--	-768 768	Average
160	300	180	166	--	--	--	128	Rms
160	300	768 -1024*	-1150 1024*	--	--	--	-1280 +?*	Average

Notes:

The asterisk means an occasional shift to oscillations about the noted mean level.

1) The static strains were recorded immediately prior to the conduct of the 139 db and 160 db runs.
2) The dynamic rms strain
3) The strain about which strain fluctuations were observed.
4) These average strains are not corrected for temperature induced apparent strain.

TABLE B-12. TEMPERATURES OF SPECIMEN A-1-2

SFL	Nominal Temperature	Temperature			Nominal Temperature	Temperature		
		T_1	T_3	T_2		T_1	T_3	T_2
(db)	(F)	(F)	(F)	(F)	(F)	(F)	(F)	(F)
Ambient	Ambient	74	74	74	150	135	147	135
Ambient	80	77	81	80	200	180	201	176
Ambient	85	84	86	85	250	225	253	218
Ambient	90	87	89	90	300	266	301	258
Ambient	95	92	97	94	200	195	194	191
Ambient	100	97	101	98	Ambient	81	81	81
Ambient	125	115	125	118				
139	Ambient	75	75	75				
139	100	97	99	94				
139	200	180	200	178				
139	300	-	301	272				
160	Questionable temperature data							

TABLE B-13 MEMBRANE AND BENDING STRAIN

OF SPECIMEN A-1-2

Nominal Temperature	Strains					
	$\frac{e_2 + e_1}{2}$	$\frac{e_2 - e_1}{2}$	$\frac{e_4 + e_3}{2}$	$\frac{e_4 - e_3}{2}$	$\frac{e_6 + e_5}{2}$	$\frac{e_6 - e_5}{2}$
(F)	(μ"/")	(μ"/")	(μ"/")	(μ"/")	(μ"/")	(μ"/")
75	15	33	18	28	15	30
80	-49	-34	-9	59	-15	-36
85	-69	-96	-19	100	-30	-107
90	-73	-134	-23	128	-38	-148
95	-88	-208	-33	188	-55	-235
100	-91	-244	-35	220	-58	-275
125	-108	-418	-53	379	-82	-466
150	-117	-536	-65	495	-97	-596
200	-137	-771	-95	729	-123	-847
250	-141	-954	-117	918	-135	-1038
300	-150	-1110	-140	1092	-149	-1194
200	-122	-713	-98	754	-117	-763
80	37	60	54	110	68	68

TABLE B-14 STRAIN RECORDS OF SPECIMEN A-2-1 AT AMBIENT SPL

Nominal Temperature	Strain									
	e_1	e_2	e_3	e_4	e_5	e_6	e_7	e_8	e_9	e_{10}
(F)	(μ"/")	(μ"/")	(μ"/")	(μ"/")	(μ"/")	(μ"/")	(μ"/")	(μ"/")	(μ"/")	(μ"/")
78	-10	-9	-88	83	-34	-59	-49	-126	-10	-15
100	18	-84	-126	65	-32	-14	-61	56	-18	25
150	-19	-31	-103	87	-4	-43	-64	84	-11	48
200	40	-206	-164	65	42	-41	-142	125	-100	130
250	87	-286	-188	22	58	-54	-170	134	-101	121
300	155	-324	-220	20	56	-66	-211	121	-132	84
200	-19	45	-20	93	134	-58	8	161	20	19
100	48	8	-35	60	68	-22	10	142	15	-42

TABLE B-15 DYNAMIC RMS STRAIN RECORDS OF SPECIMEN A-2-1

SPL	Nominal Temperature	Strains									
		e_1	e_2	e_3	e_4	e_5	e_6	e_7	e_8	e_9	e_{10}
(db)	(F)	(μ"/")	(μ"/")	(μ"/")	(μ"/")	(μ"/")	(μ"/")	(μ"/")	(μ"/")	(μ"/")	(μ"/")
139	87	56	51	79	79	36	90	96	96	120	118
139	100	56	49	74	74	—	90	96	96	113	113
139	200	69	54	64	64	—	92	96	90	105	108
139	300	66	49	59	60	—	96	90	88	100	[illegible]
160	75	410	395	—	425	—	435	460	525	460	—
160	100	435	425	—	450	—	460	—	—	485	—
160	200	480	450	—	475	—	485	—	—	435	—
160	300	500	—	—	—	—	—	—	—	—	—

TABLE B-16 AVERAGE STRAINS IN THERMAL-ACOUSTIC TESTS

Specimen	SPL	Nominal Temp.	Strain										
			e_1	e_2	e_3	e_4	e_5	e_6	e_7	e_8	e_9	e_{10}	e_{11}
	(db)	(F)	(μ"/")	(μ"/")	(μ"/")	(μ"/")	(μ"/")	(μ"/")	(μ"/")	(μ"/")	(μ"/")	(μ"/")	(μ"/")
A-2-1	139	Ambient	0	13	-26	26	26	0	51	-51	-105	-105	
	139	100	-23	41	-74	41	-	-61	28	-61	-151	-138	
	139	200	-94	-184	-158	21	-	-56	-107	-94	-222	-158	
	139	300	-	-240	-256	51	-	-192	-179	-141	-245	-205	
	160	Ambient	0	0	-	64	-	0	128	-	128	-	
	160	100	-74	54	-	118	-	246	-	-	246	-	
	160	200	-235	162	-	226	-	98	-	-	354	-	
	160	300	-256	-	-	-	-	-	-	-	0	-	
A-1-1	139	Ambient	-26	-26	-128	-102	-52	-102	0	-51	-102	-179	-153
	139	100	-87	-177	-36	0 (1) -368	195 (1) -368	0 (1) -358	118	0 (1) -215	-138	-189	0 (1) -522
	139	200	-143	-440	560	-950	-1160	-900	556	-542	-312	-158	534
	139	300	-128	-590	793	-1150	-1380	-970	640	-640	-410	-205	665
	160	Ambient	-26	-26	-128	-205	-153	-205	-103	-256	-256	-205	-256
	160	100	-62	-62	-	-112	-138	-	0	-215	-215	-112	-246
	160	200	-82	-440	-	502 -797	610 -797	-	482 -542	72 -678	-	-158 98	128 -1180
	160	300	26 (1) -128	184 (1) -256	-	716 -1150	-	-	767 -767	512 -767	-	-102 102	60 -1530

(1) Occasionally

TABLE B-17 TEMPERATURES OF SPECIMEN A-2-1

SPL	Nominal Temperature	Temperature (1)											
		T_1	T_2	T_3	T_4	T_5	T_6	T_7	T_8	T_9	T_{10}	T_{11}	T_{12}
(db)	(F)	(F)	(F)	(F)	(F)	(F)	(F)	(F)	(F)	(F)	(F)	(F)	(F)
Ambient	Ambient	78	78	78	78	78	78	78	78	78	78	78	78
Ambient	100	100	100	100	100	95	93	100	100	101	94	97	94
Ambient	150	150	144	150	150	142	135	146	144	150	140	141	136
Ambient	200	203	191	200	200	189	176	200	193	202	186	188	176
Ambient	250	254	235	250	250	234	215	250	238	251	231	231	214
Ambient	300	302	286	295	295	285	250	299	281	301	272	271	250
Ambient	200	224	200	218	220	225	205	208	196	200	224	206	201
Ambient	100	101	99	101	102	104	103	99	99	99	105	101	101
139	Ambient	87	87	87	87	87	87	87	87	87	87	87	87
139	100	101	101	101	101	99	99	100	100	101	99	99	99
139	200	182	181	185	183	158	151	188	188	200	154	171	155
139	300	285	275	284	287	250	235	284	283	300	246	264	241
160	Ambient	78	78	78	78	78	78	78	78	78	78	78	78
160	100	97	97	98	99	93	90	98	99	100	90	95	94
160	200	195	195	192	193	179	171	193	197	202	162	183	172
160	300	276	268	273	280	260	244	275	276	300	238	257	238

(1) Temperatures T_5, T_6, T_{10}, and T_{12} are at the four corners of the specimen. T_5 is downstream at the panel top, T_{10} is upstream at the panel top, T_6 is upstream at the panel bottom, and T_{12} is downstream at the panel bottom.

TABLE B-18 STRAIN RECORDS OF SPECIMEN A-2-2 AT AMBIENT SPL

TEMPERATURE	STRAIN									
	e_1	e_2	e_3	e_4	e_5	e_6	e_7	e_8	e_9	e_{10}
(F)	(μ"/")	(μ"/")	(μ"/")	(μ"/")	(μ"/")	(μ"/")	(μ"/")	(μ"/")	(μ"/")	(μ"/")
70	-89	93	-6	38	-38	120	-79	12	-124	116
100	-304	404	120	-126	-394	445	-95	-50	-204	25
150	-490	668	138	-255	-706	803	-109	-135	-255	-67
200	-675	574	320	-620	-940	1011	-366	-59	-424	-116
250	-958	932	494	-808	-1125	1292	-543	-67	-624	-226
300	-1196	1280	624	-954	-1335	1535	-720	-67	-789	-310
200	-570	738	535	-726	-815	740	-232	18	-293	-28
90	-1	-7	-48	55	-22	34	55	160	-50	197

TEMPERATURE	STRAIN									
	e_{11}	e_{12}	e_{13}	e_{14}	e_{15}	e_{16}	e_{17}	e_{18}	e_{19}	e_{20}
(F)	(μ"/")	(μ"/")	(μ"/")	(μ"/")	(μ"/")	(μ"/")	(μ"/")	(μ"/")	(μ"/")	(μ"/")
70	12	-101	18	-153	48	-150	-440	245	-246	3
100	-97	-270	412	-389	-60	-356	-470	174	45	-240
150	227	-462	599	-326	-208	-535	-490	99	134	-358
200	-286	-650	640	-176	-344	-772	-544	210	-1344	848
250	-404	-985	663	-73	-522	-1003	-571	261	-1667	1265
300	-506	-1285	647	-35	-652	-1230	-606	334	-1820	1518
200	-192	-400	246	62	-197	-461	-459	275	-990	541
90	59	-70	20	16	71	-95	-450	230	-310	127

TABLE B-19 MEMBRANE AND BENDING STRAINS OF SPECIMEN A-2-2 AT AMBIENT SPL

TEMPERATURE	STRAIN									
	$\frac{\varepsilon_2+\varepsilon_1}{2}$	$\frac{\varepsilon_2-\varepsilon_1}{2}$	$\frac{\varepsilon_4+\varepsilon_3}{2}$	$\frac{\varepsilon_4-\varepsilon_3}{2}$	$\frac{\varepsilon_6+\varepsilon_5}{2}$	$\frac{\varepsilon_6-\varepsilon_5}{2}$	$\frac{\varepsilon_8+\varepsilon_7}{2}$	$\frac{\varepsilon_8-\varepsilon_7}{2}$	$\frac{\varepsilon_{10}+\varepsilon_9}{2}$	$\frac{\varepsilon_{10}-\varepsilon_9}{2}$
(F)	(μ"/")	(μ"/")	(μ"/")	(μ"/")	(μ"/")	(μ"/")	(μ"/")	(μ"/")	(μ"/")	(μ"/")
70	2	47	16	22	41	79	-33	46	-4	120
100	40	354	-13	-121	16	419	-82	22	-99	115
150	64	579	-93	-146	23	755	-147	-13	-186	94
200	-80	625	-180	-470	6	975	-246	153	-300	154
250	-18	945	-172	-651	68	1208	-320	288	-440	199
300	42	1238	-165	-789	100	1435	-394	327	-550	240
200	54	654	-126	-630	-68	788	-137	126	-190	132
100	-14	-3	-6	-52	-4	28	98	53	68	124

TEMPERATURE	STRAIN									
	$\frac{\varepsilon_{12}+\varepsilon_{11}}{2}$	$\frac{\varepsilon_{12}-\varepsilon_{11}}{2}$	$\frac{\varepsilon_{14}+\varepsilon_{13}}{2}$	$\frac{\varepsilon_{14}-\varepsilon_{13}}{2}$	$\frac{\varepsilon_{16}+\varepsilon_{15}}{2}$	$\frac{\varepsilon_{16}-\varepsilon_{15}}{2}$	$\frac{\varepsilon_{18}+\varepsilon_{17}}{2}$	$\frac{\varepsilon_{18}-\varepsilon_{17}}{2}$	$\frac{\varepsilon_{20}+\varepsilon_{19}}{2}$	$\frac{\varepsilon_{20}-\varepsilon_{19}}{2}$
(F)	(μ"/")	(μ"/")	(μ"/")	(μ"/")	(μ"/")	(μ"/")	(μ"/")	(μ"/")	(μ"/")	(μ"/")
70	-45	-56	67	-85	-51	-99	-98	342	-121	-125
100	-193	-86	2	-400	-218	-148	-158	322	-107	-142
150	-369	-118	111	-462	-356	-163	-220	295	-137	-246
200	-498	-182	202	-408	-588	-213	-202	377	-278	+1096
250	-709	-291	265	-368	-777	-240	-170	416	-216	+1466
300	-895	-389	306	-341	-961	-289	-136	470	-151	+1669
200	-326	-104	122	-92	-299	-132	-122	372	-255	+765
100	-16	-65	8	-2	2	-83	-120	340	-112	+218

TABLE B-20 NONDIMENSIONAL MEMBRANE STRESS OF SPECIMEN A-2-2 AT AMBIENT SPL

TEMPERATURE	NONDIMENSIONAL MEMBRANE STRESS, $\frac{S(1-\mu^2)}{E} = \frac{8S}{9E}$									
(F)	$\frac{S_1+S_2}{2}$	$\frac{S_3+S_4}{2}$	$\frac{S_5+S_6}{2}$	$\frac{S_7+S_8}{2}$	$\frac{S_9+S_{10}}{2}$	$\frac{S_{11}+S_{12}}{2}$	$\frac{S_{13}+S_{14}}{2}$	$\frac{S_{15}+S_{16}}{2}$	$\frac{S_{17}+S_{18}}{2}$	$\frac{S_{19}+S_{20}}{2}$
70	-13	38	24	-66	-84	-44	72	-37	-109	-122
100	-24	-12	-57	-135	-135	-180	-2	-213	-185	-140
150	-59	-56	-109	-220	-232	-348	80	-388	-269	-199
200	-246	-113	-193	-313	-393	-525	142	-586	-284	-378
250	-254	-184	-191	-377	-512	-715	208	-754	-277	-363
300	-256	-63	-214	-439	-600	-881	251	-908	-267	-334
200	-55	-157	-168	-178	-275	-308	-134	-322	-168	-318
100	-19	-7	-3	58	31	-21	-4	1	-87	-89

TABLE B-21 NONDIMENSIONAL BENDING STRESS OF SPECIMEN A-2-2 AT AMBIENT SPL

TEMPERATURE	NONDIMENSIONAL BENDING STRESS, $\frac{S(1-\mu^2)}{E} = \frac{8S}{9E}$									
(F)	$\frac{S_2-S_1}{2}$	$\frac{S_4-S_3}{2}$	$\frac{S_6-S_5}{2}$	$\frac{S_8-S_7}{2}$	$\frac{S_{10}-S_9}{2}$	$\frac{S_{12}-S_{11}}{2}$	$\frac{S_{14}-S_{13}}{2}$	$\frac{S_{16}-S_{15}}{2}$	$\frac{S_{18}-S_{17}}{2}$	$\frac{S_{20}-S_{19}}{2}$
70	77	-6	46	160	78	-24	-78	-73	349	-85
100	325	-256	370	129	68	32	-441	-8	329	-104
150	540	-317	701	85	12	75	-527	89	291	-215
200	564	-606	904	279	519	26	-565	112	428	1147
250	848	-774	1128	427	688	24	-585	163	512	1532
300	1108	-903	1339	484	796	24	-604	189	579	1749
200	629	-661	744	250	387	117	-312	131	414	809
100	-25	-53	0	166	197	-66	-19	-74	358	259

TABLE B-22 NONDIMENSIONAL STRESSES OF SPECIMEN A-2-2 AT AMBIENT SPL

TEMPERATURE	NONDIMENSIONAL STRESS OF $\frac{8S \times 10^{-6}}{9E}$									
(F)	S_1	S_2	S_3	S_4	S_5	S_6	S_7	S_8	S_9	S_{10}
70	-85	59	0	-13	-22	70	-226	94	-206	117
100	-346	304	-27	-266	-424	314	-262	-2	-199	-65
150	-591	489	-87	-389	-800	600	-297	-127	-235	-211
200	-800	327	77	-709	-1085	724	-577	-19	-902	-197
250	-1108	589	258	-847	-1314	943	-748	5	-1197	181
300	-1365	852	408	-966	-1552	1125	-922	44	-1396	196
200	-674	575	438	-725	-911	556	-415	80	-653	122
100	9	-40	-51	50	-8	-8	-105	227	-163	229

TEMPERATURE	NONDIMENSIONAL STRESS OF $\frac{8S \times 10^{-6}}{9E}$									
(F)	S_{11}	S_{12}	S_{13}	S_{14}	S_{15}	S_{16}	S_{17}	S_{18}	S_{19}	S_{20}
70	-18	-70	16	-139	35	-110	-466	249	-287	42
100	-208	-145	442	-441	-201	-218	-512	147	-33	-242
150	-415	-186	620	-436	-468	-292	-551	29	24	-405
200	-541	-489	717	-513	-687	-465	-691	160	-1515	779
250	-738	-689	813	-357	-912	-567	-767	224	-1890	1165
300	-905	-858	855	-353	-1097	-718	-846	312	-2083	1415
200	-412	-184	394	-210	-499	-244	-566	251	-1113	502
100	59	-82	-6	-12	54	-94	-442	273	-337	183

TABLE B-23 TEMPERATURES OF SPECIMEN A-2-2

RUN NO.	SPL	NOMINAL TEMPERATURE	TEMPERATURE				
			T_1 (1)	T_2 (1)	T_3 (1)	T_4 (1)	T_5 (1)
	(db)	(F)	(F)	(F)	(F)	(F)	(F)
	Ambient	Ambient	70	70	70	70	70
	Ambient	100	88	89	95	94	102
	Ambient	150	120	122	139	134	150
	Ambient	200	158	160	187	180	200
	Ambient	250	200	200	237	225	252
	Ambient	300	245	243	285	273	301
	Ambient	200	195	184	208	205	200
	Ambient	90	92	90	90	92	90
1	139	Ambient	74	74	74	74	74
1	139	100	84	87	92	92	100
1	139	200	142	145	171	170	200
1	139	300	212	216	258	257	300
1	160	Ambient	80	80	80	80	80
1	160	100	86	87	94	94	100
1	160	200	150	146	178	170	out (2)
1	160	300	215	200	258	250	out (2)
2	139	Ambient	70	70	70	70	out (2)
2	139	100	86	86	92	92	out (2)
2	139	200	140	140	170	169	out (2)
2	139	300	208	-	258	257	out (2)

(1) T_1 and T_2 are at the middle of the short ends; T_3 and T_4 are at the long edges; and T_5 is at the panel center. All five of the thermocouples are on the surface not exposed to the lamps.

(2) The thermocouple T_5 came off the panel during the 160 db run. The control of the panel temperature was changed to the average of T_3 and T_4 using the T_3 vs T_4 vs T_5 relation established in run number 1 at 139 db.

TABLE B-24 DYNAMIC RMS STRAIN RECORDS[4] OF SPECIMEN A-2-2

RUN NO.	SPL	NOMINAL TEMPERATURE	STRAINS									
			e_2	e_4	e_6	e_8	e_{10}	e_{12}	e_{14}	e_{16}	e_{18}	e_{20}
	(db)	(F)	(μ"/")	(μ"/")	(μ"/")	(μ"/")	(μ"/")	(μ"/")	(μ"/")	(μ"/")	(μ"/")	(μ"/")
1	139	74	92	77	103	20	20	20	64	49(1)	43(1)	77
1	139	100(3)	128	56	123	24	24	24	103	51(1)	43(1)	87
1	139	200	92	36	51(1)	20	24	24	67	51(1)	43(1)	46
1	139	300	107	36	69(1)	20	24	26	46	51(1)	43(1)	87
1	160	80	410	356	422	44	44	61	235	87	54	358
1	160	100	435	396	460	49	49	66	305	100	59	out
1	160	200(3)	715	690	765	77	51	136	435	176	72	out
1	160	300	143	97	103	36	33	46	77	72	46(1)	out
2	139	74	108	100	118	23	23	23	82	51(1)	44(1)	out
2	139	100	97	76	103	23	23	23	97	51(1)	44(1)	out
2	139	200	20	20	36	23	23	26	51	51(1)	44(1)	out
2	139	300	20	23	23	23	23	23	44	51(1)	44(1)	out

(Continued on next page)

TABLE B-24 DYNAMIC RMS STRAIN RECORDS[4] OF SPECIMEN A-2-2 (COMPLETED)

RUN NO.	SPL	NOMINAL TEMPERATURE	STRAINS									
			e_1	e_3	e_5	e_7	e_9	e_{11}	e_{13}	e_{15}	e_{17}	e_{19}
	(db)	(°)	(μ"/")	(μ"/")	(μ"/")	(μ"/")	(μ"/")	(μ"/")	(μ"/")	(μ"/")	(μ"/")	(μ"/")
1	139	74	80	92	92	18	22	22	72	40(1)	44(1)	92
1	139	100(3)	98	122	66	22	22	22	138	40(1)	40(1)	138
1	139	200	30	66	30	20	22	26	64	40(1)	40(1)	72
1	139	300	38	30	26	26	22	22	46	40(1)	40(1)	48
1	160	80	384	384	420	42	42	62	230	76	48	410
1	160	100	396	408	460	42	52	72	308	82	52	436
1	160	200(3)	716	640	870	76	60	134	486	134	64	486
1	160	300	84	128	-	42	38	82	128	92	40(1)	98
2	139	74	100	115	out	20	23	23	84	41(1)	41(1)	97
2	139	100(2)	79	104	out	20	23	23	97	41(1)	41(1)	97
2	139	200	20	41	out	20	23	26	51	41(1)	41(1)	46
2	139	300	20	26	out	20	23	23	46	41(1)	41(1)	46

(1) The reading is in the noise floor of the recording and playback instrumentation

(2) On the threshold of oil canning

(3) Oil canning

(4) All strain gages with odd numbers are on the surface that is not exposed to the heating lamps and all strain gages with even numbers are on the surface that is exposed to the heating lamps.

TABLE B-25 AVERAGE STRAIN RECORDS[2] OF SPECIMEN A-2-2

RUN NO.	SPL	NOMINAL TEMPERATURE	STRAIN									
			e_2	e_4	e_6	e_8	e_{10}	e_{12}	e_{14}	e_{16}	e_{18}	e_{20}
	(db)	(F)	(μ"/")	(μ"/")	(μ"/")	(μ"/")	(μ"/")	(μ"/")	(μ"/")	(μ"/")	(μ"/")	(μ"/")
1	139	74	-103	-154	-256	-204	-256	-307	51	0	0	0
1	139	100	154	-307	0				-308			-204
			-307	103	-512	-282	-307	-410	256	-154	-51	256
1	139	200	512	-512	615	-409	-562	-895	-384	-562	-230	-615
1	139	300	767	-920	895	358	-715	-1530	-204	-1280	0	1280
1	160	80	-128	-256	-256	-128	-256	-205	51	205	128	out
1	160	100	-128	-256	-256	-154	-282	-256	103	128	0	out
1	160	200	615	-562	512	-358	-512	-615	-256	-358	-128	out
1	160	300	1025	-920	1025	-665	-715	-895	0	-715	-205	out
2	139	74	0	-153	-256	-256	-384	-512	0	-128	103	0
2	139	100	0	-256	-256	-307	-410	-512	-128	-102	153	out
2	139	200[1]	-766	766	512	-384	563	-512	512	-256	154	
			766	-766	-1025	-154	-256	-768	-256	-768	0	out
2	139	300	-1025	1025	-1280	-768	-820	-768	51	-640	-410	out

(Continued on next page)

TABLE B-25 AVERAGE STRAIN RECORDS[2] OF SPECIMEN A-2-2 (COMPLETED)

RUN NO.	SPL	NOMINAL TEMPERATURE	STRAIN									
			e_1	e_3	e_5	e_7	e_9	e_{11}	e_{13}	e_{15}	e_{17}	e_{19}
	(db)	(F)	(μ"/")	(μ"/")	(μ"/")	(μ"/")	(μ"/")	(μ"/")	(μ"/")	(μ"/")	(μ"/")	(μ"/")
1	139	74	-128	-256	-205	-205	-256	-308	51	0	51	205
1	139	100[1]	-308 102	-51	-460 256	-205	-282	-410	-256 256	-128	0	256
1	139	200	-640	0	-700	-256	-410	-640	564	410	0	715
1	139	300	-1080	256	1330	-715	-820	-1540	665	-640	-154	-1150
1	160	80	0	-256	0	-230	-308	-384	0	-128	128	256
1	160	100	0	-256	0	-256	-308	-460	128	-102	179	256
1	160	200[1]	-512 768	512 -1020	-895 768	-154 -410	-384	-564 -895	615 -384	-256 -512	0 -154	768 -768
1	160	300	1025	-1075	1025	-154	562	-1025	-522	-640	102	1410
2	139	74	-256	-308	out	-102	-179	-256	51	0	205	307
2	139	100	-205	-256	out	-128	-230	-256	102	0	153	307
2	139	200	-715	51	out	-179	-358	-512	410	-256	102	870
2	139	300	-920	154	out	-256	-485	-870	485	-562	153	1280

(1) Oil canning.

(2) All strain gages with odd numbers are on the surface that is not exposed to the heating lamps and all strain gages with even numbers are on the surface that is exposed to the heating lamps. These average strains were not corrected for temperature induced apparent strain.

TABLE B-26 STRAIN RECORDS OF SPECIMEN A-3-1 AT AMBIENT SPL

Nominal Temperature	Strain										
	e_1	e_2	e_3	e_{11}	e_5	e_6	e_7	e_8	e_9	e_{10}	e_4
(F)	(μ"/")	(μ"/")	(μ"/")	(μ"/")	(μ"/")	(μ"/")	(μ"/")	(μ"/")	(μ"/")	(μ"/")	(μ"/")
78	-133	-113	1	44	-180	-232	72	-108	-11	10	0
100	-198	-224	408	464	-610	-552	383	-222	-83	42	-370
150	-244	-328	735	760	-960	-762	582	-362	-185	48	-670
200	-263	-450	850	858	-1150	-840	604	-435	-246	37	-815
250	-274	-528	924	875	-1240	-861	560	-470	-276	10	-910
300	-292	-606	954	869	-1294	-918	570	-530	-314	-37	-975
200	-160	-237	27	40	-36	-347	-3	-250	-78	-51	-205
100	-66	104	10	30	82	65	39	114	39	19	231

TABLE B-27 AVERAGE AND BENDING STRAINS FOR PANEL A-3-1 AT AMBIENT SPL

TEMPERATURE	STRAINS (1)					
	$\frac{e_4 + e_3}{2}$	$\frac{e_4 - e_3}{2}$	$\frac{e_{11} + e_5}{2}$	$\frac{e_{11} - e_5}{2}$	$\frac{e_6 + e_7}{2}$	$\frac{e_6 - e_7}{2}$
(F)	(μ"/")	(μ"/")	(μ"/")	(μ"/")	(μ"/")	(μ"/")
Ambient	0	-1	-68	-112	-80	-152
100	9	-389	-83	-537	-94	-468
150	7	-702	-125	-860	-115	-672
200	-13	-832	-176	-1004	-148	-722
250	-8	-917	-197	-1052	-165	-710
300	-10	-964	-212	-1082	-174	-744
200	-119	-116	-28	-38	-205	-172
100	100	120	16	26	42	13

(1) These strains have been corrected for temperature induced apparent strain.

TABLE B-28 TEMPERATURE OF SPECIMEN A-3-1

SPL	Nominal Temperature	Temperature (1)											
		T_1	T_2	T_3	T_4	T_5	T_6	T_7	T_8	T_9	T_{10}	T_{11}	T_{12}
(db)	(F)	(F)	(F)	(F)	(F)	(F)	(F)	(F)	(F)	(F)	(F)	(F)	(F)
Ambient	Ambient	73	73	73	73	73	73	73	73	73	73	73	73
Ambient	100	99	96	91	96	94	90	100	90	90	90	90	100
Ambient	150	146	140	125	139	134	121	150	122	120	122	123	150
Ambient	200	192	181	156	179	172	150	200	159	150	159	159	200
Ambient	250	239	224	190	220	210	182	250	192	182	194	194	250
Ambient	300	288	270	225	265	252	216	300	234	218	238	238	300
Ambient	200	202	195	226	189	184	168	200	191	180	194	188	201
Ambient	100	105	107	108	105	105	105	101	120	119	122	120	101
139	Ambient	79	79	79	79	79	79	79	79	79	79	79	79
139	100	96	94	90	97	97	92	100	90	90	90	90	100
139	200	176	168	142	185	178	152	200	144	143	146	149	200
139	300	264	248	202	278	264	216	300	210	208	214	217	300
160	Ambient	82	82	82	82	82	82	82	82	82	82	82	82
160	100	99	98	93	99	98	93	100	93	92	92	93	100
160	200	179	170	140	190	180	150	200	150	153	148	162	200
160	300	254	241	192	266	254	206	300	202	208	200	218	300

(1) Note that temperatures T_6 through T_{11} are measured along the panel center lines. T_6 is upstream, T_9 is downstream, T_{10} is at the top of the panel and T_{11} is at the bottom of the panel. T_3 is on the upstream stiffener and T_8 is on the downstream stiffener.

TABLE B-29 DYNAMIC RMS STRAIN RECORDS OF SPECIMEN A-3-1

SPL	Nominal Temperature	Strains										
		e_1	e_2	e_3	e_4	e_5	e_6	e_7	e_8	e_9	e_{10}	e_{11}
(db)	(F)	(μ"/")	(μ"/")	(μ"/")	(μ"/")	(μ"/")	(μ"/")	(μ"/")	(μ"/")	(μ"/")	(μ"/")	(μ"/")
139	79	20	33	64	72	82	87	69	46	34	23	87
139	100	31	39	133	108	123	123	148	46	34	28	164
139	200	31	21	26	30	33	43	41	36	30	26	31
139	300	36	23	26	30	31	41	36	36	30	23	28
160	82	110	225	260	280	360	380	335	320	180	123	350
160	100	126	280	–	345	410	–	360	345	192	144	410
160	200	172	360	–	505	590	–	515	487	–	169	640
160	300	200	410	–	610	–	–	565	540	–	195	760

TABLE B-30 STRAIN RECORDS OF SPECIMEN A-3-2 AT AMBIENT S?L

NOMINAL TEMPERATURE	STRAIN											
	e_1	e_2	e_3	e_4	e_5	e_6	e_7	e_8	e_9	e_{10}	e_{11}	e_{12}
(F)	(μ"/")	(μ"/")	(μ"/")	(μ"/")	(μ"/")	(μ"/")	(μ"/")	(μ"/")	(μ"/")	(μ"/")	(μ"/")	(μ"/")
68	20	-30	-34	-31	54	-128	-63	-84	-123	59	-22	-12
100	198	-136	428	-434	369	-460	12	-366	-620	545	-32	53
150	398	-146	749	-701	556	-656	65	-546	-966	860	11	157
200	574	-184	941	-874	652	-763	151	-632	-1160	1012	48	243
250	692	-218	1018	-967	628	-752	372	-612	-1290	1078	68	282
300	464	-420	982	-1024	596	-720	574	-572	-1380	1118	64	287
200	104	-276	322	-478	266	-482	6	-442	-688	492	66	216
76	0	-35	-140	55	-32	-32	-6	-10	-35	-71	96	83

TABLE B-31 MEMBRANE AND BENDING STRAINS OF SPECIMEN A-3-2 AT AMBIENT SPL

TEMPERATURE	STRAIN (1)					
	$\frac{e_4 + e_3}{2}$	$\frac{e_4 - e_3}{2}$	$\frac{e_{10} + e_9}{2}$	$\frac{e_{10} - e_9}{2}$	$\frac{e_6 + e_5}{2}$	$\frac{e_6 - e_5}{2}$
(F)	(μ"/")	(μ"/")	(μ"/")	(μ"/")	(μ"/")	(μ"/")
68	-32	2	-32	91	-37	-90
100	-13	-431	-48	582	-56	-415
150	-1	-725	-75	916	-75	-616
200	4	-908	-104	1086	-86	-708
250	10	-943	-121	1184	-77	-690
300	4[illegible]	-1003	-131	1249	-62	-658
200	-106	-400	-128	590	-138	-374
76	-42	96	-53	-18	-32	0

(1) The strain corrections for temperature induced apparent strain are based upon the nominal temperature of the run, rather than on the actual temperature of the gage.

TABLE B-32 TEMPERATURES OF SPECIMEN A-3-2

SPL	NOMINAL TEMPERATURE	TEMPERATURE							NOTES
(db)	(F)	T_1 (F)	T_3 (F)	T_4 (F)	T_6 (F)	T_7 (F)	T_{10} (F)	T_{11} (F)	
Ambient	Ambient	68	68	68	68	68	68	68	
Ambient	100	97	90	94	89	100	85	91	
Ambient	150	142	125	134	120	150	114	128	
Ambient	200	197	156	176	147	200	144	162	
Ambient	250	234	192	220	180	250	180	204	
Ambient	300	280	227	264	214	300	220	245	
Ambient	200	199	174	186	164	200	181	192	On cool down
Ambient	Ambient	76	76	76	76	76	76	76	On cool down
139	Ambient	76	76	76	76	76	76	76	
139	100	95	90	97	90	101	86	91	
139	200	174	145	185	153	200	140	160	
139	300	154	205	276	218	300	206	234	
160	Ambient	70	70	70	70	70	70	70	
160	100	94	85	97	86	100	85	92	
160	200	171	136	180	142	195	141	161	
160	300	257	206	280	216	299	208	240	

TABLE B-33 DYNAMIC RMS STRAIN RECORDS OF SPECIMEN A-3-2

SPL	NOMINAL TEMPERATURE	STRAINS											
		e_1	e_2	e_3	e_4	e_5	e_6	e_7	e_8	e_9	e_{10}	e_{11}	e_{12}
(db)	(F)	(μ"/")	(μ"/")	(μ"/")	(μ"/")	(μ"/")	(μ"/")	(μ"/")	(μ"/")	(μ"/")	(μ"/")	(μ"/")	(μ"/")
139	76	36	23	92	67	69	69	38	36	82	90	26	28
139	100	46	21	59	26	44	36	74	36	33	51	26	26
139	200	33	18	20	20	49	69	148	64	25	23	20	20
139	300	38	18	20	20	31	31	46	46	26	23	20	20
160	70	230	254	282	282	282	358	282	308	358	358	85	123
160	100	286	282	333	333	333	410	384	396	435	435	138	189
160	200(1)	332	308	384	384	384	435	410	410	510	510	164	215
160	300(1)	332	256	282	282	256	308	410	308	384	384	112	128

(1) Oil Canning

TABLE B-34 STRAIN GAGE CORRESPONDENCE

STRAIN GAGE OF PANEL A-3-1	STRAIN GAGE OF PANEL A-3-2
3	3
4	4
7	5
6	6
5	9
11	12

TABLE B-35 AVERAGE STRAIN RECORDS OF SPECIMEN A-3-2

SPL	NOMINAL TEMPERATURE	STRAINS											
		e_1	e_2	e_3	e_4	e_5	e_6	e_7	e_8	e_9	e_{10}	e_{11}	e_{12}
(db)	(F)	(μ"/")	(μ"/")	(μ"/")	(μ"/")	(μ"/")	(μ"/")	(μ"/")	(μ"/")	(μ"/")	(μ"/")	(μ"/")	(μ"/")
139	76	0	0	-154	-102	-102	-154	0	0	-102	-102	-128	-128
139	100	0	-102	51	-359	103	-459	-52	-256	-469	256	-256	-128
139	200	256	-256	512	-714	406	-769	307	-512	-1024	768	-256	-26
139	300	410	-359	666	-924	406	-769	768	-512	-1154	896	-256	0
160	70	-51	0	-128	-52	-154	0	0	0	0	0	-204	-128
160	100(1)	-51	-52	-154	-154	-154	-256	-52	-102	0	0	-256	-204
			512										
160	200(2)	-51	-256	256	-512	256	-512		-512	-512	0	-307	
		0	512	-512	410	-769	768	128	512	768	-2304	384	-128
160	300(2)	256	-384	563	-769	358	-614		-512	-2304	768	-256	
		-51	512	-769	410	-769	768	256	512	768	-2304	256	-128

(1) Threshold of oil canning
(2) Oil canning

TABLE B-36 NATURAL MODES OF PANEL A-3-2

FREQUENCY	STRAINS (NONDIMENSIONAL)		
(Hz)	S_7	S_9	S_1
131	-13	37	-13
240	23	9	13
300	64	23(1)	-38

(1) A phase harmonic existed

TABLE B-37. STRAIN DATA OF SPECIMENS A-4-1 AND A-4-2 AT AMBIENT SPL

Panel	Nominal Temperature	Strain(1)					
		e_2	e_4	e_6	e_8	e_9	e_{10}
	(F)	(μ"/")	(μ"/")	(μ"/")	(μ"/")	(μ"/")	(μ"/")
A-4-1	70	25	-14	-9	-46	20	-64
A-4-1	100	-64	-78	-44	-178	-372	162
A-4-1	200	-103	-254	-197	-353	-896	602
A-4-1	300	-76	-334	-288	-425	-1126	768
A-4-1	400	-26	-380	-382	-451	-1261	864
A-4-1	500	61	-377	-430	-444	-1168	1077
A-4-1	600	234	-273	-391	-368	-1139	1086
A-4-1	400	-36	-145	-82	-327	-575	178
A-4-1	200	123	52	87	-45	9	-69
A-4-1	95	56	-6	-17	-78	13	-82
A-4-2	81	-80			-80	-64	-63
A-4-2	100	-4			14	222	-336
A-4-2	200	83			129	521	-690
A-4-2	300	111			178	705	-911
A-4-2	400	130			182	850	-1048
A-4-2	500	180			200	987	-1058
A-4-2	600	330			298	1139	-969
A-4-2	400	34			-54	210	-508
A-4-2	200	51			22	-78	-4
A-4-2	90	19			8	95	-224

(1) The strains are corrected for temperature induced apparent strain.

TABLE B-38 MEMBRANE AND BENDING STRAIN OF PANELS A-4-1 AND A-4-2 AT AMBIENT SPL.

Nominal Temperature	Panel A-4-1 Strain		Panel A-4-2 Strain	
	$\frac{e_{10}+e_9}{2}$	$\frac{e_{10}-e_9}{2}$	$\frac{e_{10}+e_9}{2}$	$\frac{e_{10}-e_9}{2}$
(F)	(μ"/")	(μ"/")	(μ"/")	(μ"/")
Ambient	-22	-42	-64	1
100	-105	267	-57	-279
200	-147	749	-85	-605
300	-179	947	-103	-808
400	-198	1062	-99	-949
500	-45	1122	-35	-1022
600	-27	1112	85	-1054
400	-198	376	-149	-358
200	-30	-39	-42	37
Ambient	-35	-47	-60	-159

TABLE B-39 NATURAL MODES OF PANELS A-4-1 AND A-4-2

Mode Number	Panel A-4-1					Panel A-4-2				
	Frequency (HZ)	Damping Factor (5)	Phase Relation (1) Bay 1	Bay 2	Bay 3	Frequency (HZ)	Damping Factor (5)	Phase Relation (1) Bay 1	Bay 2	Bay 3
1	120		+	-	+	128	0.012	(2)	+	(2)
2	216		+	(3)	+	215		+	+(3)	+
3	255		NA(4)	NA	NA	251		NA	NA	NA
4	304		NA	NA	NA	319		NA	NA	NA

(1) The phase relation was predicted by observing data from accelerometers at the center of the outer two bays and from a strain gage at the center of the middle bay. Bay 1 is the center bay.

(2) Phase harmonic

(3) Very low amplitude

(4) Not available

(5) No damping factors were obtained in the test of panel A-4-1. A viscous damping factor of 0.012 was obtained in the test of panel A-4-2 under loudspeaker excitation at 128 Hz.

TABLE B-40 TEMPERATURES OF SPECIMEN A-4-1

SPL	Temperature								
	Target	T_1	T_3	T_4	T_6	T_7	T_{10}	T_{11}	Notes
(db)	(F)	(F)	(F)	(F)	(F)	(F)	(F)	(F)	
Ambient	Ambient	70	70	70	70	70	70	70	
Ambient	100	98	78	86	76	100	80	82	
Ambient	200	190	90	160	90	200	136	134	
Ambient	300	276	110	240	108	296	205	190	
Ambient	400	370	135	330	132	395	282	242	
Ambient	500	465	170	420	170	496	370	310	
Ambient	600	570	215	520	212	596	465	400	
Ambient	400	410	200	375	196	400	340	285	On Cooldown
Ambient	200	210	145	195	142	200	205	185	On Cooldown
Ambient	Ambient	95	95	95	95	95	95	95	On Cooldown
139	Ambient	80	80	80	80	80	80	80	
139	200	170	95	180	95	196	145	142	
139	400	345	140	372	145	400	285	150	
139	600	520	200	560	210	595	450	390	
160	Ambient	80	80	80	80	80	80	80	
160	200	175	92	180	92	200	142	139	
160	400	345	130	365	135	400	280	250	
160	600	550	205	578	215	600	448	400	

TABLE B-41. TEMPERATURES OF SPECIMEN A-4-2

SPL		Temperature						
	Target	T_1	T_3	T_4	T_6	T_7	T_{10}	T_{11}
(db)		(F)	(F)	(F)	(F)	(F)	(F)	(F)
Ambient	Ambient	81	81	8[illegible]	81	81	81	81
Ambient	100	100	85	93	85	102	95	95
Ambient	200	195	105	160	102	200	140	137
Ambient	300	285	125	240	122	300	210	190
Ambient	400	380	155	345	150	400	290	250
Ambient	500	475	190	430	185	500	380	325
Ambient	600	575	235	530	230	600	470	420
Ambient	400	395	190	335	185	400	330	280
Ambient	200	200	150	170	145	200	195	175
Ambient	Ambient	90	90	90	90	90	90	90
139	Ambient	85	85	85	85	85	85	85
139	200	165	95	165	97	200	140	135
139	400	330	140	350	143	400	280	245
139	600	510	208	535	220	600	440	400
160	Ambient	79	79	79	79	79	79	79
160	200	140	55	135	85	200	129	129
160	400	310	110	325	110	400	255	248
160	600	485	160	505	165	600	400	370

TABLE B-42 DYNAMIC RMS STRAIN RECORDS OF PANELS A-4-1 AND A-4-2

Panel	SPL	Nominal Temperature	Strain					
			e_2	e_4	e_6	e_8	e_9	e_{10}
	(db)	(F)	(μ"/")	(μ"/")	(μ"/")	(μ"/")	(μ"/")	(μ"/")
A-4-1	139	Ambient (1)	38	18	18	46	138	138
A-4-1	139	200 (1)	20	18	18	28	26	26
A-4-1	139	400 (1)	20	18	18	23	18	20
A-4-1	139	600 (1)	20	18	18	20	18	18
A-4-1	160	Ambient (1)	184	33	43	out	230	294
A-4-1	160	200 (1)	out	39	51	out	out	out
A-4-1	160	400 (1)	out	39	56	out	out	out
A-4-1	160	600 (1)	out	51	103	out	out	out
A-4-2	139	Ambient (1)	66			74	141	133
A-4-2	139	200 (1)	20			36	20	20
A-4-2	139	400 (1)	23			26	23	23
A-4-2	139	600 (1)	18			26	23	20
A-4-2	160	Ambient (1)	243			243	282	out
A-4-2	160	200 (2)	308			332	410	out
A-4-2	160	400 (1)	out			out	141	out
A-4-2	160	600 (1)	out			out	179	out

(1) No oil canning was detected in the strain signal

(2) Oil canning was detected in the strain signal

TABLE B-43 AVERAGE STRAINS OF PANELS A-4-1 AND A-4-2

Panel	SPL	Nominal Temperature	Strain (1)					
			e_2	e_4	e_6	e_8	e_9	e_{10}
	(db)	(F)	(μ"/")	(μ"/")	(μ"/")	(μ"/")	(μ"/")	(μ"/")
A-4-1	139	Ambient	-8	-8	-160	-59	-8	-59
A-4-1	139	200	-212	-212	-342	-342	-805	474
A-4-1	139	400	-152	-382	-634	-404	-985	680
A-4-1	139	600	40	-216	-631	-246	-828	1014
A-4-1	160	Ambient	-8	-59	-162	-8	out	-136
A-4-1	160	200	out	-313	-291	out	out	out
A-4-1	160	400	out	-330	-514	out	out	out
A-4-1	160	600	out	-892	-570	out	out	out
A-4-2	139	Ambient	-67			-16	-16	35
A-4-2	139	200	-441			-441	-1115	805
A-4-2	139	400	-548			-788	-1496	1065
A-4-2	139	600	-372			-956	-1524	1411
A-4-2	160	Ambient	-8			-8	-8	out
A-4-2	160	200 (2)	-456 56			-324 188	-884 704	out
A-4-2	160	400	out			out	-1290	out
A-4-2	160	600	out			out	-1274	out

(1) The strains have been corrected to account for temperature induced apparent strain.
(2) Oil canning was detected in the strain signal.

TABLE B-44. STRAIN DATA OF SPECIMENS A-5-1 AND A-5-2 AT AMBIENT SPL

Panel	Nominal Temperature	Strain (1)			
		e_1	e_2	e_3	e_4
	(F)	(μin/in)	(μin/in)	(μin/in)	(μin/in)
A-5-1	75	30	114	67	52
A-5-1	100	155	485	375	420
A-5-1	200	-390	1270	710	850
A-5-1	300	-850	1170	590	1000
A-5-1	400	-1020	1600	650	1100
A-5-1	500	-1000	1750	550	1300
A-5-1	600	-1150	1950	800	1700
A-5-1	700	-1350	1900	1050	1450
A-5-1	800	-650	2700	1700	2200
A-5-1	900	-600	2500	1800	2400
A-5-1	1000	-1000	1600	520	1420
A-5-2	72	-49	-27		
A-5-2	108	-285	245		
A-5-2	204	-780	610		
A-5-2	302	-1250	850		
A-5-2	400	-1300	1150		
A-5-2	500	-1950	1000		
A-5-2	600	-2900	1300		
A-5-2	700	-2250	1250		
A-5-2	800	-1750	1650		
A-5-2	900	-2900	1600		
A-5-2	1000	-2700	900		

(1) The strains are corrected for temperature induced apparent strain.

TABLE B-45. MEMBRANE AND BENDING STRAIN OF PANELS A-5-1 AND A-5-2 AT AMBIENT SPL

Target Nominal Temperature	Panel A-5-1 Strain		Panel A-5-2 Strain	
	$\frac{e_2 + e_1}{2}$	$\frac{e_2 - e_1}{2}$	$\frac{e_2 + e_1}{2}$	$\frac{e_2 - e_1}{2}$
(F)	(μin/in)	(μin/in)	(μin/in)	(μin/in)
Ambient	72	42	-38	11
100	320	165	-20	265
200	440	830	-85	695
300	160	1010	-200	1050
400	290	1310	-75	1225
500	375	1375	-475	1475
600	400	1550	-800	2100
700	275	1625	-500	1750
800	1025	1675	-50	700
900	950	1550	-650	2250
1000	300	1300	-900	1800

TABLE B-46. NATURAL MODES OF PANELS A-5-1 AND A-5-2

Mode Number	Panel A-5-1					Panel A-5-2				
			Phase Relation[1]					Phase Relation[1]		
	Frequency	Damping Factor[7]	Bay 1	Bay 2	Bay 3	Frequency	Damping Factor[7]	Bay 1	Bay 2	Bay 3
	(Hz)					(Hz)				
1	138[2]	.015	(3)	+	(3)	155[2]	.017	(3)	+	(3)
2	181[4]					209[4]				
3	258[5]					285[5]				
4	296[6]					332[4]				

(1) Bay 2 is the middle bay.

(2) The predominant response was in the middle bay.

(3) Phase harmonic

(4) One nodal line was perpendicular to the stiffeners in all three bays. The nodal line was along a center line of the panels.

(5) Two nodal lines (in the middle bay) were perpendicular to the stiffeners. There were three half waves in the central bay along its length direction.

(6) The predominant response was in the outer bays with a 1-1 mode in each of those bays.

(7) Damping factors were obtained under loudspeaker excitation.

TABLE B-47. TEMPERATURES OF PANEL A-5-1

SPL	Temperature				
	Target	T_1	T_2	T_3	T_4
(db)	(F)	(F)	(F)	(F)	(F)
Ambient	Ambient	72	71	70	70
Ambient	100	98	98	91	91
Ambient	200	202	202	173	177
Ambient	300	296	296	258	277
Ambient	400	394	394	358	378
Ambient	500	495	495	467	485
Ambient	600	595	595	565	587
Ambient	700	695	695	674	692
Ambient	800	800	796	781	796
Ambient	900	896	890	890	900
Ambient	1000	996	989	992	1002
139	Ambient	70	70	70	70
139	300	300	300	272	260
139	600	599	598	580	562
139	1000	995	985	1004	992
160	Ambient	72	72	72	72
160	300	300	300	278	262
160	600	600	598	583	565
160	1000	1000	990	1007	995

TABLE B-48. TEMPERATURES OF PANEL A-5-2

SPL	TEMPERATURE							
	Target	T_1	T_3	T_4	T_6	T_7	T_{10}	T_{11}
(db)	(F)	(F)	(F)	(F)	(F)	(F)	(F)	(F)
Ambient	Ambient	72		72	72	72	72	72
Ambient	100	102	80	94	80	108	86	87
Ambient	200	180	94	155	94	204	137	137
Ambient	300	270	122	237	122	302	195	185
Ambient	400	367	170	330	175	400	272	250
Ambient	500	460	212	415	220	500	345	315
Ambient	600	570	290	525	300	600	445	405
Ambient	700	670	360	620	370	700	540	495
Ambient	800	775	445	730	460	800	635	590
Ambient	900	880	530	835	550	900	735	685
Ambient	1000	980	610	950	635	1000	840	790
139	Ambient	80	80	80	80	80	80	80
139	300	250	120	255	125	300	200	200
139	600	530	245	555	280	600	415	400
139	1000	950	580	965	630	1000	800	790
160	Ambient	80	80	80	80	80	80	80
160	300	245	118	255	120	300	200	200
160	600	525	245	550	275	600	410	410
160	1000	945	585	965	635	1000	795	795

TABLE B-49 DYNAMIC RMS STRAIN RECORDS OF PANELS A-5-1 AND A-5-2

Panel	SPL	Nominal Temperature	Rms Strain[1]			
			e_1	e_2	e_3	e_4
	(db)	(F)	(μ"/")	(μ"/")	(μ"/")	(μ"/")
A-5-1	139	Ambient	18	20	29	17
A-5-1	139	300	low[2]	low[2]	low[2]	low[2]
A-5-1	139	600	low[2]	low[2]	low[2]	low[2]
A-5-1	139	1000	low[2]	low[2]	low[2]	low[2]
A-5-1	160	Ambient	208	263	255	174
A-5-1	160	300	76	53	-	95
A-5-1	160	600	78	57	-	100
A-5-1	160	1000	78	57	-	83
A-5-2	139	Ambient	27	29		
A-5-2	139	300	low[1]	low[1]		
A-5-2	139	600	low[1]	low[1]		
A-5-2	139	1000	low[1]	low[1]		
A-5-2	160	Ambient	195	220		
A-5-2	160	300	74	85		
A-5-2	160	600	73	84		
A-5-2	160	1000	70	87		

(1) No oil canning was detected at any of these strain readings.

(2) These strain readings were in the noise floor.

TABLE B-50 AVERAGE STRAINS OF PANELS A-5-1 AND A-5-2

Panel	SPL (db)	Nominal Temperature (F)	Strains[1] e_1 (μ"/")	e_2 (μ"/")	e_3 (μ"/")	e_4 (μ"/")
A-5-1	139	Ambient	-100	-230	-7	-28
A-5-1	139	300	-300	500	850	1300
A-5-1	139	600	-700	2400	1900	2400
A-5-1	139	1000	-2600	1750	650	800
A-5-1	160	Ambient	-330	-455	-370	-130
A-5-1	160	300	-800	650	600	700
A-5-1	160	600	-600	1300	850	1350
A-5-1	160	1000	-2200	1900	650	900
A-5-2	139	Ambient	-272	-169		
A-5-2	139	300	-1150	370		
A-5-2	139	600	-2100	900		
A-5-2	139	1000	-3200	400		
A-5-2	160	Ambient	-147	-402		
A-5-2	160	300	-1050	250		
A-5-2	160	600	-1900	900		
A-5-2	160	1000	-3200	300		

(1) The strains are corrected for temperature induced apparent strain.

B.17 REFERENCES FOR APPENDIX B.

B-1 W. J. Hurty and M. F. Rubinstein, Dynamics of Structures, Prentice-Hall, Inc., Englewoods Cliffs, New Jersey, 1965.

B-2 M. J. Jacobson, Advanced Composite Joints; Design and Acoustic Fatigue Characteristics, Technical Report AFFDL-TR-71-126, April 1972.

B-3. S. Timoshenko and J. M. Gere, Theory of Elastic Stability, McGraw Hill Book Co., 1961.

APPENDIX C. SHAKER TEST DATA

The fatigue results obtained in the room temperature and elevated temperature shaker test program are in Table C-1 of this Appendix.

In Table C-1, when two strain entries at the line of rivets are separated by a semicolon, each strain of the pair is the average strain that persisted after th snap-throughs in oil canning. It was the repetition of large strain and stress reversals during the snap-throughs that was the predominant factor in producing the fatigue damage in the specimens.

The snap-throughs were detected by observing the strain signal on the oscilloscope and also by observing the test specimen respond to the shaker excitation.

TABLE C-1 Shaker Fatigue Test Results

Specimen	Temperature	Rise Time	Dwell Time	Cumulative Dwell Time	Strain at Line of Rivets		Discussion
					RMS	Average	
	(F)	(min)	(min)	(min)	(μ"/")	(μ"/")	
S-1-1	75 (Ambient)	–	169.5	169.5	766	0	The specimen broke in half.
S-1-2	(Ambient)	–	209.5	209.5	766	0	A fatigue crack was observed at the strain gage and extended to 0.1 inch below the bottom rivet.
S-1-3	(Ambient)	–	202.1	202.1	766	0	The fatigue crack extended from the lower rivet to the middle rivet.
S-9-1	(Ambient)	–	8.5	8.5	766	0	The specimen broke in half.
S-9-2	(Ambient)	–	5.5	5.5	766	0	The specimen broke in half.
S-9-3	(Ambient)	–	10.8	10.8	766	0	The fatigue crack extended from one edge nearly to the other edge.
S-10-1	(Ambient)	–	62.0	62.0	460	0	The fatigue crack extended from each rivet to an adjacent rivet.
S-10-2	(Ambient)	–	200.0	200.0	460	0	The fatigue crack extended from each rivet to an adjacent rivet and to one edge of the specimen.
S-10-3	(Ambient)	–	253.0	253.0	460	0	The fatigue crack extended from the top rivet past the middle rivet and half way to the bottom rivet.

TABLE C-1 (continued)

Specimen	Temperature (F)	Rise Time (min)	Dwell Time (min)	Cumulative Dwell Time (min)	Strain at Line of Rivets RMS (μ"/")	Strain at Line of Rivets Average (μ"/")	Discussion
S-2-1	5 to 300	0.9	2.0	2.0	460	1280;-4100	There was a 0.1 inch fatigue crack at 13.4 cumulative dwell minutes; 0.2 inch at 15.4 minutes; 1.8 inch at 17.4 minutes; and the specimen broke in half at 17.8 minutes.
	100 to 300	0.8	2.0	4.0	460		
	100 to 300	0.8	2.0	6.0	out		
	100 to 300	0.7	2.0	8.0			
	100 to 300	0.7	1.4	9.4			
	100 to 300	0.8	2.0	11.4			
	100 to 300	0.7	2.0	13.4			
	100 to 300	0.8	2.0	15.4			
	85 to 300	0.6	2.0	17.4			
	75 to 300	0.7	0.4	17.8			
S-2-2	76 to 300	0.7	2.0	2.0	460	1280;-6120	A fatigue crack from 0.1 inch above the top rivet to 0.1 inch below the center rivet was observed at 16.0 minutes of cumulative dwell time. The specimen broke in half at 17.0 minutes.
	100 to 300	0.7	2.0	4.0			
	100 to 300	0.6	2.0	6.0			
	100 to 300	0.6	2.0	8.0			
	100 to 300	0.8	2.0	10.0			
	100 to 300	0.6	2.0	12.0			
	100 to 300	0.7	2.0	14.0			
	100 to 300	0.6	2.0	16.0			
	100 to 300	0.6	1.0	17.0			
S-2-3	76 to 300	0.7	2.0	2.0	460	1790;-5120	Fatigue cracks were observed at each rivet at 16.0 minutes of cumulative dwell time. The test was terminated at 18.0 minutes of cumulative dwell time with the fatigue crack extending from the top to bottom rivet.
	100 to 300	0.7	2.0	4.0			
	100 to 300	0.7	2.0	6.0			
	100 to 300	0.6	2.0	8.0			
	100 to 300	0.7	2.0	10.0			
	100 to 300	0.6	2.0	12.0			
	100 to 300	0.6	2.0	14.0			
	100 to 300	0.6	2.0	16.0			
	100 to 300	0.6	2.0	18.0			

TABLE C-1 (continued)

Specimen	Temperature (F)	Rise Time (min)	Dwell Time (min)	Cumulative Dwell Time (min)	Strain at Line of Rivets RMS (μ"/")	Strain at Line of Rivets Average (μ"/")	Discussion
S-3-1	93 (Ambient)	0	1.0	1.0	768	0	Cumulative dwell time is for shaker excitation only. The test was terminated with a fatigue crack nearly along the entire specimen width.
	300	0.6	2.0	1.0	0	-5120	
	77 (Ambient)	0	1.0	2.0	768	-1430	
	300	0.6	2.0	2.0	0	-6400	
	83 (Ambient)	0	1.0	3.0	768	out	
	300	0.6	2.0	3.0	0		
	84 (Ambient	0	0.8	3.8	out		
S-3-2	74 (Ambient	0	1.0	1.0	768	0	Cumulative dwell time is for shaker excitation only. The test was terminated with a fatigue crack nearly along the entire specimen width.
	300	0.8	2.0	1.0	0	-4350	
	81 (Ambient)	0	1.0	2.0	768	-1280	
	300	0.7	2.0	2.0	0	-5370	
	66 (Ambient)	0	1.0	3.0	768	-1800	
	300	0.8	2.0	3.0	0	-6150	
	71 (Ambient)	0	1.0	4.0	768	-2150	
	300	0.7	2.0	4.0	0	-6400	
	72 (Ambient)	0	1.0	5.0	768	-2040	
	300	0.7	2.0	5.0	0	-6000	
	70 (Ambient)	0	1.0	6.0	768	out	

TABLE C-1 (continued)

Specimen	Temperature (F)	Rise Time (min)	Dwell Time (min)	Cumulative Dwell Time (min)	Strain at Line of Rivets RMS (μ"/")	Strain at Line of Rivets Average (μ"/")	Discussion
S-3-3	69 (Ambient)	0	1.0	1.0	768	0	Cumulative dwell time is for shaker excitation only. In contrast to specimens S-3-1 and S-3-2, there were some thermal cycles when a tensile strain was recorded at 300F. The test was terminated with a fatigue crack nearly along the entire specimen width.
	300	0.7	2.0	1.0	0	-4220	
	73 (Ambient)	0	1.0	2.0	768	-1320	
	300	0.7	2.0	2.0	0	-4220	
	74 (Ambient)	0	1.0	3.0	768	-1430	
	300	0.7	2.0	3.0	0	-4300	
	76 (Ambient	0	1.0	4.0	768	-1550	
	300	0.8	2.0	4.0	0	+2040	
	83 (Ambient)	0	1.0	5.0	768	-69	
	300	0.7	2.0	5.0	0	+2040	
	79 (Ambient)	0	1.0	6.0	768	-480	
	300	0.7	2.0	6.0	0	-4600	
	80 (Ambient)	0	1.0	7.0	768	-2090	
	300	0.7	2.0	7.0	0	+1150	
	82 (Ambinet)	0	1.0	8.0	768	-1000	
	300	0.7	2.0	8.0	0	-5620	
	82 (Ambient)	0	1.0	9.0	768	-3120	
	300	0.7	2.0	9.0	0	+1020	
S-4-1				26.0	460 (under shaker excitation at ambient temperature and at 300 F)	The steady strains were similar to data given for the S-2 and S-3 series of specimens	The total cumulative dwell time is for shaker excitation at 300F only. The test was terminated with a fatigue crack nearly along the entire specimen width. At some unknown time in the test, one of the four shear pins failed and quite possibly resulted in an increase of fatigue life because of relaxation of in-plane strain.

TABLE C-1 (continued)

Specimen	Temperature	Rise Time	Dwell Time	Cumulative Dwell Time	Strain at Line of Rivets		Discussion
					RMS	Average	
	(F)	(min)	(min)	(min)	(μ"/")	(μ"/")	
S-4-2				20.0	460 (under shaker excitation at ambient temperature and 300F)	See S-4-1 entry	The total cumulative dwell time is for shaker excitation at 300F only. The test was terminated when a fatigue crack was observed between two adjacent rivets.
S-4-3				16.0	460 (under shaker excitation at ambient temperature and 300F)	See S-4-1 entry	The total cumulative time is for shaker excitation at 300F only. The specimen broke in half.
S-5-1	600	0	117	117	460	-2560;2560	The test was terminated with 0.1 inch cracks from each rivet.
S-5-2	600	0	231	231	460	-1800;2300	The test was terminated with small cracks from each rivet. Pop throughs were occurring more often than in the case of specimen S-5-1. The pop throughs were occurring at about 25 per minute.
S-5-3	600	0	133	133	460	-890;3200	The specimen broke in half.

TABLE C-1 (continued)

Specimen	Temperature	Rise Time	Dwell Time	Cumulative Dwell Time	Strain at Line of Rivets		Discussion
					RMS	Average	
	(F)	(min)	(min)	(min)	(μ"/")	(μ"/")	
S-8-1	300	–	120.0	120.0	561 to 645	0	The strain level was raised after 120 minutes to prevent a long duration test. The specimen broke in half after 129.8 minutes of excitation.
	300	–	9.8	129.8	820	0	
S-8-2	300	–	140.0	140.0	320	0	The test was terminated with a visible crack of 1.2 inch.
S-8-3	300	–	138.0	138.0	320	0	The test was terminated with fatigue cracks extending almost from each rivet to the adjacent rivet. At an inspection at 126 minutes of excitation, a fatigue crack of 0.1 inch from each side of one rivet was observed.
S-7-1	300	–	14.3	14.3	460	1540;-3580 (corrected)	The specimen broke in half. Pop throughs occurred at about 5 to 10 per minute.
S-7-2	300	–	8.6	8.6	460	1530;-5120	The specimen broke in half. Pop throughs occurred at about 5 to 10 per minute.
S-7-3	300	–	24.6	24.6	460	1530;-5120	The test was terminated with a fatigue crack extending about the entire width of the specimen. Pop throughs occurred at about 5 per minute.

TABLE C-1 (completed)

Specimen	Temperature	Rise Time	Dwell Time	Cumulative Dwell Time	Strain at Line of Rivets		Discussion
					RMS	Average	
	(F)	(min)	(min)	(min)	μ"/"	μ"/"	
S-6-1	1000	0	32	32			The material was not aged at 1400F for 16 hours. No strain data are reported. There were approximately four pop throughs per minute.
S-4-2	1000	0	58	58	-	2625; 2615	The material was properly aged at 1400F for 16 hours. The double amplitude 5250 μ"/" was recorded during a pop through before the gage went out. There were approximately 2 pop throughs per minute
S-6-3	1000	0	25	25	-	-	The material was not aged at 1400F for 16 hours. No strain data are reported. There were approximately 4 pop throughs per minute.

Unclassified

Security Classification

DOCUMENT CONTROL DATA - R & D

(Security classification of title, body of abstract and indexing annotation must be entered when the overall report is classified)

1. ORIGINATING ACTIVITY (Corporate author) NORTHROP CORPORATION AIRCRAFT DIVISION, HAWTHORNE, CA. 90250	2a. REPORT SECURITY CLASSIFICATION Unclassified 2b. GROUP

3. REPORT TITLE

EFFECTS OF STRUCTURAL HEATING ON THE SONIC FATIGUE OF AEROSPACE VEHICLE STRUCTURES

4. DESCRIPTIVE NOTES (Type of report and inclusive dates)

Final Technical Report - March 1972 to March 1973

5. AUTHOR(S) (First name, middle initial, last name)

MARCUS J. JACOBSON
PAUL E. PINWALL

6. REPORT DATE January 1974	7a. TOTAL NO. OF PAGES 164	7b. NO. OF REFS 32
8a. CONTRACT OR GRANT NO. F33615-72-C-1198 b. PROJECT NO 4437 c. d.	9a. ORIGINATOR'S REPORT NUMBER(S) NOR 73-45 9b. OTHER REPORT NO(S) (Any other numbers that may be assigned this report) AFFDL-TR-73-56	

10. DISTRIBUTION STATEMENT Distribution limited to U.S. Government agencies only; test and evaluation; statement applied April 1973. Other requests for this document must be referred to AF Flight Dynamics Laboratory (FY), Wright-Patterson, AFB, Ohio 45433.

11. SUPPLEMENTARY NOTES	12. SPONSORING MILITARY ACTIVITY AF Flight Dynamics Laboratory Wright-Patterson AFB, Ohio 45433

13. ABSTRACT

The results of an analytic and experimental investigation to identify and determine the influence of effects of structural heating on the dynamic response characteristics of randomly excited aerospace structures and on the combined environment-acoustic fatigue properties of structural components are presented. Thermal and thermal-acoustic tests were conducted on 2024-T81, Ti-6Al-4V and Rene' 41 nickel-base alloy panel specimens. Effects of the temperature increase and sound pressure on the stress response and oil canning of the panels were observed. A semi-empirical criterion for predicting oil canning of panels in thermal-acoustic environments was developed. Shaker tests were conducted on 2024-T81 aluminum alloy specimens to determine the effect of the different sequences and combinations of heating and shaker excitation on the fatigue life of the specimens when oil canning is a factor. Elevated temperature fatigue tests under steady-state random (shaker) excitation were also conducted with Ti-6Al-4V titanium alloy and Rene' 41 nickel-base alloy specimens.

DD FORM 1 NOV 68 1473

Unclassified

Security Classification

14 KEY WORDS	LINK A		LINK B		LINK C	
	ROLE	WT	ROLE	WT	ROLE	WT
Thermal-acoustic Fatigue						
Dynamic Response						
Dynamic Instability						
Random S-N Data						
Cross-Stiffened Panels						

*U.S. Government Printing Office: 1974 — 750-431/168